

DETERMINE INITIAL CAUSE FOR CURRENT PREMATURE PORTLAND CEMENT CONCRETE PAVEMENT DETERIORATION

FINAL REPORT

Sponsored by the Project Development Division
of the Iowa Department of Transportation
and the Iowa Highway Research Board
Iowa DOT Project TR-406
CTRE Management Project 97-13

OCTOBER 2000



*Center for Transportation
Research and Education*

IOWA STATE UNIVERSITY



Iowa Department
of Transportation

The opinions, findings, and conclusions expressed in this publication are those of the authors and not necessarily those of the Iowa Department of Transportation.

CTRE's mission is to develop and implement innovative methods, materials, and technologies for improving transportation efficiency, safety, and reliability, while improving the learning environment of students, faculty, and staff in transportation-related fields.

DETERMINE INITIAL CAUSE FOR CURRENT PREMATURE PORTLAND CEMENT CONCRETE PAVEMENT DETERIORATION

FINAL REPORT

Principal Investigator

Scott Schlorholtz
Scientist

Department of Civil and Construction Engineering, Iowa State University

Sponsored by the Project Development Division
of the Iowa Department of Transportation
and the Iowa Highway Research Board
Iowa DOT Project TR-406

Preparation of this report was financed in part
through funds provided by the Iowa Department of Transportation
through its research management agreement with the
Center for Transportation Research and Education,
CTRE Management Project 97-13.

Center for Transportation Research and Education Iowa State University

ISU Research Park
2901 South Loop Drive, Suite 3100
Ames, Iowa 50010-8632
Telephone: 515-294-8103
Fax: 515-294-0467
<http://www.ctre.iastate.edu>

October 2000

TABLE OF CONTENTS

ABSTRACT.....	ix
INTRODUCTION	1
RESEARCH APPROACH	1
EQUIPMENT AND PROCEDURES.....	2
RESULTS AND DISCUSSION.....	7
Field Study.....	7
General Descriptions.....	7
Air Void Measurements.....	7
Petrographic Examination.....	15
Laboratory Study.....	18
Bulk Materials.....	18
Premature Stiffening Tests (Mortar Method).....	21
Restrained Shrinkage Tests (Paste Method).....	28
Unrestrained Shrinkage Tests (Paste Method).....	30
Shrinkage During Setting and Hardening (Mortar Method).....	35
SUMMARY AND CONCLUSIONS	35
Closing Comments.....	40
Recommendations.....	43
Recommendations for Further Research.....	44
ACKNOWLEDGMENTS	45
REFERENCES.....	46
APPENDIX A: MODIFIED ASTM C 359 TEST METHOD AND TEST RESULTS	47
APPENDIX B: CORE LOGS.....	51
APPENDIX C: IOWA DOT ASTM C 666 DATA	95
APPENDIX D: PETROGRAPHIC SUMMARIES AND SITE INFORMATION.....	104
APPENDIX E: RESULTS OF SHRINKAGE TESTING	125
APPENDIX F: HYPOTHESIS FOR PREMATURE CONCRETE DETERIORATION.....	129

LIST OF FIGURES

FIGURE 1	Illustration of how the pavement cores were sectioned for analysis.	4
FIGURE 2	Illustration of the Blaine restrained shrinkage ring (taken from [4]).	6
FIGURE 3	Good section of US 20.....	9
FIGURE 4	Bad section of US 20.....	9
FIGURE 5	Illustration of the use of X-ray maps to highlight the ettringite-filled air voids.	10
FIGURE 6	Higher magnification image from Figure 4; note the filled voids.....	10
FIGURE 7	Results of the image analysis measurements for air content.....	12
FIGURE 8	Illustration of segregation in a core extracted from I-80 in Iowa county.....	14
FIGURE 9	Examples from the XRD and DSC studies to quantify cement sulfate phases.	20
FIGURE 10	X-ray diffractogram of the fly ash sample used in this study.....	21
FIGURE 11	Illustration of mortars exhibiting false set and flash set.....	22
FIGURE 12	Influence of water-cement ratio on the premature stiffening tests.....	24
FIGURE 13	Relationship between premature stiffening and bassanite content.....	26
FIGURE 14	Abnormal behavior in the premature stiffening tests caused by admixtures.....	27
FIGURE 15	Results of the restrained shrinkage tests (cracking ring tests).....	29
FIGURE 16	Expanded view of the restrained shrinkage tests (no Kaiser cement).....	29
FIGURE 17	Unrestrained shrinkage during air curing for the various mixes.....	31
FIGURE 18	Unrestrained expansion during water curing for the various mixes.....	32
FIGURE 19	Influence of fly ash on the unrestrained shrinkage tests.....	33
FIGURE 20	Influence of water reducer and fly ash on unrestrained shrinkage.....	33
FIGURE 21	Results of the ASTM C 827 tests for the five control cements.....	34
FIGURE 22	Influence of fly ash and water reducer on the ASTM C 827.....	34
FIGURE 23	Model for concrete deterioration (adapted from Farny and Kosmatka [12]).	42
FIGURE 24	Holistic model for concrete deterioration (extracted from Mehta [13]).....	42

LIST OF TABLES

TABLE 1	Summary of the Pavement Sites Investigated in This Study	2
TABLE 2	Summary of Field Inspection and Core Logs for Sites Included in This Study	8
TABLE 3	Summary of the Hardened Air Contents for Pavement Sites Included in This Study	11
TABLE 4	Air Void Rating Scheme That Is Applicable to This Study.....	12
TABLE 5	Estimates of the Hardened Air Parameters for Pavements Included in This Study.....	13
TABLE 6	Summary of the Petrographic Examination of Cores Included in This Study.....	16
TABLE 7	Bulk Chemistry of the Cements and Fly Ash Used in This Study.....	19
TABLE 8	Measured Sulfate Compounds in the Cements and Fly Ash Used in This Study.....	19
TABLE 9	Summary of the Premature Stiffing Study for the Control Cements ($w/c = 0.30$).....	23
TABLE 10	Results of the Restrained Shrinkage Tests on the Control Cements.....	28

ABSTRACT

A detailed investigation has been conducted on core samples taken from 17 portland cement concrete pavements located in Iowa. The goal of the investigation was to help to clarify the root cause of the premature deterioration problem that has become evident since the early 1990s. Laboratory experiments were also conducted to evaluate how cement composition, mixing time, and admixtures could have influenced the occurrence of premature deterioration. The cements used in this study were selected in an attempt to cover the main compositional parameters pertinent to the construction industry in Iowa.

The hardened air content determinations conducted during this study indicated that the pavements that exhibited premature deterioration often contained poor to marginal entrained-air void systems. In addition, petrographic studies indicated that sometimes the entrained-air void system had been marginal after mixing and placement of the pavement slab, while in other instances a marginal to adequate entrained-air void system had been filled with ettringite. The filling was most probably accelerated because of shrinkage cracking at the surface of the concrete pavements. The results of this study suggest that the durability—more specifically, the frost resistance—of the concrete pavements should be less than anticipated during the design stage of the pavements.

Construction practices played a significant role in the premature deterioration problem. The pavements that exhibited premature distress also exhibited features that suggested poor mixing and poor control of aggregate grading. Segregation was very common in the cores extracted from the pavements that exhibited premature distress. This suggests that the vibrators on the paver were used to overcome a workability problem. Entrained-air voids formed in concrete mixtures experiencing these types of problems normally tend to be extremely coarse, and hence they can easily be lost during the paving process. This tends to leave the pavement with a low air content and a poor distribution of air voids. All of these features were consistent with a premature stiffening problem that drastically influenced the ability of the contractor to place the concrete mixture. Laboratory studies conducted during this project indicated that most premature stiffening problems can be directly attributed to the portland cement used on the project. The admixtures (class C fly ash and water reducer) tended to have only a minor influence on the premature stiffening problem when they were used at the dosage rates described in this study.

INTRODUCTION

Recent observations have identified several portland cement concrete (PCC) pavements in Iowa that have exhibited cracking after only approximately three to five years of service. Distress could not be specifically linked to design or materials constraints. However, materials-related difficulties, such as plastic concrete problems (workability), and materials incompatibilities were reported during the construction of several of the projects. Consultants were asked to evaluate several of the projects and to assess the most probable reason(s) for the observed distress. No consensus was reached by the various consultants. Alkali-silica reaction (ASR) and freeze-thaw deterioration were considered the most probable reasons attributed to the distress observed in the pavements. However, the consultants failed to satisfy the expectations of the Iowa Department of Transportation (Iowa DOT) because they failed to reach a consensus and they never really identified the root cause of the distress. Reactive shale particles were identified in the sand fraction of several portions of the distressed pavements; however, the same shale particles were also present in roadways that exhibited no distress after 20 years of service. In addition, the rapidity of the distress (the distress was evident after approximately three years of service) suggested that the shale particles were only minor culprits in the deterioration. The rapid onset of deterioration was also contrary to field service records for the aggregates used in the various projects.

The purpose of this research project was to refine the investigation of several of the pavements that exhibited premature deterioration. The goal of the project was to provide a better explanation of the root cause of the problem.

RESEARCH APPROACH

The research program consisted of both a field study and a laboratory study. The purpose of the field study was to provide forensic evidence pertaining to the deterioration mechanisms observed in 17 pavement sites across Iowa. The purpose of the laboratory study was to attempt to simulate some of the field-related problems in a laboratory environment so that the significance of the key constituents could be more clearly defined.

The field study utilized cores from the pavements summarized in Table 1. Approximately half the pavements that were cored represented "good" sites (i.e., pavements that exhibited no apparent signs of abnormal deterioration). The remaining sites all exhibited some level of deterioration that was considered excessive for the age of the pavement. The cores were subjected to petrographic examination and the air content of specific sections of the cores were evaluated using image analysis.

The laboratory study used two common admixtures that have consistently been recognized by Iowa DOT personnel to cause field problems in pavement jobs, and a suite of five different portland cements. Three of the cements were chosen to represent those commonly available in Iowa. Two additional cements, a low-alkali cement and a high-alkali cement, were also included in the laboratory study to expand the composition ranges of the cements. The admixtures consisted of (1) a class C fly ash with a very high analytical calcium content from Council Bluffs No. 3 power plant and (2) a low-range water reducer (Plastocrete 161, ASTM type A chemical admixture [1]). The laboratory study evaluated the premature stiffening

characteristics of a series of different combinations of portland cement, fly ash, and water reducer. Volume stability during setting and hardening was monitored using ASTM C 827 (1). The shrinkage of paste specimens containing the various constituents was evaluated during the study by means of unrestrained shrinkage and restrained shrinkage tests. The laboratory study also included the use of thermal analysis techniques and X-ray diffraction techniques to quantify the sulfur compounds that were present in the cements and fly ash.

TABLE 1 Summary of the Pavement Sites Investigated in This Study

Site	Road	County	Year Paved	Project Number	Location	Premature Distress?
1	US 20	Webster	1986	F-520-3(12)-20-94	Westbound, milepost 127.55, station 2002	No
2	US 20	Hamilton	1986	F-520-4(26)-16-40	Westbound, milepost 135.4, station 49	Yes
3	US 169	Webster	1990	F-169-6(31)-20-94	Southbound, near station 2002	Yes
4	Hwy 175	Hamilton	1980	F-175-7(13)-20-40	Westbound lane, milepost 156.2, station 143	No
5	Hwy 175	Hamilton	1980	F-175-7(13)-20-40	Eastbound lane, milepost 157.5, station 191	No
6	Hwy 175	Hamilton	1980	F-175-7(13)-20-40	Eastbound lane, milepost 158.3, station 244	No
7	Hwy 330	Marshall	1983	F-330-2(19)-20-64	Northbound lane, milepost 6.8, station 74	Yes
8	I-80	Iowa	1988	IR-80-6(119)-12-48	Eastbound, milepost 210.36, station 298	Yes
9	I-80	Dallas	1989	IR-80-3(57)106	Eastbound, milepost 107.55, station 509	No
10	I-80	Dallas	1989	IR-80-3(57)106	Eastbound, milepost 113.25, station 810	Yes
11	I-80	Dallas	1989	IR-80-3(57)106	Eastbound, milepost 116.2, station 966	No
12	I-80	Cass	1988	IR-80-2(108)61-12-15	Westbound, milepost 68, station 1019	No
13	Hwy 2	Fremont	1986	F-2-1(23)-20-36	Westbound, milepost 2.6, station 1499	Yes
14	Hwy 160	Polk	1985	F-415-1(11)-20-77	Eastbound, near station 362	Yes
15	US 218	Johnson	1983	F-518-4(12)-20-52	Southbound, milepost 95.45, station 1658	Yes
16	US 218	Johnson	1983	F-518-4(12)-20-52	Northbound, milepost 91.96, station 1498	Yes
17	US 61	Scott	1981	FFD-561-1(6)-2N-82	Northbound, milepost 125, station 525	No

EQUIPMENT AND PROCEDURES

Core samples having a nominal diameter of 102 millimeters (4 inches) were extracted from each site by Iowa DOT personnel. All of the cores represented the full depth of the pavement slab unless noted otherwise. The core specimens were sectioned using a Buehler LAPRO slab saw. The saw was equipped with a 457-millimeter (18 inch) diameter notched-rim diamond blade. Reagent grade propylene glycol was used as the lubricant-coolant during the cutting process. Preliminary cuts were made to section the cores into thirds (i.e., top, middle, and

bottom of each core). This was done to preserve information about air content versus depth. Test specimens were cut from each section by making two longitudinal cuts (see Figure 1). Hence, the nominal section area that was available for analysis on any given specimen was about 77 cm² (12 in², in accordance with ASTM C 457 [1], assuming a nominal coarse aggregate size of 25 millimeters [1 inch]). The sections were then prepared for analysis using a LECO VP-50 variable speed grinder/polisher. The VP-50 was equipped with a 300-millimeter (12 inch) diameter brass wheel. Fixed grit silicon carbide grinding paper was used throughout the study. The exact details of the specimen preparation technique have been summarized in a previous report (2).

A Hitachi S-2460N low-vacuum scanning electron microscope was used for collecting the digital images obtained during this project. All of the digital images were collected using an Oxford Instruments LINK TETRA back-scattered electron detector. The digital images were then analyzed using image analysis techniques to provide estimates of air content, specific surface and spacing factor. X-ray maps were also collected for specific samples using an Oxford Instruments GEM X-ray detector and a LINK ISIS X-ray acquisition system.

The X-ray maps provide important information pertaining to some of the deterioration processes that could have occurred in the pavements. Detailed summaries of the equipment and standard operating procedures for the image analysis technique can be found in an earlier report (2). Several different microscopes were used for the light microscopy phase of this study. Thin sections were viewed with an Olympus BH-2 transmitted light microscope or a Unitron polarizing microscope. Bulk or polished specimens were viewed in reflected light with an Olympus BH reflected light microscope or an Olympus SZH stereo microscope.

A TA Instruments differential scanning calorimeter (DSC, Model 2910) was used to analyze portions of the portland cement samples. A typical experiment was conducted on a 10-milligram specimen that was heated from 25°C to about 300°C using a heating rate of 10 degrees per minute. All specimens were hermetically sealed in aluminum specimen containers prior to analysis. Nitrogen gas was purged through the system to avoid oxidation of the DSC cell. The method was calibrated using a series of synthetic standards that were manufactured from pure gypsum, bassanite, and a portland cement clinker that contained neither of the minerals.

A Siemens D-500 X-ray diffractometer (XRD) was used to analyze the cements and fly ash that were used in this study. A typical experiment used a copper X-ray tube (excitation conditions 50 kV and 27 mA) and a diffracted beam monochromator. Specimens were back-loaded into a sample holder for analysis. Scanning rates were 1.5 degrees per minute for the initial qualitative runs. Quantitative measurements were conducted using a scanning rate of 0.5 degrees per minute. Silicon metal was used as an internal standard in all quantitative runs. The method was calibrated using a series of synthetic standards. The standards were manufactured by mixing known amounts of the pure minerals (gypsum, bassanite, and anhydrite) with a portland cement clinker that contained no detectable amount of these three different minerals.

A Philips PW 2404 X-ray fluorescence spectrometer (XRF) was used for measuring the bulk elemental composition of the various materials used in this project. The spectrometer is equipped with a rhodium target X-ray tube, a 167 specimen sample changer (only sixty positions active at this time) and is fully computer controlled. All of the specimens were presented to the spectrometer as fused disks. The spectrometer was calibrated using NIST-grade standard reference materials that had been fused into glass disks.

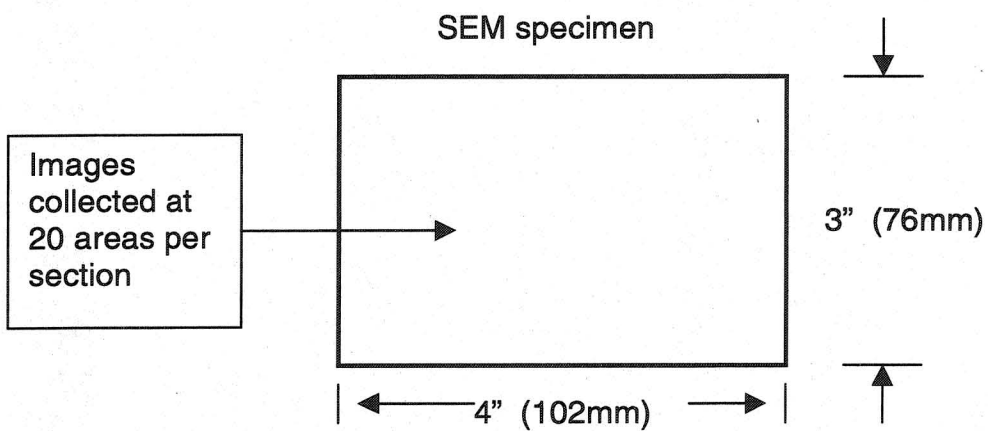
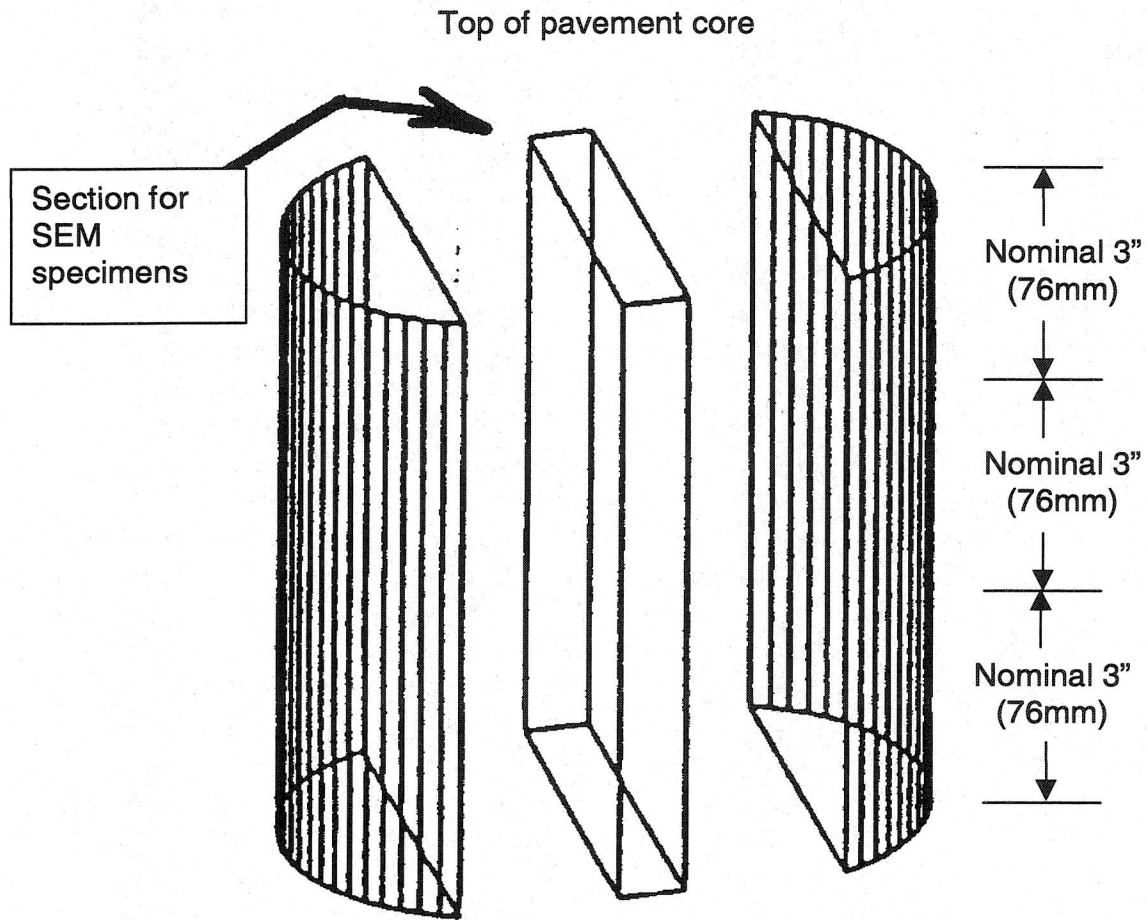


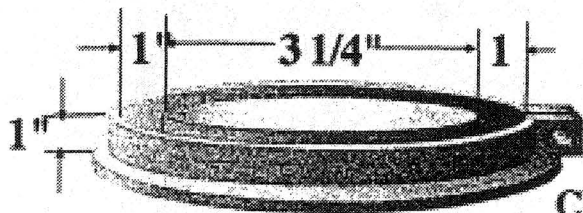
FIGURE 1 Illustration of how the pavement cores were sectioned for analysis.

The procedure described in ASTM C 827 (1) was used for monitoring the shrinkage of mortar test specimens during the setting and hardening process. Briefly, the procedure was as follows. The standard mortar mixing procedure given in ASTM C 305 (3) was used for all mixes. Enough water was added to each mix to produce a plastic consistency (i.e., a mortar flow between 100 and 125). When needed, the water-reducing admixture was added to the mix after the sand, just before the mixer was switched to speed 2. This ensured that the cement was in contact with water for about a minute prior to being dosed with water reducer. The mortar mixture was then compacted into a cylinder mold (50-millimeter [2 inch] diameter, 100 millimeters [4 inches] tall) that had been oiled. Then a polystyrene bead (12-millimeter diameter, density = 1.13 grams per cubic centimeter) was gently pressed into the top of the mortar specimen. The mortar specimen was then positioned in an apparatus similar to that described in ASTM C 827, except that the projection system only produced a nominal magnification of 80X (not the 90X to 110X required in ASTM C 827). The exact magnification factor for each experiment was determined by using a drill bit and the procedure outlined in ASTM C 827. The drill bit had a diameter of 3.1 millimeters. The approximate setting time of the mortar was determined using a soil pocket penetrometer and the excess mortar from any given mix. The excess mortar was placed in container (75-millimeter [3 inch] diameter by 50 millimeters [2 inches] tall) and then probed with the penetrometer at half-hour time increments. The mortar was considered to have set when the penetrometer reached its maximum reading (430 kN per square meter). This technique is not a conventional method for determining the setting time of mortar, but it was deemed adequate for the needs of this testing program.

The unrestrained drying shrinkage characteristics of various mixtures were measured using prismatic bar specimens (nominal dimensions of 25 millimeters by 25 millimeters by 300 millimeters [1 inch by 1 inch by 11.25 inches], effective gage length of 250 millimeters [10 inches]). The paste specimens were mixed with enough water to attain normal consistency and then placed in the molds. When needed, the water-reducing admixture was added to the mix after the scrape down procedure described in ASTM C 305 (3). This ensured that the cement was in contact with water for about a minute prior to being dosed with water reducer. The test specimens were cured under plastic at ambient room temperature for one day. Note, this is not the normal moist curing cycle that is commonly used for autoclave bar specimens. Then the test specimens were separated into two equal groups. The first group (i.e., half of the of test specimens that were molded) was exposed to ambient temperature and humidity conditions (temperature = $23 \pm 2^\circ\text{C}$, relative humidity = 57 ± 7 percent). The other group of test specimens was subjected to lime water curing (i.e., an ideal curing case with no shrinkage). Shrinkage or expansion, depending on the group of specimens, was monitored at regular intervals after the first four hours of exposure to the test environment. It was not possible to maintain the relative humidity of the laboratory at the 57 percent level after approximately the first 40 days of exposure. This was due to the start of the winter months. During these months, the relative humidity fluctuated between about 35 percent and 45 percent, and this did lead to an observed increase in the shrinkage of most of the test specimens.

Restrained shrinkage was conducted using paste specimens and a shrinkage ring described by Burrows (4). Burrows indicated that this was basically the apparatus described by Blaine et al. (5). A diagram of the shrinkage ring, the directions for performing the test, and the suggested rating scheme for interpreting the test results are given in Figure 2. When needed, the water-reducing admixture was added to the mix after the scrape-down procedure described in ASTM C 305 (3). This ensured that the cement was in contact with water for about a minute

prior to being dosed with water reducer. The curing and storage conditions for the shrinkage ring tests were identical to those for the unrestrained shrinkage tests described above (i.e., curing under plastic for 24 hours, followed by exposure to ambient room conditions, temperature = $23 \pm 2^\circ\text{C}$, relative humidity = 57 ± 7 percent).



DIRECTIONS FOR TEST
MIX TO NORMAL CONSISTENCY
W/C = 0.23 - 0.26
CURE AT 73°F, > 95% RH FOR 24 HRS
DEMOLD AND DRY AT 73°F, 50% RH

<u>BREAK TIME</u>	<u>RATING</u>
< 1 hour	Poor
1 to 4 hours	Questionable
4 to 15 hours	Good
> 15 hours	Excellent

FIGURE 2 Illustration of the Blaine restrained shrinkage ring (taken from [4]).

Premature stiffening tests, often called false set tests, were conducted using two different procedures. ASTM C 359 (3) was the first procedure that was used. The second procedure, which will be referred to as the “modified C 359,” used a shorter mix cycle than the procedure described in ASTM C 359. The procedure for the modified C 359 test is given in Appendix A. The modified C 359 test is considered the more rigorous of the two test methods. This was deemed appropriate because of the rather short mix cycles that are used in pavement concrete mixes. When needed, the water-reducing admixture was added to the mix during the final 30 seconds of the mix cycle. This ensured that the cement was in contact with water for at least 30 seconds prior to being dosed with water reducer. Briefly, both test methods evaluate the premature stiffening behavior of mortars for the first 10 or 11 minutes after water was added to the mix. The mortars were then subjected to a remix cycle to evaluate if the premature stiffening was caused by flash set or false set. Flash set mortars typically exhibit low penetration values even after the remix cycle. For the purpose of this research program, the mortars were evaluated for an additional 20 to 30 minutes after the remix cycle. This was done to lengthen the observation period to about 30 minutes after the water was added to the mix.

RESULTS AND DISCUSSION

Field Study

General Descriptions

The general details noted during the field inspection of the pavements are summarized in Table 2. The core logs, which were generated during the laboratory inspection of the cores, are given in Appendix B. Important details from the core logs have also been summarized in Table 2.

Air Void Measurements

The image analysis procedure utilized a series of low-magnification (40x) digital images to measure the air voids present in a test specimen. Typical digital images obtained from “good” and “bad” sections of pavement are illustrated in Figures 3 and 4, respectively. The images represent concrete from the top three inches of cores that had been taken from the midpanel region of two different pavement slabs. Both figures contain similar features; however, the good section contained more entrained-air voids than did the bad section. This discrepancy could be due to the fact that (1) the air void system in the bad section was lower to start with (because of improper admixture dosage, poor mixing, or excessive vibration) or (2) because the air voids have been filled with a sulfate mineral that has a chemical composition close to the mineral ettringite [$\text{Ca}_6\text{Al}_2(\text{SO}_4)(\text{OH})_{12-25}\text{H}_2\text{O}$]. The image analysis technique cannot count the air voids that have been filled with ettringite because of the very poor contrast between the cement paste and the filled voids. However, another analytical procedure, commonly referred to as X-ray mapping, can be used to produce a detailed image of the initial air void system. This is illustrated in Figure 5. The figure shows that the initial air void system has been filled with a phase that is rich in sulfur (ettringite in this instance, as determined by energy dispersive X-ray analysis). Likewise, the silicon map exhibits dark areas (holes) where the initial air voids resided in the cement paste.

Higher magnification (see Figure 6) can also be used to distinguish the filled voids from the cement paste. However, this causes a dramatic increase in the number of images that need to be collected to provide a reliable estimate of the air content of the sample. The image shown in Figure 6 indicates that, in this particular specimen, most of the air voids with diameters less than about 100 microns have been filled with ettringite. This should have a negative impact on the freeze-thaw resistance of the concrete because it causes an increase in the spacing factor of the concrete.

Presently, there are several strategies available for quantifying the amount of voids that are filled in any given sample. The first strategy is to use X-ray mapping to directly measure the sulfur rich phase present in the air voids. Another strategy is to stain the material in the voids with a dye this facilitates their measurement using conventional (light) microscopes. The third strategy is to use a solvent to selectively remove the ettringite from the air voids. This coupled with an additional measurement cycle would allow one to evaluate the amount of voids that had been filled.

TABLE 2 Summary of Field Inspection and Core Logs for Sites Included in This Study

Site	Road	Description of Pavement Distress	Description of Distress Noted in Cores
1	US 20	No distress observed	No cracks evident; entrapped air voids common
2	US 20	Severe cracking at joints, similar to D-cracking, but some cracks extend the length of the panels on 450-mm (18 inch) to 600-mm (24 inch) spacing	Cracking noted in all cores, typically subparallel to top of core; many large, entrapped air voids; shale pop outs common on sides of core
3	US 169	Staining and faint to moderate cracking noted only at joint area	Poor core extraction, broke off at about 125 mm (5 inches); cracking noted, typically subparallel to top of core
4	Hwy 175	No distress observed	No cracks evident; some staining around shale particles; entrapped air voids common
5	Hwy 175	No distress observed	No cracks evident; some staining around shale particles; entrapped air voids common
6	Hwy 175	No distress observed	One fine crack at base of core, ran halfway around the core; some staining around shale particles; entrapped air voids common.
7	Hwy 330	Staining and moderate cracking noted only at joints	Cracking evident; some cracking due to gravel aggregate particles
8	I-80	Severe cracking radiating from transverse joints through the length of the panel—often on 450-mm (18 inch) to 600-mm (24 inch) spacing	Cracking noted at top surface and bottom of core; some segregation noted; large entrapped air voids common
9	I-80	No distress observed	No cracks evident; shale particles common, some have white residue surrounding them
10	I-80	Severe cracking at joints; few cracks propagate through length of panel	Some surface cracking evident; some coarse aggregate particles exhibit staining; entrapped voids as large as 25-mm (1 inch) diameter observed near mid-depth of some cores
11	I-80	No distress observed	No cracking noted; some coarse aggregate particles exhibit staining; entrapped voids common
12	I-80	No distress observed	Slight cracking noted at bottom of cores; entrapped voids common but all less than 18-mm (0.75 inch) diameter.
13	Hwy 2	Cracking at joints, typically perpendicular to joints but at random spacing; some cracking on panel	Surface cracking common
14	Hwy 160	Cracking only at joints; cracks did not extend through the panel	No cracking evident except for pop outs due to shale particles
15	US 218	Faint longitudinal cracks; appeared to be on a 450-mm (18 inch) to 600-mm (24 inch) spacing	No cracking evident; some white residue noted around shale particles
16	US 218	Severe cracking radiating from transverse joints through the length of the panel, often on 450-mm (18 inch) to 6000-mm (24 inch) spacing	Cracking common at top surface of cores taken from the joints; some shale and chert particles noted, often surrounded by white residue
17	US 61	No distress observed	Cracking common at the bottom of all cores; most cracks pass through the coarse aggregate particles

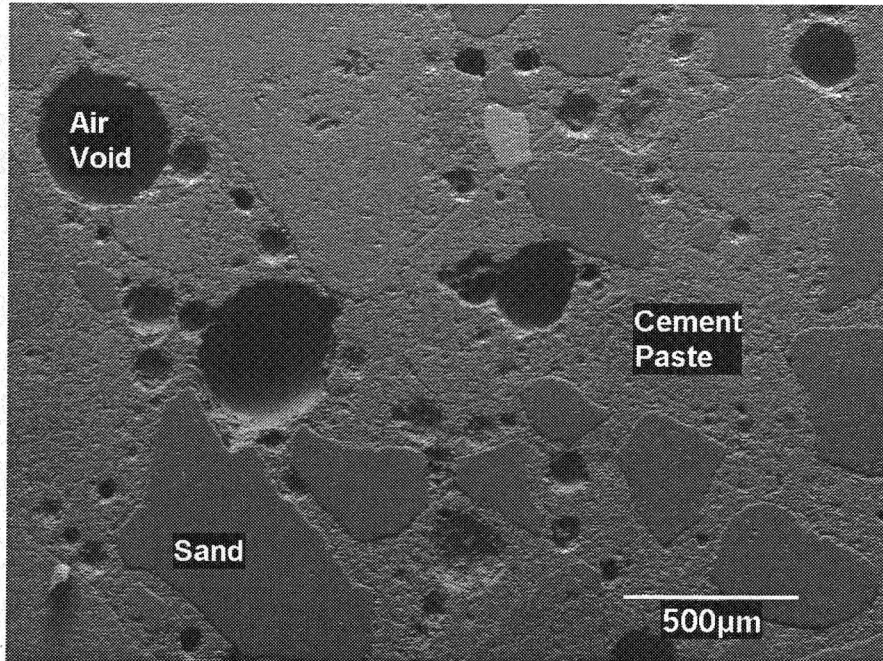


FIGURE 3 Good section of US 20.

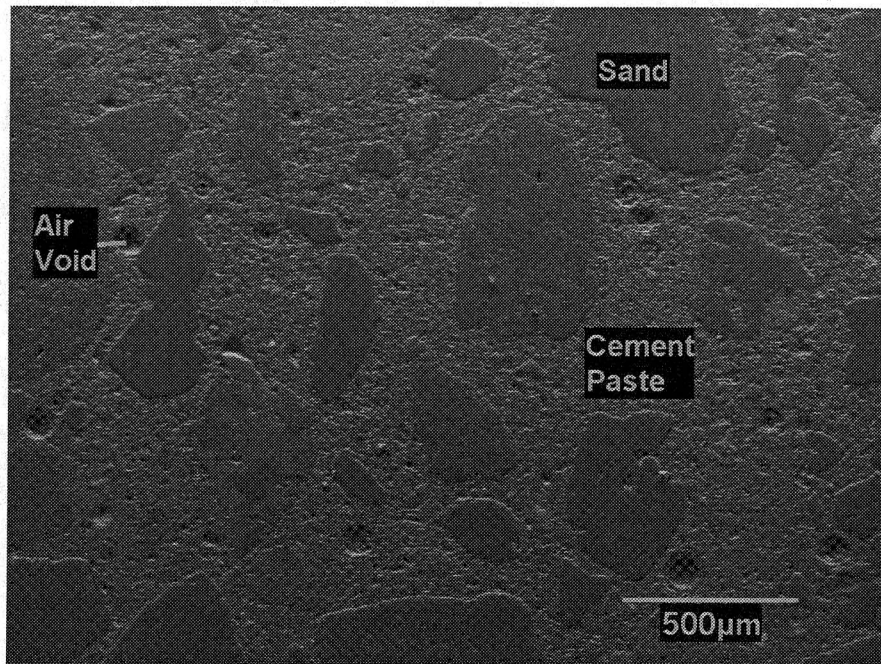


FIGURE 4 Bad section of US 20.

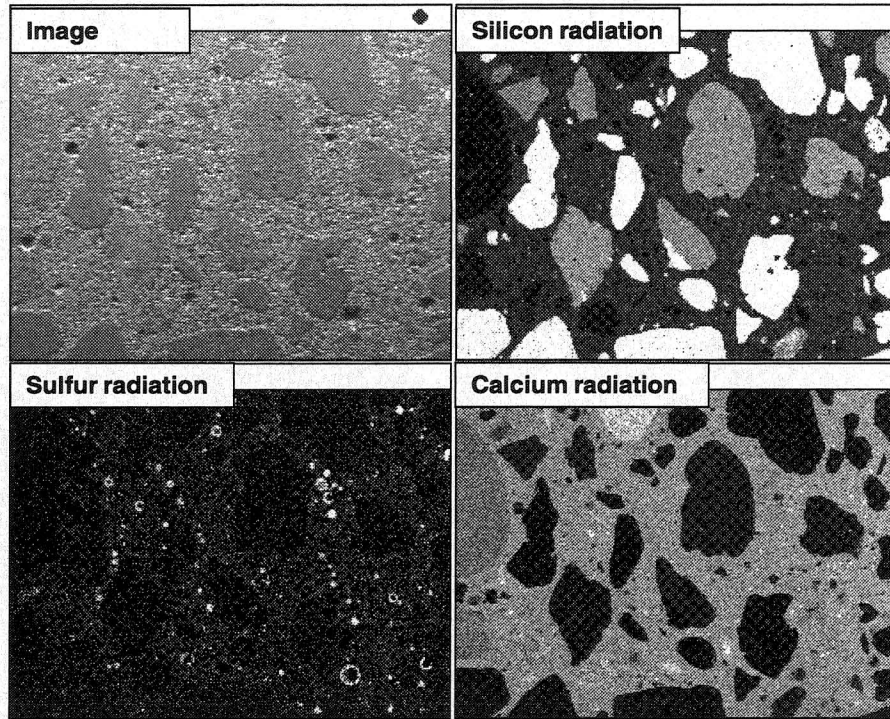


FIGURE 5 Illustration of the use of X-ray maps to highlight the ettringite-filled air voids.

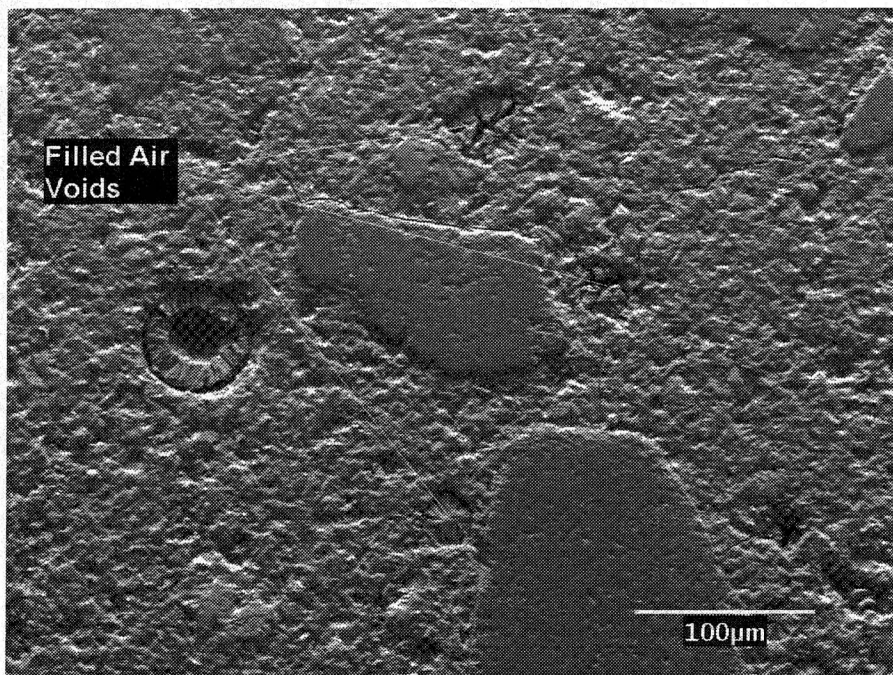


FIGURE 6 Higher magnification image from Figure 4; note the filled voids.

The results of the hardened air content determinations that were conducted for this study are summarized in Table 3 and are depicted graphically in Figure 7. The results shown in the figure have been sorted by location (i.e., joint vs. midpanel) to help spread out the information. For the purpose of this discussion the numerical values have been expressed as air contents based on the mortar fraction of the concrete specimens (i.e., ignoring the coarse aggregate fraction of the concrete). Previous research (6, 7) has indicated that concrete containing mortar air contents of 9 ± 1 percent typically exhibit good to excellent resistance to freezing and thawing. Recent work at this lab (2) has produced test results in good agreement with these earlier studies.

TABLE 3 Summary of the Hardened Air Contents for Pavement Sites Included in This Study

Site	Road	County	Mortar Air			Number of Determinations	Premature Deterioration?
			Average (%)	Low Value (%)	High Value (%)		
1	US 20	Webster	6.9	4.9	8.5	4	No
2	US 20	Hamilton	5.0	3.9	6.2	4	Yes
3	US 169	Webster	7.2	4.9	9.6	3	Yes
4	Hwy 175	Hamilton	7.6	6.4	8.8	5	No
5	Hwy 175	Hamilton	6.4	5.0	8.1	4	No
6	Hwy 175	Hamilton	8.9	8.1	10.5	4	No
7	Hwy 330	Marshall	5.3	5.0	5.7	4	Yes
8	I-80	Iowa	5.1	3.3	8.3	6	Yes
9	I-80	Dallas	6.1	5.2	7.3	4	No
10	I-80	Dallas	5.2	2.8	8.4	4	Yes
11	I-80	Dallas	5.1	3.9	6.4	4	No
12	I-80	Cass	9.1	8.0	10.9	5	No
13	Hwy 2	Fremont	4.0	2.7	5.0	4	Yes
14	Hwy 160	Polk	2.2	2.0	2.4	3	Yes
15	US 218	Johnson	4.7	3.6	5.4	3	Yes
16	US 218	Johnson	5.8	4.9	7.8	5	Yes
17	US 61	Scott	7.0	5.4	8.7	5	No

Table 4 summarizes the relationship between the measured mortar air content and the corresponding bulk concrete air content for an Iowa DOT C-3 concrete mix. Also included in Table 4 is a qualitative rating scheme that can be used to assess the overall suitability of the air void system to resist freeze-thaw deterioration. The rating scheme was developed using past research conducted at this laboratory in combination with the Iowa DOT data summarized in Appendix C. The critical air content (defined as "marginal" in Table 4) is not a constant for all carbonate aggregates, and the data included in Appendix C clearly indicate that some discretion must be used when interpreting values in that region. Typically, the information indicates that concrete test specimens tested for freeze-thaw durability using ASTM C 666 (1) exhibit approximately a 50 percent loss of durability factor in this region. However, some coarse grain limestones and dolomites may be able tolerate air contents in this region (e.g., see the test results for Alden, Sedgwick, and Shaffton given in Appendix C).

The results summarized in Table 3 and shown in Figure 7 indicate that the pavements that exhibited premature deterioration tended to have a wide range of mortar air contents (roughly from two to 10 percent). The average mortar air content for the pavements that exhibited premature distress was 5.1 percent, and only seven out of the 39 specimens that were tested had

air contents greater than 6 percent. In contrast, the pavements that exhibited good field performance had a slightly narrower range of air contents (range from four to 11 percent). The average mortar air content for the good pavements was 7.3 percent and only eight out of the 32 specimens that were tested had air contents less than 6 percent.

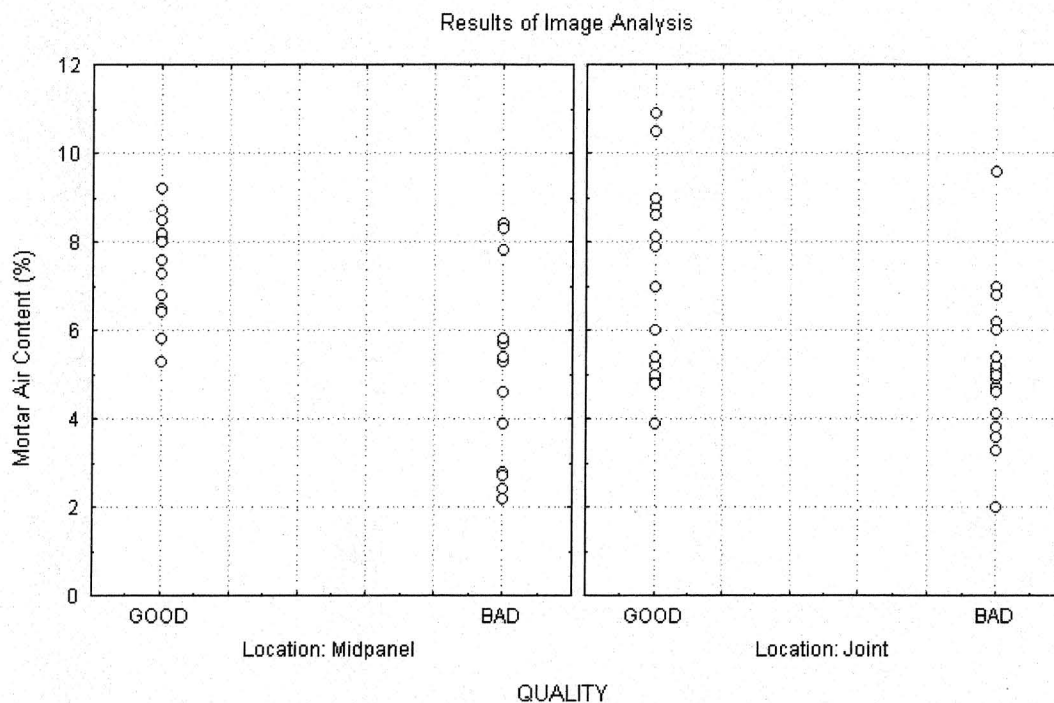


FIGURE 7 Results of the image analysis measurements for air content.

TABLE 4 Air Void Rating Scheme That Is Applicable to This Study

Qualitative Rating Scheme	Mortar Air Content (%)	Equivalent Concrete Air Content ^a (%)
Excellent	10	6.3
Excellent	9	5.7
Good	8	5.0
Adequate	7	4.4
Marginal	6	3.8
Marginal	5	3.2
Poor	4	2.5
Poor	3	1.9
Poor	2	1.3
Poor	1	0.9

^aApplies to a C-3 mix only.

Other global concrete properties, such as specific surface and spacing factor calculations, are summarized in Table 5. These calculations were conducted in a manner similar to that used in previous research (e.g., 2). However, it is important to understand that some assumptions had to be made to simplify the calculations. First, the paste content and the bulk air content of each pavement site had to be estimated using the nominal mix proportions (i.e., theoretical or as specified by Iowa DOT documents). This is a drastic oversimplification because sometimes things simply do not go right in the field. The standard ASTM test (C 457) allows for the measurement of paste content and this needs to be added to the image analysis test method to make it more robust. Some of the concrete cores that were evaluated in this study exhibited severe segregation. This is illustrated in Figure 8. This particular concrete mix should have been a C-3WR-C mix with about 38 percent coarse aggregate and 25 percent paste (by volume). It is apparent in Figure 8 that the actual (or measurable) mix proportions deviate significantly from the theoretical mix proportions. This means that the spacing factor calculated for the section will be in error. Second, no attempt has been made to transform the observed circle diameter distribution into the theoretical sphere diameter distribution prior to performing the spacing factor calculations. Ignoring the transform greatly simplified the calculations, but it also inflates the spacing factor values since the transform tends to increase the number of small voids at the expense of the larger voids. Hence, the values summarized in Table 5 will be referred to as "apparent spacing factors." The apparent spacing factor estimates (as rough as they were) still separated the concrete cores into two rough groups that corresponded closely to the observation of distress in the cores. Cores having apparent spacing factor values less than about 0.21 millimeters (0.0083 inches) exhibited little distress. Cores having apparent spacing factor values above 0.24 millimeters (0.0094 inches) nearly always exhibited distress. These test results suggest that the premature distress was at least partially related to inadequate or marginal entrained-air void systems in the hardened concrete pavements.

TABLE 5 Estimates of the Hardened Air Parameters for Pavements Included in This Study

Site	Road	County	Apparent Specific Surface (mm ⁻¹)	Apparent Spacing Factor (mm)	Deterioration Noted in Cores?
1	US 20	Webster	25.4	0.20	No
2	US 20	Hamilton	24.1	0.24	Yes
3	US 169	Webster	23.0	0.22	Yes
4	Hwy 175	Hamilton	25.7	0.19	No
5	Hwy 175	Hamilton	25.3	0.21	No
6	Hwy 175	Hamilton	26.5	0.17	No
7	Hwy 330	Marshall	19.5	0.29	Yes
8	I-80	Iowa	24.0	0.25	Yes
9	I-80	Dallas	21.9	0.24	No
10	I-80	Dallas	24.3	0.25	Yes
11	I-80	Dallas	30.6	0.19	No
12	I-80	Cass	26.2	0.17	No
13	Hwy 2	Fremont	29.3	0.23	Yes
14	Hwy 160	Polk	26.2	0.34	Yes
15	US 218	Johnson	21.4	0.28	Yes
16	US 218	Johnson	24.0	0.24	Yes
17	US 61	Scott	20.6	0.25	Yes

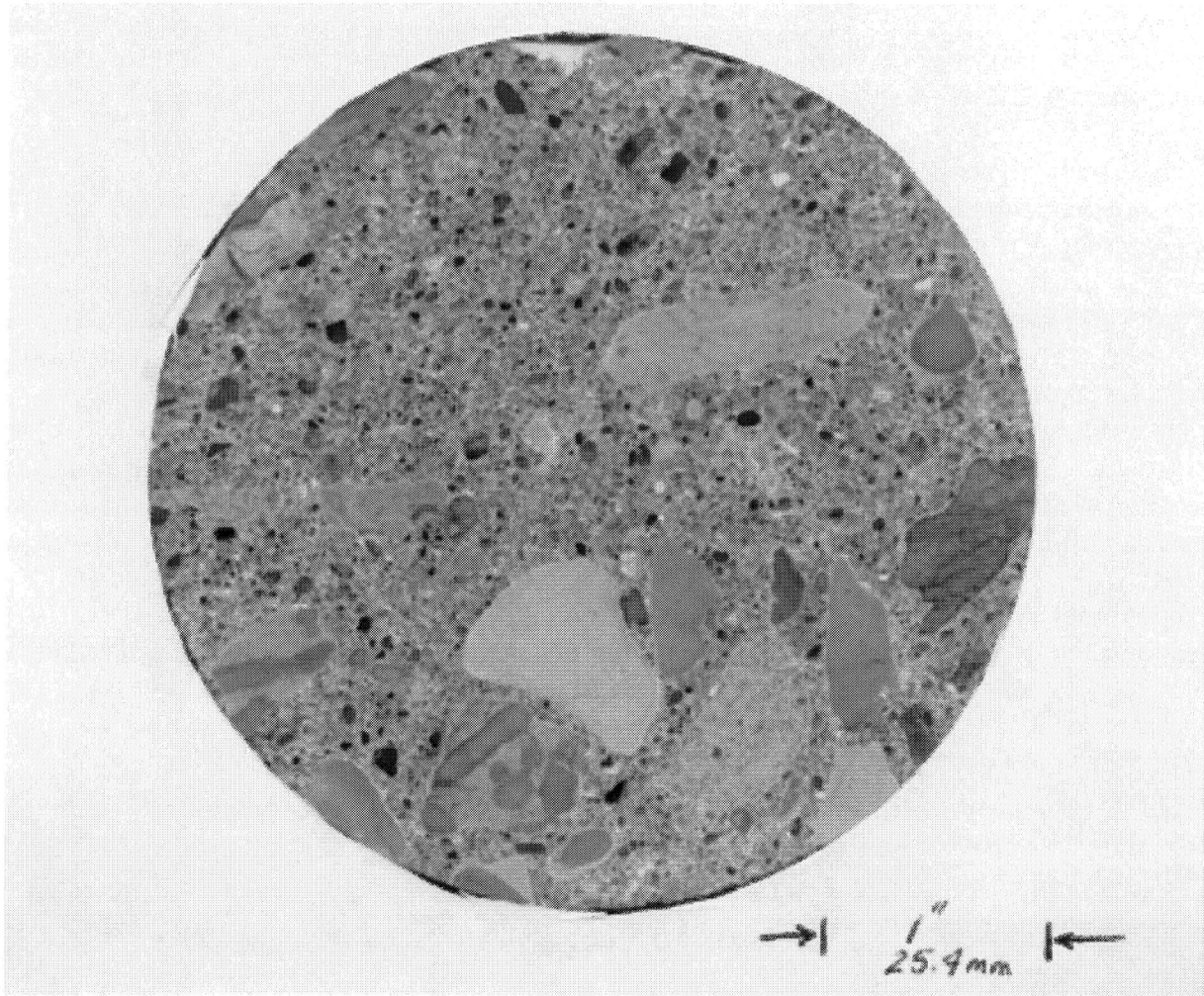


FIGURE 8 Illustration of segregation in a core extracted from I-80 in Iowa county.

Petrographic Examination

Cores from each site were subjected to a general petrographic examination. The examinations were conducted in a manner similar to that summarized in a previous research project (8); however, it is important to note that the current study used specimens obtained from longitudinal sectioning of the core specimens (refer to Figure 1). The previous study (8) produced very limited information about the top inch of the concrete pavement cores because the investigation was limited to horizontal sections taken from a depth of 25 millimeters (1 inch) below the top of the core. The purpose of this section is simply to tabulate the pertinent information (see Table 6). Detailed information for each site is given in Appendix D.

In general, the study indicated a few instances where the durability of the coarse aggregate could be questioned. Most notably sites 7 (Hwy 330), 8 (I-80 in Iowa county) and 17 (US 61) need some explanation.

Cores from site 7 had a gravel coarse aggregate. This was not consistent with the Iowa DOT documentation on the project (9). The gravel did contain several suspect particles that have exhibited cracking or staining in the cores. Since this coarse aggregate appears to be an anomaly (i.e., the coarse aggregate should have been a crushed carbonate stone) this site was not subjected to extensive study. The cores from site 8 were highly distressed and it was difficult to determine whether the coarse aggregate was part of the problem. Several individual particles appeared to contain some chert that was causing some cracking. However, this same aggregate (Conklin quarry) was also used in sites 15 and 16 and normally appeared to be sound in those two pavements. Site 17 was chosen as a good pavement site because it did not exhibit any evidence of surface cracking. However, the cores indicate that the pavement has become critically saturated at the base. This is causing the pavement to fail from the bottom up. Much of the failure appears to originate from the crushed dolomite aggregate. Cracking in the coarse aggregate and paste is very common in the bottom third of the pavement. Air voids near the bottom of the cores tend to be filled with ettringite. Air voids near the top of the pavement were not filled with ettringite. This suggests that drainage was poor. It is interesting to note that site 12 presently exhibits the early symptoms of distress very similar to those observed at site 17. In both instances, it is difficult to place blame only on the coarse aggregate when the actual deterioration mechanism is really related to the presence of excess water. For this same reason, this author disagrees with the conclusion proposed by Stutzman (10) that the deterioration at site 2 (US 20 in Hamilton County) can be partially attributed to the coarse aggregate particles. In the vast majority of cores extracted from the poor (and good!) sections of US 20, this author has seen little evidence of a consistent failure of the coarse aggregate particles. Rather, in its early stages, the deterioration is most prevalent in the mortar phase of the concrete and typically passes around aggregate particles. It seems much more likely that the aggregate has cracked because it has also become critically saturated due to the extensive cracking in the pavement. This would also be in better agreement with the field service record (based on many different projects) for this particular aggregate.

Many occurrences of reactive shale particles were noted in the fine aggregate fraction of the core specimens. The shale particles were observed in cores from pavements sites that exhibited both "good" and "bad" field performance. The shale particles were undergoing alkali silica reaction, but the distress associated with the particles was very limited and very rarely radiated from the fine aggregate particle. This is in good agreement with earlier studies (8, 10). Chert particles were also observed in the fine aggregate fraction of several cores. The chert

particles exhibited negligible distress in cores from sites 11 and 12. However, sites 3, 10, 15, and 16 all contain chert particles that had cracks. The chert particles in sites 15 and 16 typically exhibit active cracking due to alkali-silica reaction. The damage associated with the cracking was small and the percentage of chert in the fine aggregate was also small; however, the distress was not negligible in this instance because the cracks did occasionally propagate several millimeters into the cement paste.

TABLE 6 Summary of the Petrographic Examination of Cores Included in This Study

Site	Road	Mix Design	Aggregates	Voids	Cracking	Comments
1	US 20	C-3WR	Limestone coarse aggregate sound; sand sound except for shale	Many entrapped air voids, most smaller than 10 mm	None evident except in shale particles	Cores appeared to be sound and durable
2	US 20	C-3C	Limestone coarse aggregate sound; sand sound except for shale	Many entrapped air voids, some as large as 25 mm; many small voids filled	Major cracks subparallel to top of core; fine vertical (shrinkage) cracks in top 50 mm of cores	Segregation or gradation problems evident in most cores (gap graded?); fly ash present
3	US 169	C-3WR	Limestone coarse aggregate sound; sand sound except for shale and chert particles	Many entrapped air voids, some as large as 25 mm; many small voids filled	Major cracks subparallel to top of core; shale and chert particles are cracked	Only joints exhibit cracking; segregation is common in cores; many mortar-rich regions
4	Hwy 175	A-3-F	Limestone coarse aggregate sound; sand sound except for shale	Entrapped air voids common but generally smaller than 10 mm	None evident except in shale particles	Cores appeared to be sound and durable; fly ash present
5	Hwy 175	A-3-C	Limestone coarse aggregate sound; sand sound except for shale	Some small voids lined but not filled	None evident except in shale particles	Cores appeared to be sound and durable; fly ash present
6	Hwy 175	A-3	Limestone coarse aggregate sound; sand sound except for shale	Some voids lined; some small voids filled	None evident except in shale particles	Cores appeared to be sound and durable
7	Hwy 330	C-5WR	Gravel coarse aggregate exhibits some cracking due to ASR	Very coarse air void system	Random cracking often radiates from aggregate particles; some surface cracking noted	This was supposed to be a limestone coarse aggregate
8	I-80	C-3WR-C	Limestone coarse aggregate exhibits some cracking; sand exhibits some cracking	Entrapped air voids as large as 20 mm common; many small voids filled	Surface (shrinkage) cracks penetrate 10 to 20 mm; other cracks tend to be subparallel to the top of the core	Segregation is common in the core; fly ash present
9	I-80	C-4WR-C	Dolomite coarse aggregate sound; sand sound except for shale	Most entrain air voids were open; few entrapped voids	One surface crack penetrated to 8 mm; shale particles cracked	Cores generally looked good; fly ash present but looked less than in sites 10 and 11

10	I-80	C-4WR-C	Limestone coarse aggregate sound; sand sound except for shale and occasional chert	Entrapped air voids as large as 15 mm; many small air voids filled	Surface cracking noted (one crack penetrated 30 mm into core); major cracks were subparallel to top of the core; some shale and chert cracked	Segregation and/or poor gradation common in the cores; fly ash present
11	I-80	C-4WR-C	Limestone coarse aggregate sound; sand sound except for shale	Agglomerated, distorted entrained-air voids in some cores	One very fine surface crack (shrinkage) found in core from joint area; cracked shale	Cores looked OK; chert noted in sand but no cracking evident; fly ash present
12	I-80	C-4WR-C	Dolomite coarse aggregate mostly sound; sand particles sound (some chert observed)	Air void system looked OK—dispersed and very little filling (except at bottom of cores)	A few of the coarse aggregate particles were cracked in the lower half of the cores	Cores look sound except for infilling in the bottom third of the cores; fly ash present
13	Hwy 2	47-B Class V	Limestone coarse aggregate sound; sand contains some reactive particles	Few voids observed in cores; many small voids filled	Major cracks subparallel to top of core; surface cracks common, some penetrate to 40 mm; fine aggregate has some ASR cracking	Very strange gradation—all cores appear to be very mortar-rich; one section only contains three coarse aggregate particles!
14	Hwy 160	?	Mixed limestone and dolomite coarse aggregate sound; sand sound except for shale	Coarse entrained-air void system; many small voids filled	Surface crack (shrinkage) penetrates 11 mm into core; cracked shale particles	Segregation or gap-graded coarse aggregate evident in many cores
15	US 218	C-3WR	Limestone coarse aggregate sound; sand contains some reactive (chert) particles	Many entrapped air voids in top 75 mm of cores; many small voids filled	Fine surface cracks penetrate 5 to 10 mm into cores; some fine aggregate particles show active ASR cracking	No major cracking noted; consolidation problem noted; some coarse aggregate particles have gaps around them
16	US 218	C-3WR	Limestone coarse aggregate sound; sand contains some reactive (chert) particles	Coarse, agglomerated air voids; many small voids filled	Major surface crack penetrates 30 mm into one core; major cracks most often oriented subparallel to top of cores; however, some are random	Consolidation problem noted; chert particles often exhibit active ASR cracking
17	US 61	C-3WR	Dolomite coarse aggregate exhibits cracking at base of core; sand sound	Air void system looked OK—dispersed and very little filling (except at very bottom of cores where the voids were filled)	Major cracks subparallel to top of core; the cracks are near the bottom third of the core; many cracks intersect dolomite aggregate particles	Joints show more deterioration than the midpanel cores—this pavement is failing from the bottom up

Laboratory Study

The laboratory study was conducted to evaluate how different portland cements, class C fly ash, and a water-reducing admixture influenced premature stiffening and shrinkage characteristics of pastes and mortars. This was done to evaluate the potential for mix incompatibilities to cause field problems.

Bulk Materials

The results of the X-ray analysis of the cements and fly ash used in this study are given in Table 7. The estimates for the primary cement minerals (C_3S , C_2S , C_3A , and C_4AF) were calculated using the appropriate equations summarized in ASTM C 150 (3). Table 8 contains estimates for gypsum ($CaSO_4 \cdot 2H_2O$), bassanite ($CaSO_4 \cdot 0.5H_2O$), and anhydrite ($CaSO_4$) contents that were measured using quantitative X-ray diffraction, and estimates for gypsum and bassanite contents that were measured using a thermal analysis (DSC) technique. The anhydrite content of the fly ash was also measured using quantitative X-ray diffraction.

The cements exhibited a wide range of mineral compositions. This was especially true for the sulfate compounds present in the different samples. Thermal curves and X-ray diffractograms of the extreme cases noted in this project are illustrated in Figure 9. It is apparent that the major benefit of the X-ray method, when compared with the thermal analysis method, is that the mineral anhydrite can be quantified directly. This is important because anhydrite was a principal sulfate phase in three of the five cements that were used in this study. The thermal analysis technique can also be used estimate the anhydrite content of a cement; however, an assumption has to be made prior to performing the calculation. The assumption is based on the equivalence of the bulk SO_3 content (obtained via XRF and corrected for the theoretical alkali sulfate content) to the sum of the other principal sulfate phases (i.e., gypsum, bassanite, and anhydrite). Bassanite appeared to be the most common sulfate compound observed in this study. It is also interesting to note that gypsum was not present (or present in very small concentrations) in three out of the five cements. The gypsum contents determined by the two different techniques were not in good agreement; this was due to preferred orientation in the XRD determinations. Gypsum is notorious for preferred orientation, and it proved to be a difficult task to make the cement samples behave like the standards used in this study. Hence, the DSC measurements probably give a better estimate of the actual gypsum content of the various cement specimens.

The fly ash used in this project was typical for that which is normally produced at Council Bluffs generating station unit No. 3. The fly ash contained a high analytical calcium content and was very reactive with water. Slaking the fly ash with 30 percent water caused the paste mixture to stiffen and harden in approximately five minutes. Considerable heat was evolved during the setting and hardening process. This is consistent with other samples of fly ash obtained from this particular power plant (11). In addition to the anhydrite present in the fly ash, it also contained a small amount of tetra-calcium tri-aluminate sulfate (an expansive cement compound that is commonly found in shrinkage compensating cements). An X-ray diffractogram of the fly ash is given in Figure 10.

TABLE 7 Bulk Chemistry of the Cements and Fly Ash Used in This Study

	Holnam (mass %)	LaFarge (mass %)	Lehigh (mass %)	Kaiser (mass %)	Dixon Marquette (mass %)	Fly Ash (mass %)
Loss on ignition	0.92	1.57	1.01	1.14	1.50	0.3
Na ₂ O	0.12	0.11	0.06	0.16	0.08	1.5
MgO	3.37	2.96	3.57	1.38	4.12	7.3
Al ₂ O ₃	4.64	4.25	5.43	3.58	4.51	17.4
SiO ₂	21.08	20.59	21.38	21.17	19.70	31.4
P ₂ O ₅	0.29	0.10	0.03	0.24	0.05	0.8
SO ₃	2.85	2.55	3.00	2.55	3.72	4.0
K ₂ O	0.47	0.65	0.61	0.19	1.18	0.28
CaO	62.48	63.26	62.36	65.53	61.66	29.2
TiO ₂	0.21	0.19	0.20	0.29	0.20	1.4
Fe ₂ O ₃	3.05	3.26	2.34	3.86	3.03	6.1
SrO	0.03	0.04	0.03	0.10	0.06	0.43
Mn ₂ O ₃	0.10	0.53	0.06	0.06	0.06	Not measured
BaO	Not measured	Not measured	Not measured	Not measured	Not measured	0.74
Total	99.67	100.14	100.09	100.26	99.87	100.8
Calculated Compounds:						
C ₃ S	50.4	60.6	43.0	69.0	56.1	Not calculated
C ₂ S	22.4	13.3	28.8	8.6	14.2	Not calculated
C ₃ A	7.1	5.7	10.4	2.9	6.8	Not calculated
C ₄ AF	9.3	9.9	7.1	11.7	9.2	Not calculated

TABLE 8 Measured Sulfate Compounds in the Cements and Fly Ash Used in This Study

	Holnam (mass %)	LaFarge (mass %)	Lehigh (mass %)	Kaiser (mass %)	Dixon Marquette (mass %)	Fly Ash (mass %)
XRD method						
Gypsum	1.6	0.0	0.0	0.0	3.3	0.0
Bassanite	2.6	1.9	2.1	3.4	0.0	0.0
Anhydrite	0.0	1.6	2.8	0.0	2.2	5.2
Sum	4.2	3.5	4.9	3.4	5.5	5.2
Expressed as SO ₃	2.2	2.0	2.8	1.9	2.8	3.1
XRF SO ₃	2.85	2.55	3.00	2.55	3.72	4.0
DSC method						
Gypsum	1.0	0.1	0.1	0.1	2.2	Not measured
Bassanite	2.6	1.7	2.1	3.4	0.6	Not measured
Calculated Anhydrite	0.7	1.5	2.0	0.4	2.1	Not measured

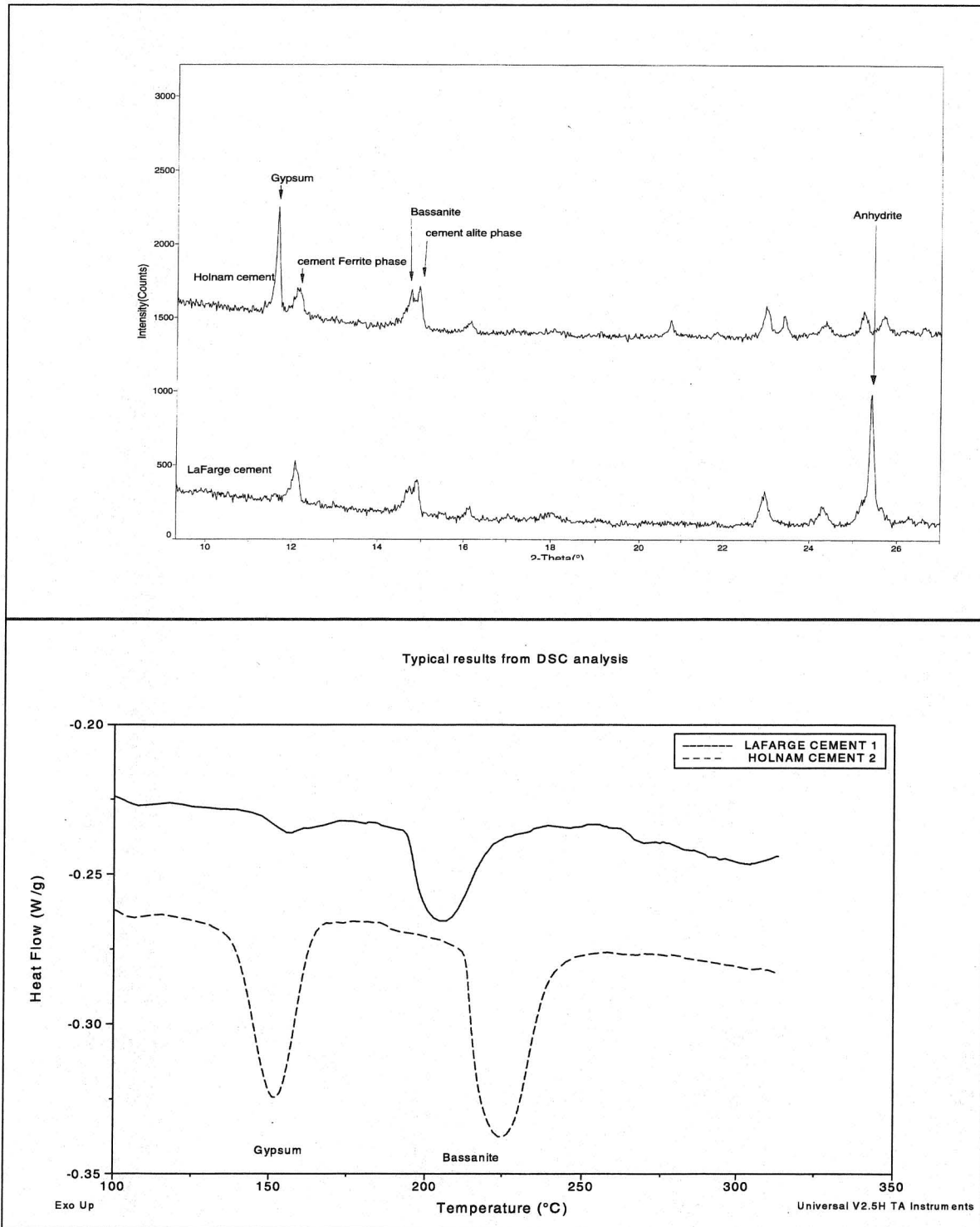


FIGURE 9 Examples from the XRD and DSC studies to quantify cement sulfate phases.

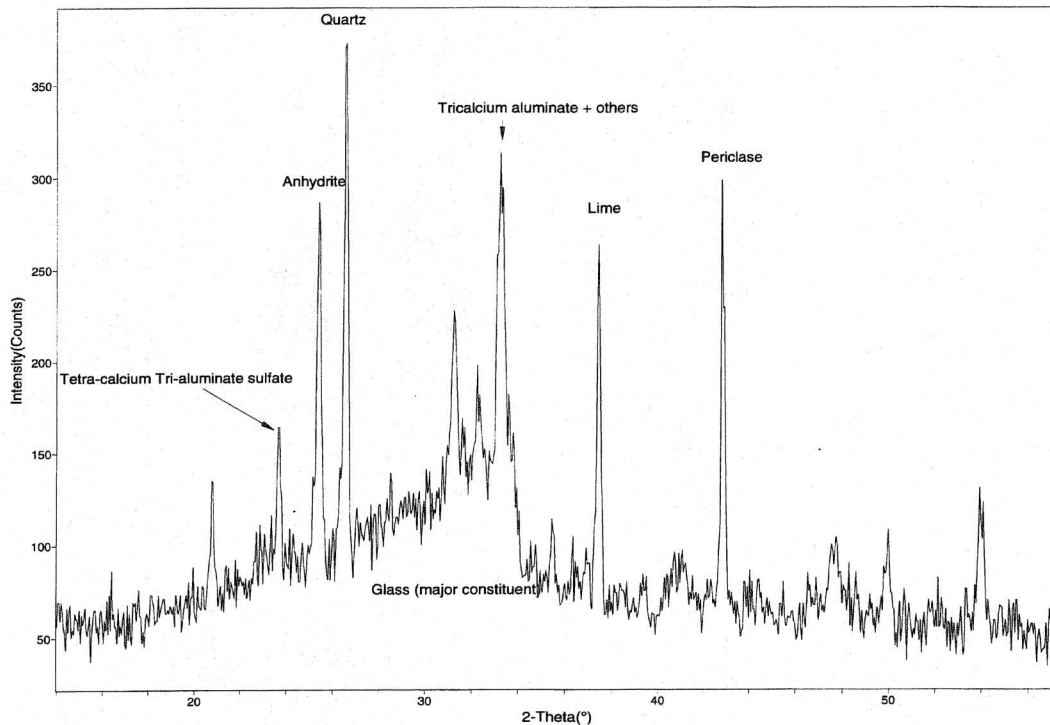


FIGURE 10 X-ray diffractogram of the fly ash sample used in this study.

Premature Stiffening Tests (Mortar Method)

Typical test results expected from this test method are illustrated in Figure 11. The top graph illustrates a mixture that exhibits neither false set nor flash set. This mixture remained plastic and exhibited a high penetration value for the duration of the test. The middle graph illustrates a mixture that exhibits false set. The penetration values decreased during the test; however, the remix cycle replenished the plasticity of the mixture (i.e., high penetration values after the remix, for the duration of the test). Note that the test procedure does not allow for the addition of water to the remix cycle. The bottom graph depicts a mixture that rapidly lost its plasticity and did not regain it during the remix cycle. This behavior is normally associated with quick set or flash set.

The results of the premature stiffening tests conducted on the five different cements are summarized in Table 9. This was done because all five of the cements produced very similar test results. All five of the cements exhibited severe premature stiffening. In fact, the results were so similar that it would have been difficult to distinguish between the various cements or the two different mixing procedures on any type of a graph. Since the mixes appeared to be rather dry at the specified water-cement ratio ($w/c = 0.30$), several different water contents were evaluated to see how that would influence the test results. In addition, the influence of fly ash and water reducer was also studied. Many of the tests were conducted using both the standard mix cycle and the modified mix cycle. This was done to evaluate the influence of mixing on the test results. Raw data are summarized in Appendix A.

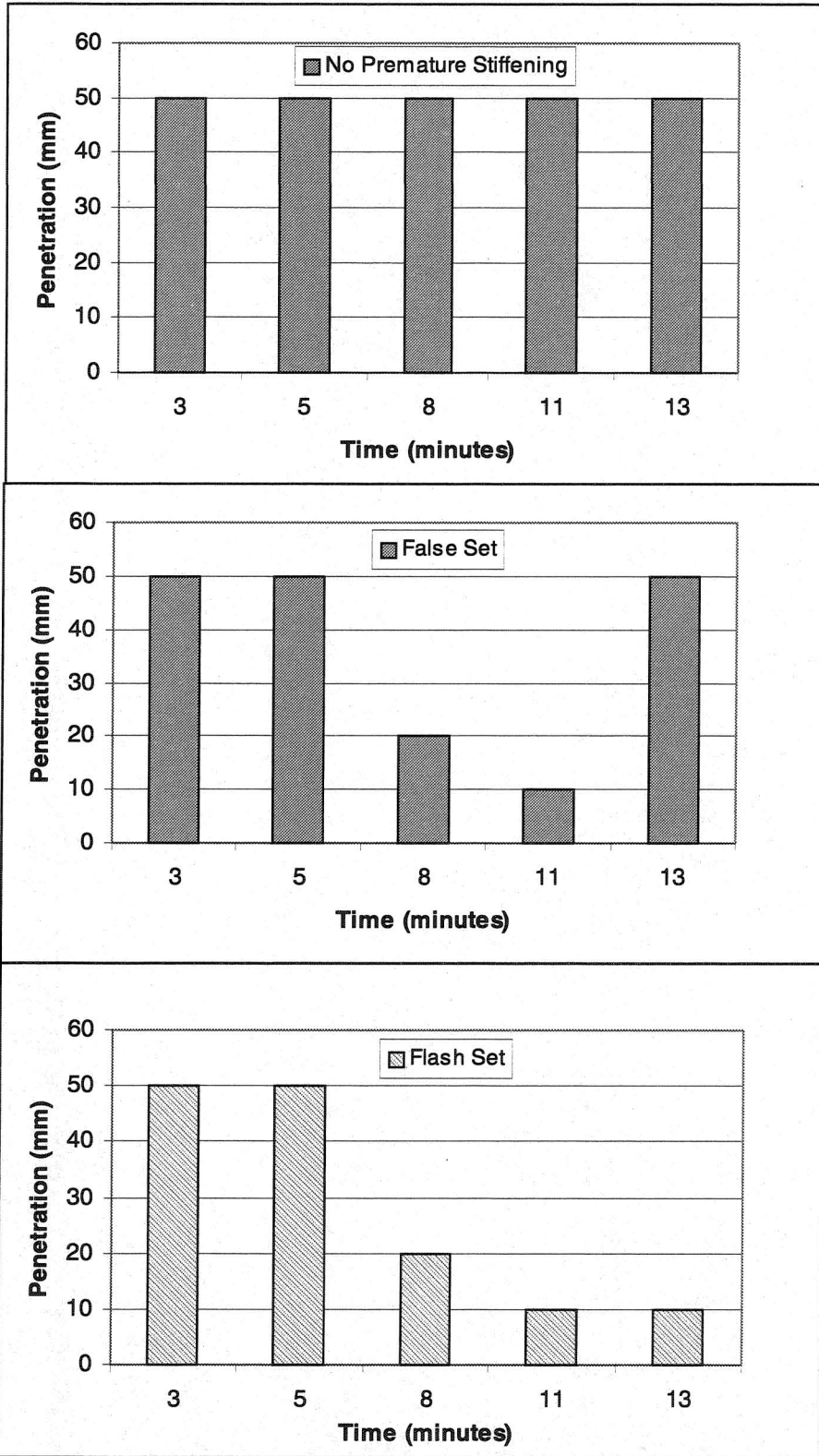


FIGURE 11 Illustration of mortars exhibiting false set and flash set.

TABLE 9 Summary of the Premature Stiffing Study for the Control Cements ($w/c = 0.30$)

Mix Cycle	Cement	Mix Temperature (°C)	Penetration				
			1 (mm)	2 (mm)	3 (mm)	4 (mm)	5 (After Remix Cycle) (mm)
Standard	Dixon Marquette	25.8	7	4	3	2	6
Standard	Holnam	24.7	3	2	1	1	50
Standard	Kaiser	22.6	4	1	1	1	50
Standard	LaFarge	22.9	50	4	2	1	50
Standard	Lehigh	25.8	5	2	2	1	15
Modified	Dixon Marquette	—	5	2	2	2	9
Modified	Holnam	—	24	2	1	1	50
Modified	Kaiser	—	4	1	1	1	50
Modified	LaFarge	—	50	4	1	1	50
Modified	Lehigh	—	9	3	3	15	49

From the information summarized in Table 9, three of the cements could be classified as false setting (LaFarge, Holnam, and Kaiser). One of the cements could be classified as quick setting (Dixon Marquette), and one of the cements (Lehigh) showed a mixed behavior since it regained its plasticity in one of the tests. These initial classifications will be re-evaluated after the presentation of the rest of the test results because it will become apparent that they are oversimplifications of a very complex phenomenon. The behavior becomes even more complex when admixtures are included in the mortars. The test results were in general agreement with those reported by other researchers (see the test data summarized in Appendix A). It is also important to note that the mortar temperatures for the Lehigh and Dixon Marquette mortars were outside the range dictated by the test method ($23 \pm 2^\circ\text{C}$). Both of the mortars reached 25.8°C , and this also suggests that rapid hydration (flash set) was occurring. Lehigh cement had the highest tricalcium aluminate content of the five cements in the study, while Dixon Marquette had a high alkali content and an intermediate tricalcium aluminate content. No attempt was made to reduce the temperature of the mortar because the study also included a series of mixes with higher water contents, which brought the mortar temperature into the appropriate range.

The influence of water content on premature stiffening was relatively consistent among the various samples of cement. Increasing the water content caused a small delay in the onset of premature stiffening. At a water-cement ratio of 0.33, or above, neither the Lehigh nor the Dixon Marquette cements exhibited any tendency for flash set. This was true for both of the mixing procedures that were used.

The different mix cycles also had an influence on the test results. Typically, the modified mix cycle aggravated the premature stiffing problems. This is best illustrated by the Kaiser cement (see Figure 12). This particular cement contained only bassanite ($\text{CaSO}_4 \cdot 0.5\text{H}_2\text{O}$) and it had a very low concentration of tricalcium aluminate (about 3 percent). Hence, it is a good example of a cement that is prone to false set. The cement exhibited similar behavior using either the standard or the modified test procedure. The mortar always regained its plasticity after the remix cycle. In fact, the Kaiser cement even exhibited premature stiffening when the standard C 109 mortar cube mixing procedure was used. This mix cycle consists of 90 seconds of mixing, 90 seconds of rest, and then an additional 60 seconds of mixing.

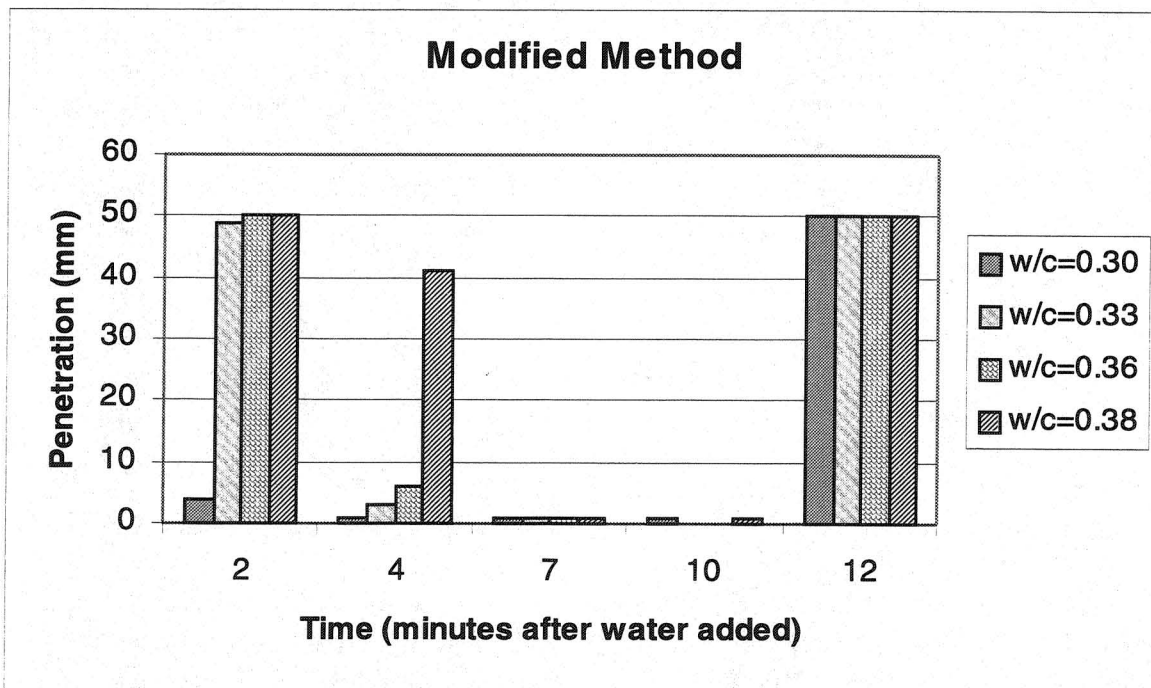
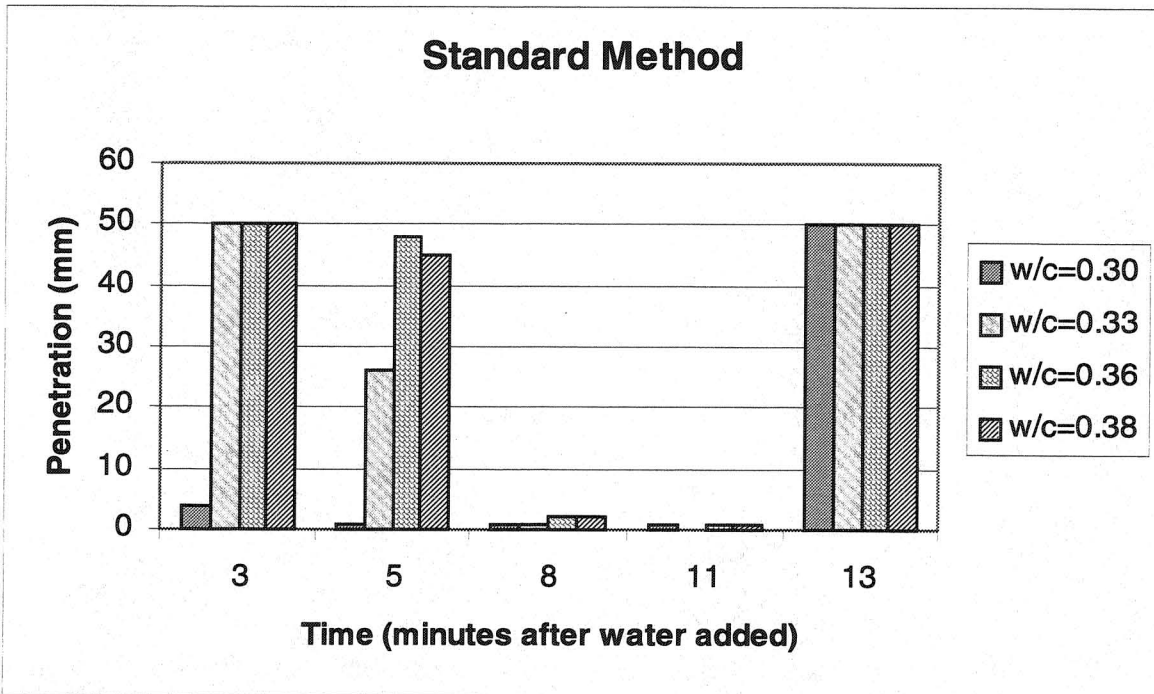


FIGURE 12 Influence of water-cement ratio on the premature stiffening tests.

In this study, most of the cements tended to exhibit premature stiffening approximately five minutes after the water was added to the cement (depending, of course, on the mixing cycle, the water-cement ratio, temperature, etc.). Hence, this suggests that the normal field mixing cycles (central batch mixer, dump trucks hauling to the paver) should aggravate this problematic behavior. No attempt was made to increase the duration of mixing past the onset of the premature stiffening (i.e., “mix through” the false set). This seemed redundant because the penetration values after the remix cycle always indicated that the mortar would regain its plasticity—it was simply a matter of remixing and time. Overall, there was a good correlation between the bassanite content of the portland cement and the false set characteristics of the mortar mixtures (see Figure 13). Again, the effects of water-cement ratio and mixing procedure on the test results are evident in the figure.

The use of fly ash and water reducer was also evaluated during this project. This tended to complicate the mix proportions because both admixtures reduce the amount of water needed to produce a mortar with a consistency equivalent to a control mortar (cement only). Hence, test mortars contained about 16 grams less water than the control mortars (i.e., about a 7 percent reduction in water content). This resulted in the proportioning the control mixes at a water-cement ratio of 0.36 and the test mixtures at a water-cement ratio of 0.33. These were considered equivalent mixtures based on mortar flow. The water-cement ratio of the control mixtures were increased from 0.30 to 0.36 because (1) at 0.30 they looked dry and harsh and were difficult to work with and (2) the minor influence of water-cement ratio on premature stiffening as was described above. At these water-cement ratios, both the control mortars and the test mortars were well mixed and easy to work with.

The fly ash used in this study typically had a minor influence on the premature stiffening properties of the five different cements. This was rather surprising due to the very high reactivity and high analytical calcium content of the fly ash. Extended observations were made of the mortar penetration and it tended to remain high (i.e., no premature stiffening) throughout the duration of the test. Some cements actually behaved better after the addition of 20 percent fly ash to the mortar.

The water reducer used in this study also appeared to have only a minor influence on the premature stiffening properties of the five different cements. Water reducer dosage was normally held constant at three ounces per 100 pounds of cement (i.e., three ounces per cwt). In some experiments, the dosage was increased to five and seven ounces per 100 pounds of cement. Typically, the mortars containing water reducer still exhibited false set behavior. Again, the modified mixing procedure tended to aggravate the premature stiffening problem.

The combined use of fly ash and water reducer tended to eliminate the premature stiffening problems in all of the mortars that were prepared using the standard mixing procedure. Premature stiffening was still evident in some of the mortars prepared using the modified mixing procedure. All of the instances of premature stiffening were classified as false set. The mortars containing the Kaiser cement behaved oddly during this testing regime. The odd behavior is illustrated in Figure 14. The mortar penetration data indicated that the mixes were experiencing premature stiffening again, approximately 10 to 20 minutes after the remix cycle (refer to the top panel of Figure 14). This behavior appeared to be associated with the water reducer dosage (see the bottom panel of Figure 14). The mortars were not subjected to a second remix cycle. This odd behavior does tend to indicate an admixture incompatibility. It also suggests that the observation period used in this study (about 30 minutes after the water was added to the mortar) may not have been long enough to catch all instances of this type of behavior. Future studies

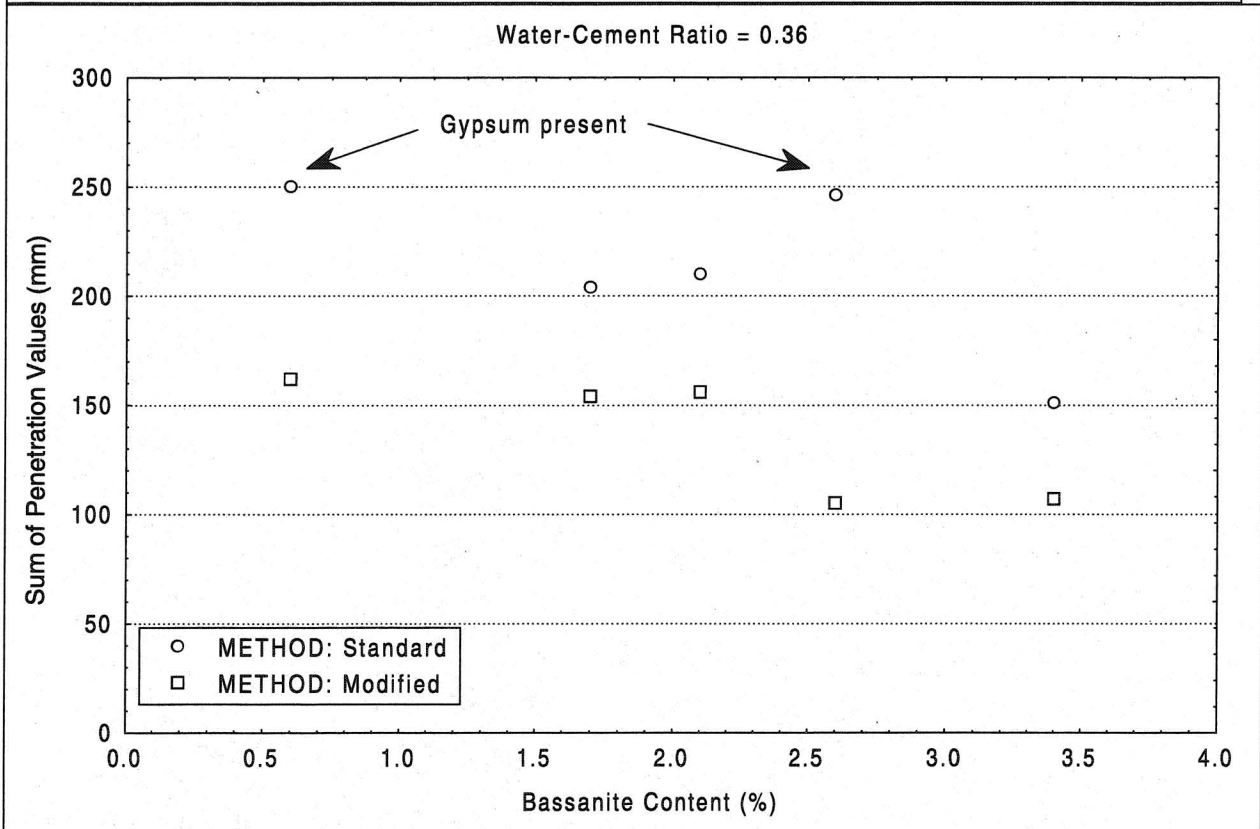
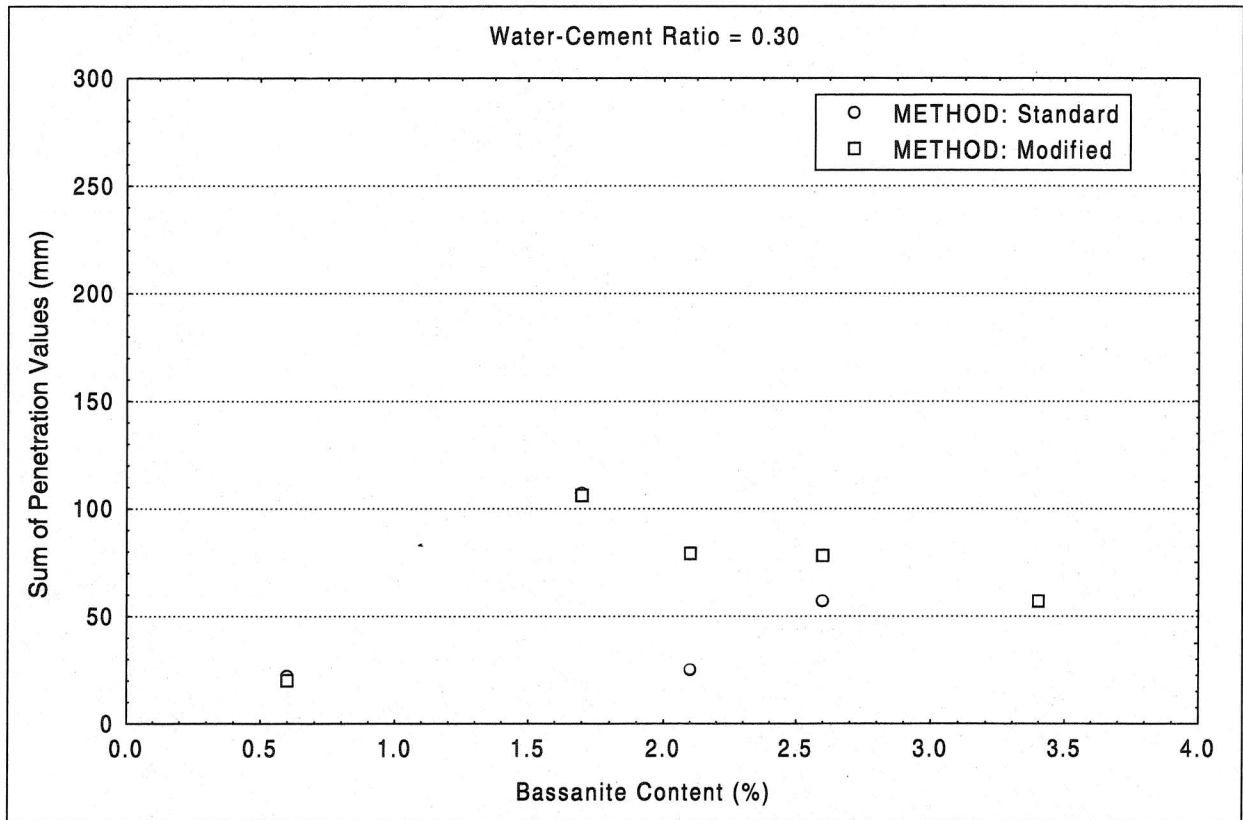


FIGURE 13 Relationship between premature stiffening and bassanite content.

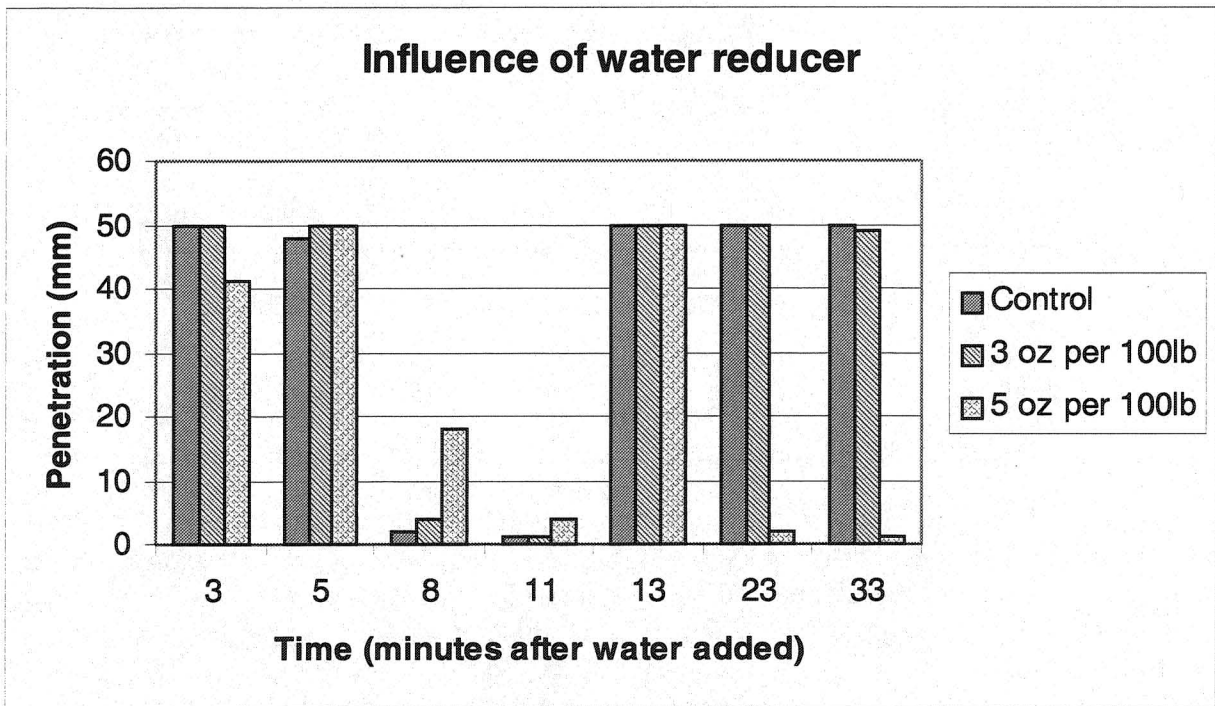
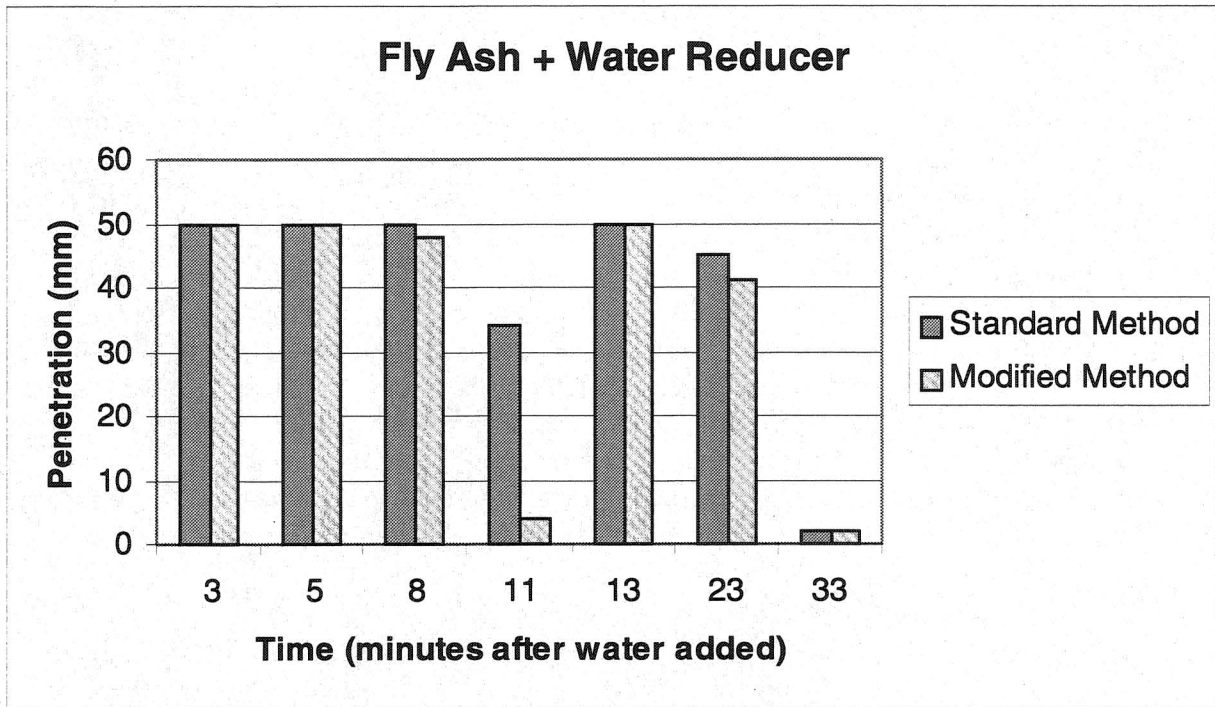


FIGURE 14 Abnormal behavior in the premature stiffening tests caused by admixtures.

should place more emphasis on fundamental aspects of this behavior because it suggests that the solubility of bassanite has been drastically reduced during the early stages of hydration (about the first 10 to 20 minutes).

In closing this section, it is important to return to the question of classifying the premature stiffening behavior of the five cements and the various admixture combinations used in this study. The classification is difficult because the categories are rather arbitrary and they depend on many different parameters (e.g., mix cycle, mix temperature, water-cement ratio, admixture dosage, etc.). Four of the five cements (Dixon Marquette, Lehigh, LaFarge, and Holnam) tended to exhibit false set characteristics in most of the experiments. The use of admixtures tended to modify the occurrence of false set and in some instances appeared to eliminate it. The remaining cement (Kaiser) exhibited a purely false set behavior when used in a control mortar. However, this cement exhibited anomalous behavior when combined with the water reducer and fly ash used in this study. The anomalous behavior appeared to be a repetition of the false set tendency of the original cement; however, it tended to be delayed (or retarded) by the water reducer. Further studies will be needed to shed more light on this odd behavior.

Restrained Shrinkage Tests (Paste Method)

The results of the restrained shrinkage tests are shown in Figure 15. The raw data are given in Appendix E. The rating scheme appropriate for this test has already been presented in Figure 2. A tabular summary of the test results for the control specimens is given in Table 10. Only the results for the control specimens were given in the table because it was not clear whether the rating scheme was appropriate for the cement pastes containing admixtures. The dosage rate for the water reducer was five ounces per 100 pounds of cement, and 20 percent fly ash was used to replace an equivalent mass of cement. None of the cements received a poor rating.

TABLE 10 Results of the Restrained Shrinkage Tests on the Control Cements

Cement	Time to Cracking (hr)	Rating
Holnam	5.5	Good
LaFarge	3.0	Questionable
Lehigh	2.7	Questionable
Kaiser	25	Excellent
Dixon Marquette	4.7	Good

When fly ash and water reducer were used, several of the tests produced only a rough estimate of the time to cracking. This was because they tended to crack after extended periods of time (i.e., odd hours outside the normal working day). Because the test relied on the presence of a technician to record the time to cracking, these particular tests failed to produce a single value. The time to cracking was roughly bracketed (see Figure 15; note the times for the Holnam and Kaiser cements). This was deemed adequate for the purpose of this study because these mixtures were consistent with “good” or “excellent” ratings. The purpose of the study was to determine which cement and admixture combinations produced “poor” or “questionable” ratings. This particular test method could be improved by implementing some type of automatic measurement strategy to remove the tedium of the long waiting periods. This would allow researchers more flexibility in designing formulations that have the potential to greatly increase the restrained cracking resistance of the paste mixtures.

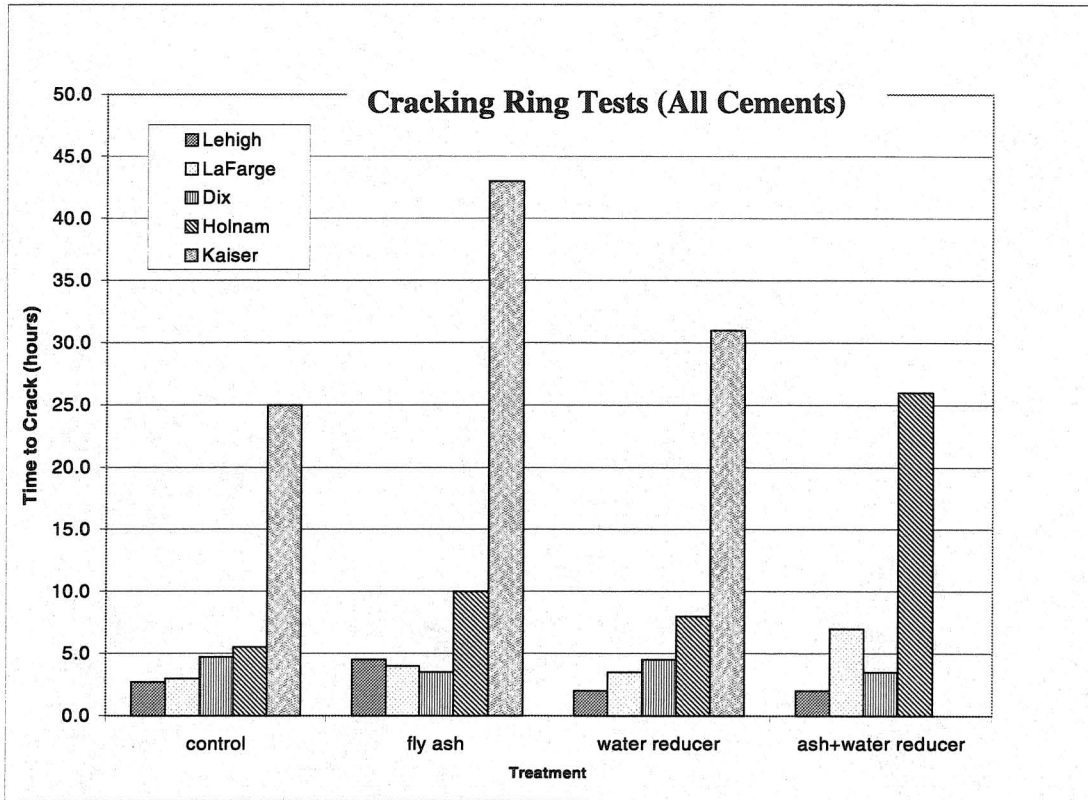


FIGURE 15 Results of the restrained shrinkage tests (cracking ring tests).

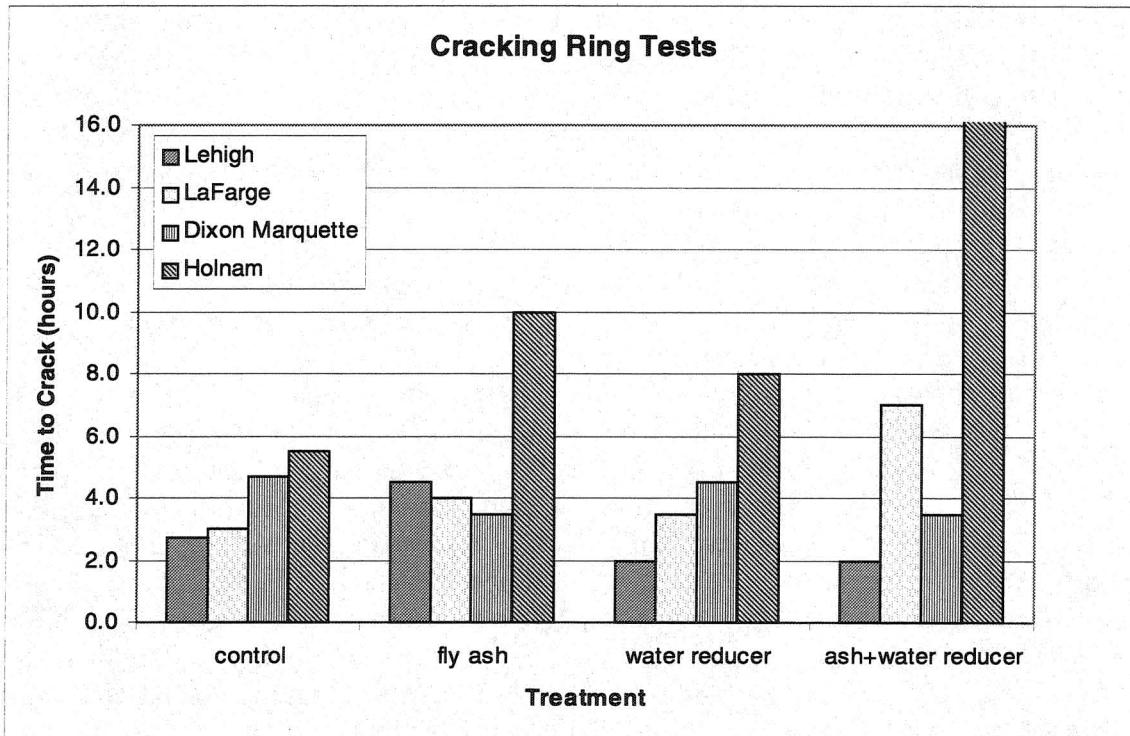


FIGURE 16 Expanded view of the restrained shrinkage tests (no Kaiser cement).

The largest variable in the test appeared to be the brand of cement that was used. The Kaiser cement exhibited exceptional behavior in this test. However, since it had a chemical composition similar to a type V cement (but was marketed as a type I-II), it will not be considered further in this discussion. The tests indicated that the use of the class C fly ash normally increased the time to cracking (refer to Figure 16). Only the Dixon Marquette cement exhibited a reduction in the time to cracking when used with 20 percent fly ash. Water reducer tended to have little influence on the time to cracking. Only the Holnam cement exhibited a significant benefit from the use of the water reducer. The other three cements (Lehigh, LaFarge, and Dixon Marquette) tended to show only small changes from the control specimens. The use of a combination of fly ash and water reducer increased the time to cracking for the mixtures containing Holnam and LaFarge cements. The remaining two cements, Lehigh and Dixon Marquette, exhibited slight reductions in the time to cracking.

Unrestrained Shrinkage Tests (Paste Method)

The results of the unrestrained shrinkage tests are shown in Figure 17. The raw data are given in Appendix E. The test results were considerably different than those obtained from the restrained shrinkage tests. The Kaiser cement still performed the best; however, it was only slightly better than the Lehigh and LaFarge cements. Holnam cement and Dixon Marquette cement performed the worst in this test. It is interesting to note that these last two cements, Holnam and Dixon Marquette, were the only cements that contained significant amounts of gypsum (i.e., greater than one percent by mass). In contrast, the restrained shrinkage tests indicated that Kaiser cement greatly outperformed the remaining cements (almost by an order of magnitude in some instances). This was followed by Dixon Marquette cement, then Holnam cement, then LaFarge cement, and finally the Lehigh cement. Hence, the two test methods only agreed on the fact that the Kaiser cement performed the best out of the five that were tested. The performance of the remaining cements almost appeared to be inversely categorized by the two different test methods.

Test specimens were also subjected to water curing to evaluate the expansion potential of the various cements (see Figure 18). Again, the Kaiser cement performed the best (i.e., least expansion during the test). It was followed by the Holnam and LaFarge cements, then the Lehigh cement, and finally the Dixon Marquette.

The use of 20 percent fly ash in a mixture reduced the unrestrained shrinkage for all of the cements that were included in this study (see Figure 17). This was in general agreement with the cracking ring study, where four out of five of the cements exhibited improved performance when fly ash was added to the mixture. Companion test specimens that were submerged in water, rather than allowed to dry in air, indicated that the fly ash had a mixed effect on the expansion of the test specimens (see Figure 18). Three of the mixes expanded slightly more than the control specimens (on the average, about 0.02 percent more expansion). Of the remaining mixes, one was too close to call, while the other mix exhibited a slight reduction in expansion (about 0.02 percent less than the control specimen). The overall effect was to reduce the extreme values in the data set (i.e., low values increased while high values decreased).

Only the Lehigh cement was used to make detailed evaluations of the influence of both fly ash plus water reducer on the unrestrained shrinkage. This was done because of a lack of materials needed to perform the testing on all of the different cements. Increasing the fly ash content tended to reduce the unrestrained shrinkage (see Figure 19). However, the mixtures appeared to be rather sensitive to the presence of water reducer. Figure 20 illustrates the

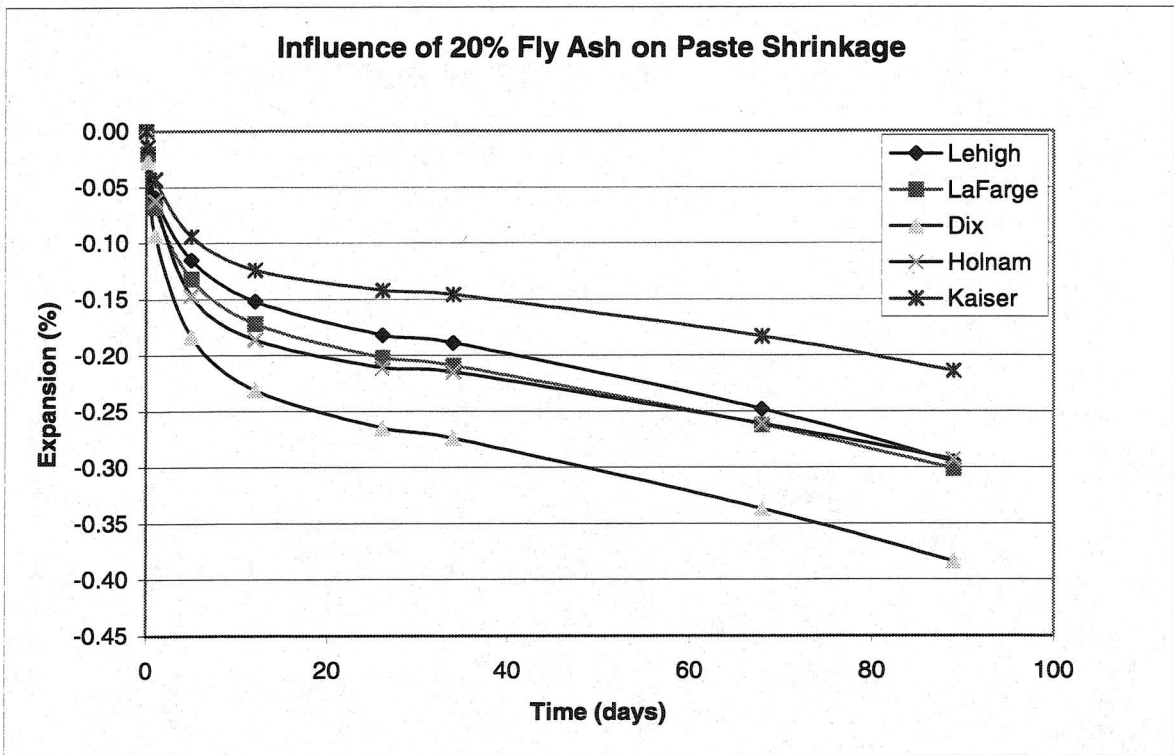
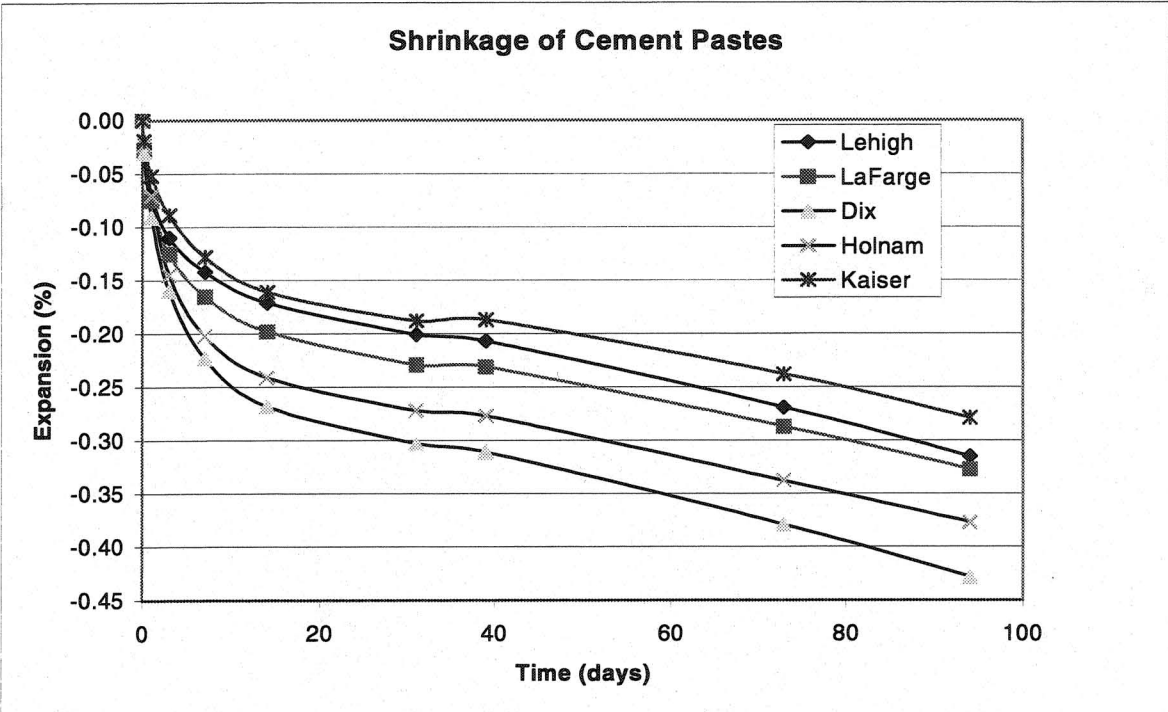


FIGURE 17 Unrestrained shrinkage during air curing for the various mixes.

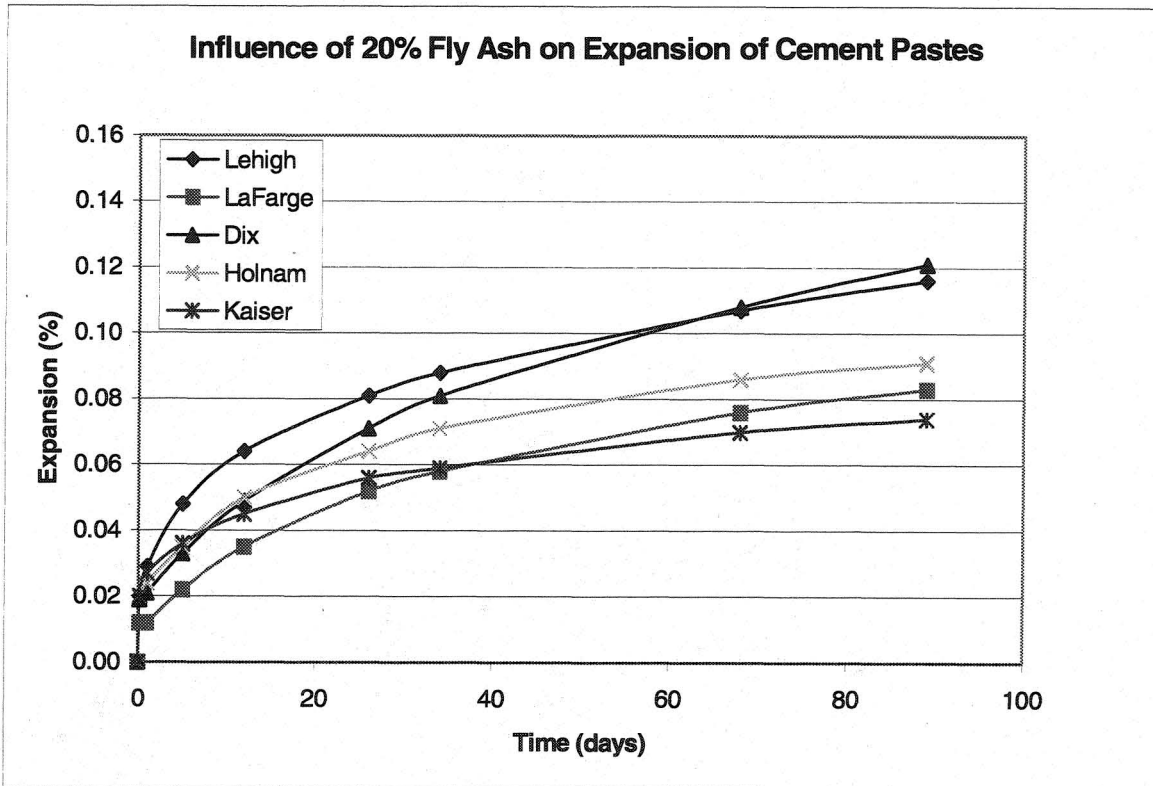
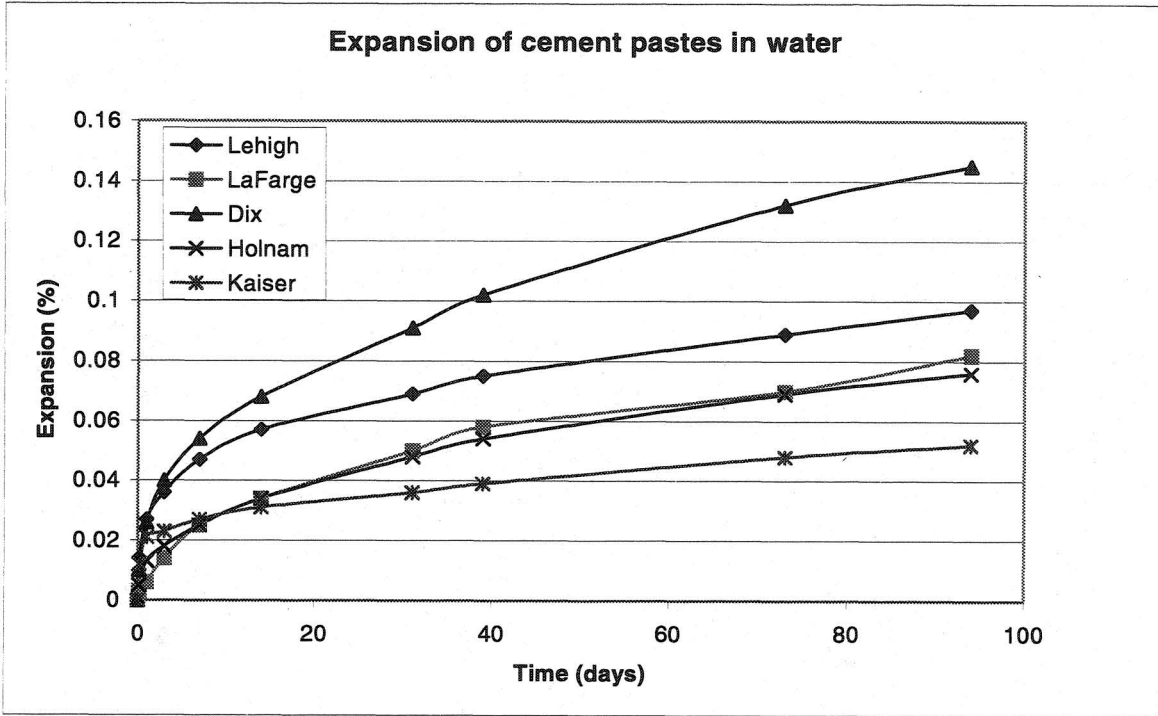


FIGURE 18 Unrestrained expansion during water curing for the various mixes.

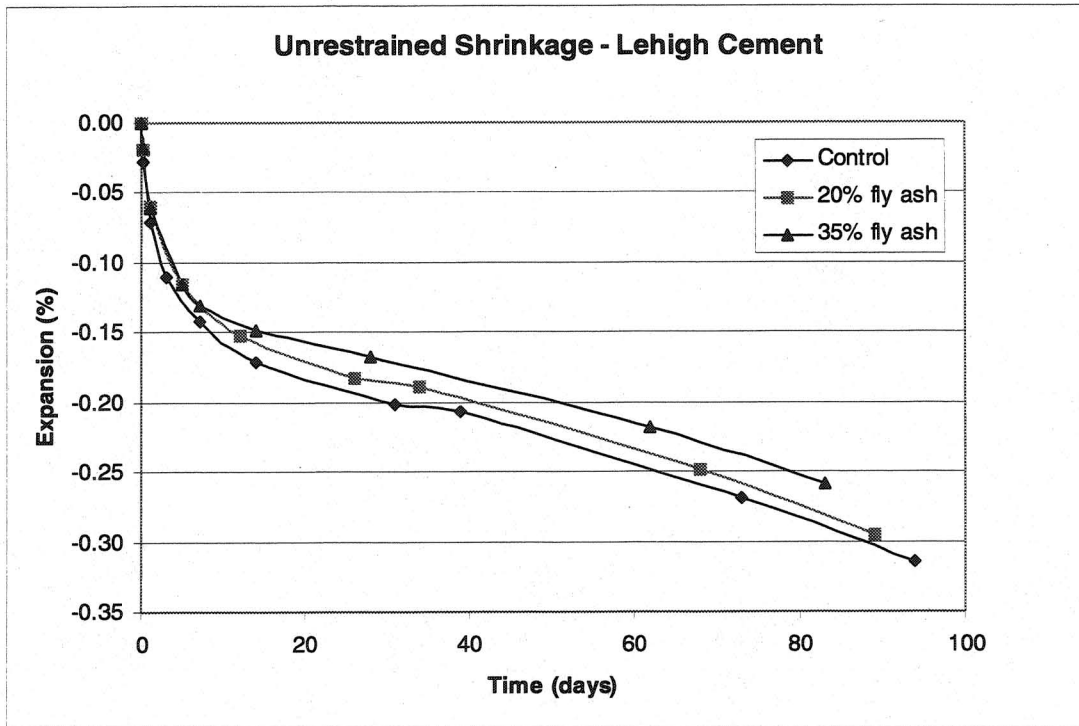


FIGURE 19 Influence of fly ash on the unrestrained shrinkage tests.

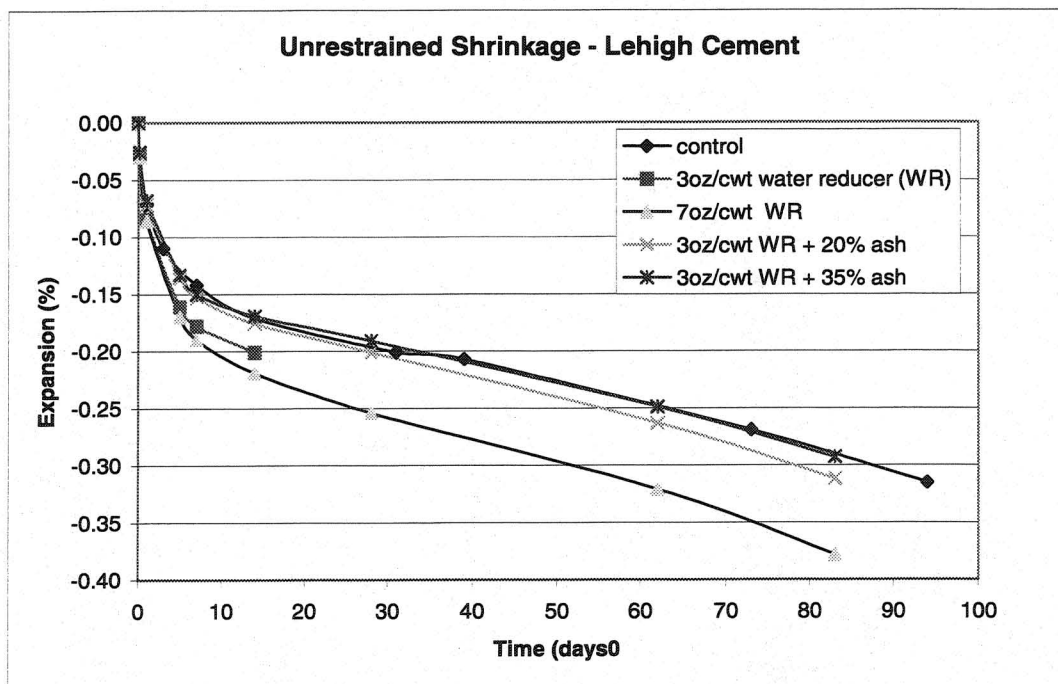


FIGURE 20 Influence of water reducer and fly ash on unrestrained shrinkage.

ASTM C 827 Mortar Tests

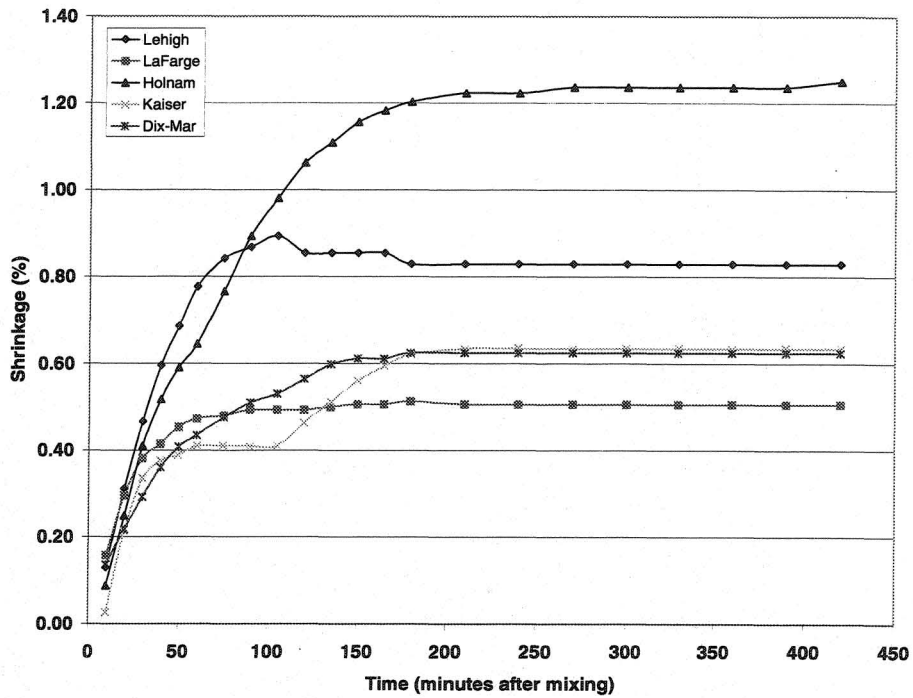


FIGURE 21 Results of the ASTM C 827 tests for the five control cements.

ASTM C 827 Tests

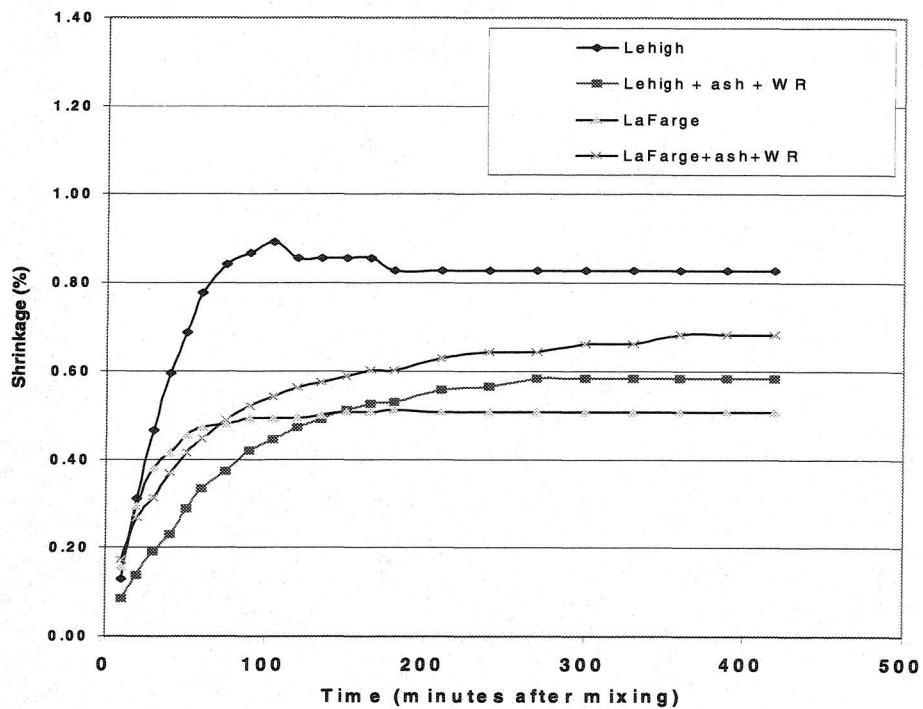


FIGURE 22 Influence of fly ash and water reducer on the ASTM C 827 tests.

influence of water reducer and water reducer plus fly ash on the unrestrained shrinkage of the paste specimens. It is evident that the unrestrained shrinkage was increased by the presence of water reducer. Increased dosage of water reducer tended to increase the early shrinkage. The beneficial influence of the fly ash was not evident when water reducer was incorporated into the mixtures.

Shrinkage During Setting and Hardening (Mortar Method)

The results of the ASTM C 827 tests are illustrated in Figure 21. The raw data are given in Appendix E. The experiments indicated that all five of the cements exhibited shrinkage during setting and hardening. The addition of fly ash and water reducer did cause some changes in the shrinkage versus time curves (see Figure 22); however, the changes were within the range of behaviors that were observed for the five control mortars. The total number of experiments was limited because of lack of sufficient materials. None of the experiments produced any significant evidence of expansive behavior during setting and hardening.

SUMMARY AND CONCLUSIONS

In summary, a detailed investigation has been conducted on core samples taken from seventeen portland cement concrete pavements located in Iowa. The goal of the investigation was to help to clarify the root cause of the premature deterioration problem that has become evident since the early 1990s. Laboratory experiments were also conducted to evaluate how cement composition, mixing time and admixtures could have influenced the occurrence of premature deterioration. However, the reader must be cautious when attempting to directly compare the lab results reported here with the field results from the study of pavement cores. This is because they only represent recent samples (circa 1997) taken from any of the cement plants. The actual cements that were used to construct the pavement sites being evaluated were manufactured almost 10 to 15 years prior to this investigation. Portland cement is like any other bulk commodity that is manufactured; as raw materials and environmental constraints change so does the finished product. The cements used in this study were selected in an attempt to cover the main compositional parameters pertinent to the construction industry in Iowa. For the purpose of this summary, the information from multiple pavement sites representing any given section of road will be presented together. This aids in comparing and contrasting differences between the individual sites.

1. US 20 in Webster and Hamilton Counties. The cores from US 20 in Webster County (site 1) exhibited no macroscopic evidence of premature deterioration. The petrographic analysis indicated some evidence of alkali-silica reaction (predominately shale in the fine aggregate); however, little distress was evident in the cores. Image analysis indicated that the hardened air content of the pavement was marginal to good.

The most probable explanation for the premature deterioration of US 20 in Hamilton County (site 2) is freeze-thaw damage. This explains the large cracks that were subparallel to the top surface of the concrete slab. Image analysis indicated that the hardened air content of the pavement was poor to marginal and that most of the small

air voids had been filled with ettringite. The premature deterioration was most probably enhanced by excessive drying shrinkage in the top surface of the concrete slab, which increased the permeability of the top surface of the pavement. The increased permeability allowed the slab to become critically saturated. The pavement also shows some evidence of alkali-silica reaction (predominately shale in the fine aggregate with an occasional chert particle). The damage caused by ASR (i.e., cracking from the aggregate extending through the cement paste) was minimal.

2. US 169 in Webster County. The most probable explanation for the premature deterioration of US 169 (site 3) is freeze-thaw damage. This explains the large cracks that were sub-parallel to the top surface of the concrete slab. Image analysis indicated that the hardened air content of the pavement varied from poor to excellent, and that many of the small air voids were in the process of being filled with ettringite. Segregation was common in all the cores and some areas tended to be mortar-rich. The pavement also shows some evidence of alkali-silica reaction (predominately shale but also small amounts of chert were noted in the fine aggregate). The damage caused by ASR (i.e., cracking from the aggregate extending through the cement paste) was minimal.
3. Iowa Highway 175 in Hamilton County. This pavement continues to perform well and exhibits only minimal evidence of deterioration (sites 4, 5, and 6). One of the six cores that were examined during this study did have very slight cracking at the base of the pavement slab near the joint region (site 6). It was not clear if the cracking was due to base saturation. In addition, many of the cores indicated that coarse aggregate particles had become exposed on the top surface (wearing surface) of the pavement; however, this is probably not uncommon for a pavement that is almost 20 years old. Image analysis indicated that the entrained-air content of the pavement ranged from marginal to excellent. However, the mortar air contents of the top three inches of cores from the three sites were all classified as good to excellent. The pavement shows some evidence of alkali-silica reaction (predominately shale in the fine aggregate). The damage caused by ASR (i.e., cracking from the aggregate extending through the cement paste) was minimal.
4. Iowa Highway 330 in Marshall County. This pavement site exhibited an anomalous aggregate type. The site was chosen because it was supposed to contain a crushed limestone aggregate. However, the site contained a gravel aggregate. Hence, no detailed studies were conducted on the cores. Image analysis indicated that the pavement had a marginal hardened air content. Petrographic analysis indicated that several different types of gravel particles (coarse aggregate fraction) exhibited active ASR cracking.
5. I-80 in Iowa County. This pavement (site 8) exhibited extensive cracking that was attributed to shrinkage and freeze-thaw attack. In addition, one of the cores had slight cracking near its bottom that may indicate saturation at the base of the pavement. Image analysis indicated that the hardened air content of the pavement slab was typically marginal to poor, especially in the top third of the core. However, one of the

lower sections from the midpanel region received an excellent rating. Segregation was common in the cores and mortar-rich regions often were observed in the top half of the cores. It was common to observe large entrapped air voids (diameter = 20 millimeters [0.8 inches]) in the top third of these cores. Cracks, mostly oriented sub-parallel to the top of the pavement core, often intersected the entrapped voids. Concerns were also raised about the coarse and fine aggregates used at this site. However, most of the cracking patterns were inconsistent with those normally caused by alkali-aggregate reaction.

6. I-80 in Dallas County. This was an interesting stretch of pavement because it encompassed three adjacent sites (sites 9, 10, and 11) that exhibited different levels of distress. Macroscopic surface cracking was observed only in the cores extracted from the joint region at site 10. However, very fine surface cracking was also observed in cores extracted from the joint region of sites 9 and 11. The very fine surface cracks required a microscope and surface wetting to enhance the features for easy viewing.

Site 9 had little distress other than a considerable amount of cracked shale particles in the fine aggregate fraction. Although this is indicative of an ASR-sensitive material, the cores and the pavement exhibited very little evidence of distress. Surface cracking was nearly absent at this site. Image analysis indicated that the hardened air content of the pavement was marginal to good. The coarse aggregate in this site consisted of Shaffton dolomite. This particular coarse-grained dolomite is rather insensitive to low entrained-air contents.

Site 10 exhibited extensive cracking at the transverse joints. Surface cracks were present in approximately the top 25 millimeters (1 inch) of the cores taken from the pavement joints. Internal distress consisted of cracks sub-parallel to the top of the core. Hence, site 10 was most probably deteriorating because of freeze-thaw attack. Image analysis indicated that the hardened air content varied from poor to excellent. Petrographic analysis indicated the fine aggregate contained shale and chert particles. The shale particles were common and were causing pop outs on the surface of the core specimens. Also, staining was noted near some of the coarse aggregate particles in the top third of the pavement cores. However, little internal distress appeared to be associated with any of these different aggregates. Entrapped air voids as large as 30 millimeters (1.25 inches) were observed on the surface of the core.

Site 11 exhibited little evidence of deterioration. Some of the coarse aggregate particles in the top third of the core did exhibit slight staining; however, no internal distress was evident. Image analysis indicated that the hardened air content of the pavement slab was poor to marginal; however, the air voids were typically of very small diameters (i.e., high specific surface) which caused the apparent spacing factor to fall below the 0.2-millimeter (0.008 inch) level. This may help to explain the lack of deterioration noted at this site. The only other significant differences between this site and site 10 were that different sources of cement were used and that different contractors performed the paving operations.

7. I-80 in Cass County. This pavement (site 12) had no evidence of premature deterioration. The only sign of distress exhibited by cores extracted from the pavement was very fine cracking at the base of each core. The cracking was always limited to the bottom 12 millimeters (0.5 inches) of the core. The significance of this feature is not evident; however, it may suggest that the base of the pavement is in the process of becoming saturated. Image analysis indicated that the hardened air content of the pavement slab was excellent and was uniform from top to bottom.
8. Iowa Highway 2 in Fremont county. This pavement (site 13) exhibited pattern cracking near the joint regions. The cracks penetrated about 25 millimeters (1 inch) below the surface of the core specimens. The cracks appeared to be due to shrinkage because they rarely intercepted aggregate particles. Pop outs were noted on the surface of a core specimen and this suggests the presence of an alkali sensitive aggregate. However, few aggregate particles appeared to be producing significant cracking in the pavement cores. Instead, the major internal cracks tended to orient themselves sub-parallel to the top surface of the pavement slab. The mix proportions used in the concrete mix design were strongly weighted to the fine aggregate fraction and this would have increased the potential for shrinkage cracking. Image analysis indicated that the hardened air content of the pavement slab was poor to marginal.
9. Iowa Highway 160 in Polk County. Site 14 exhibited cracking and broken edges that were most noticeable at the pavement joints. Cores extracted from the pavement did not show much distress. Surface cracking was slight and was observed in cores extracted from the midpanel of the pavement slab. Shale particles were producing pop outs on the surface of the cores; and hence, the sand fraction did contain some alkali-reactive particles. The shale particles did not appear to be producing significant cracking in the cores. Image analysis indicated that the hardened air content of the cores was uniformly poor. In fact, this particular pavement had an average mortar air content of less than 2.5 percent. This suggests that the air-entrainment admixture dosage was incorrect or the mixing cycle was too brief to create an adequate amount of air bubbles. Also, the grading of the coarse aggregate was questionable because it appeared to be gap graded.
10. US 218 in Johnson County. Sites 15 and 16 exhibited similar cracking patterns. However, the distress was considerably more developed at site 16. The basic cracking pattern consisted of longitudinal cracking that traversed the whole pavement panel. Vibrator trails were readily observed on many of the panels. Segregation problems and surface cracking were also noted in cores extracted from both sites. Cores from site 15 exhibited little internal cracking. Cores from site 16 exhibited significant internal cracking that was often associated with the surface cracking (branching); however, sometimes cracks having random or sub-parallel orientations were also observed. Shale and chert particles were producing pop outs on the surface of some cores; and hence, the sand fraction did contain some alkali-reactive particles. The shale particles did not appear to be producing significant internal cracking in the cores. The chert particles produced localized distress via cracking due to ASR; however, very few chert particles were observed in the cores (typically only a few per

core). Image analysis indicated that site 15 had a poor to marginal entrained-air void system, and that site 16 had a marginal to adequate entrained-air void system. The air voids at both sites were often filled with ettringite. This suggests that water has penetrated deeply into the pavement slabs. These two sites appeared to have many problems in common, which included construction-related deficiencies, poor entrained-air void systems and alkali-reactive particles in the fine aggregate.

11. US 61 in Scott County (site 17). This pavement exhibits no surface cracking but the base of the joints show extensive damage. Image analysis indicated that the entrained-air void system ranged from marginal to good; however, the marginal value occurred at the base of the pavement slab near the transverse joints. The low entrained-air value was associated with extensive ettringite deposits in the air voids. Hence, this pavement is failing from the bottom up. Core extraction was good to about 150 millimeters (6 inches) but poor from the bottom of most holes (i.e., bottom was rubble). The damage appears to be related to critical saturation and freeze-thaw attack. However, many of the coarse aggregate particles (dolomite) also exhibit cracking and rim formation in the bottom 50 to 75 millimeters (2 to 3 inches) of the pavement slab. This pavement is a good example of how service life can be incorrectly assigned when it is only based on surface observations. Better estimates of service life could be assigned if the assessments were based on both surface observations and petrographic examination of cores from the pavement. Improved drainage could have probably eliminated this problem.
12. The hardened air content determinations conducted during this study indicated that the pavements that exhibited premature deterioration often contained poor to marginal entrained-air void systems. Only one out of the nine pavements that exhibited premature deterioration had an average mortar air content greater than six percent (this corresponds to a concrete air content of about 3.8 percent). In contrast, only one out of the eight pavements that performed adequately had an average mortar air content of *less* than six percent. In addition, petrographic studies indicated that sometimes the entrained-air void system had been marginal after mixing and placement of the pavement slab, while in other instances a marginal to adequate entrained-air void system had been filled with ettringite. In either case, the results of this study suggest that the durability, more specifically the frost resistance, of the concrete pavements should be less than anticipated during the design stage of the pavements.
13. Laboratory studies indicated that all five of the cements used in this study were prone to premature stiffening problems. The problematic behavior was greatly exaggerated by reducing the water-cement ratio or decreasing the mixing cycle. In mortar mixes with plastic consistencies, the premature stiffening was most commonly classified as false set. However, these tests tended to be very sensitive to the water content of the mixture and sometimes produced inconsistent results when the water-cement ratio was held at the specified value of 0.30. The bassanite ($\text{CaSO}_4 \cdot 0.5\text{H}_2\text{O}$) content of the cements was strongly correlated to the results of the premature stiffening tests. The

fly ash and water reducer used in this study appeared to have only a minor influence on the results of the premature stiffening tests.

14. The restrained shrinkage tests indicated that two of the three portland cements commonly used in Iowa, tended to be sensitive to early shrinkage cracking. Again, the use of fly ash and/or water reducer tended to have little influence or a positive influence on the test results.
15. The unrestrained shrinkage tests produced results that were considerably different from the restrained shrinkage tests. The cement control specimens failed to produce the same performance rankings as were indicated in the restrained shrinkage tests. Companion specimens cured in water exhibited expansion that varied considerably among the five different cements. Typically, the use of fly ash tended to decrease the unrestrained shrinkage but also tended to increase the expansion in water of the various test specimens. This behavior is consistent with the observation of periclase in the fly ash. A limited number of tests were conducted that indicated that the use of water reducer tended to increase the early drying shrinkage of one of the cements that was prone to early shrinkage cracking.
16. The ASTM C 827 tests indicated that mortars containing the various cements exhibited shrinkage during setting and hardening. The magnitude of the shrinkage varied considerably with the five different brands of cement. A limited number of tests incorporating admixtures were conducted using the two cements that were identified as being prone to restrained shrinkage cracking. These tests produced results that were within the range of results obtained from the control mortars. Hence, it was tentatively concluded that mortars containing admixtures generally followed the same shrinkage tendencies exhibited by the control mortars during setting and hardening. The use of admixtures did significantly extend the mortar setting times relative to the control mortars.

Closing Comments

In closing, it seems important to give a summation of how the laboratory work may help to explain the deterioration noted in the pavement cores. Several features were consistently observed in many of the core specimens. These features included (1) large entrapped-air voids; (2) segregation; (3) surface cracking; (4) entrained-air voids filled with ettringite; (5) cracked fine aggregate particles (overwhelmingly attributed to shale particles); and (6) macrocracks and microcracks often oriented subparallel to the top surface of the core.

Features 1 and 2 suggest plastic concrete (workability) problems in the field. Problems of this type were easily predictable from the laboratory phase of this study. The problem was diagnosed as severe false set and this type of problem was primarily related to the cement used on any given project. However, as was shown in the laboratory phase of this study, water-cement ratio, temperature and admixtures sometimes can also play significant roles. Test methods (both physical and quick chemical techniques) are now available that can help to identify this problem. It is important to note that cores extracted from eight out of the 17 pavements in this study, exhibited moderate to severe segregation. All eight of the sites that exhibited segregation were

also on the list of pavements that exhibited premature deterioration. Field experience has indicated that excessive vibration is normally used to place concrete of low (and rapidly decreasing) slump. Excessive vibration causes segregation, and it also has the potential to destroy the entrained-air void system of the concrete.

Surface cracks, filled air voids, and macroscopic cracks subparallel to the top of the pavement cores (i.e., features 3, 4, and 6) were often observed in unison. The surface cracks often appeared to be caused by shrinkage. Again, this is in good agreement with the results of the laboratory study, which indicated that some of the cements were sensitive to shrinkage and restrained-shrinkage cracking. Typically, cements that exhibited early cracking in the restrained shrinkage tests were used on the majority of pavements that exhibited premature deterioration. It is important for the reader to employ great caution when interpreting this observation because the selection of sites for this study had no rigorous statistical design. Hence, there is no definitive way of testing the relationship between laboratory cracking and field cracking to see whether they are interrelated or whether they occurred by pure chance. The filled voids and subparallel cracks were often the primary features evident in the pavements that exhibited premature deterioration. These features suggest a permeability problem. This is odd because the mix designs used for Iowa pavements should be very impermeable. This is due to the high cement content and low water-cement ratio that are commonly used in the mixes. Hence, the surface cracking appears to play a significant role in this mode of deterioration because it allows water to penetrate into the pavement. Eventually the pavement reaches critical saturation and freeze-thaw attack begins. The selection of this mode of deterioration over the distress caused by alkali-silica reaction (feature 5) was mostly dictated by the size and frequency of the subparallel cracks when compared to the number of active cracks caused by ASR. In addition, many of the sites exhibited entrained-air void systems that were marginal to poor. The cracked shale particles were common in most of the pavement sites (i.e., both "good" and "bad" sites) and they rarely produced evidence of active ASR cracking. This is not meant to downplay the significance of alkali-silica reaction in Iowa pavements. This research project noted a few instances where aggregate related problems, notably chert particles in the fine aggregate, contributed to the distress observed in the pavement. However, the point of this argument is that the shrinkage cracking certainly enhances the potential for both ASR and freeze-thaw attack because it allows water to quickly penetrate into the pavement slab. Water plays such an important role in the deterioration process that all efforts should be made to minimize surface cracking. This was the crux of the hypothesis set forth by Marks, Schlorholtz, and Gress, which attempted to explain the premature deterioration problem (this hypothesis was never published but it has been reproduced in Appendix F).

Other authors have also published models that describe the importance of early cracking in the deterioration of portland cement concrete structures (12, 13). Diagrams depicting the important features of these particular models are shown in Figures 23 and 24.

The model depicted in Figure 23 was meant to explain the damage associated with ASR. However, this same model would apply to freeze-thaw damage if one would allow (1) water to flow down through the surface cracks and (2) the concrete to be exposed to cyclical freezing and thawing (better known as winter and spring in Iowa). When the concrete reaches critical saturation, freeze-thaw attack would cause the interior of the slab to expand (as depicted in the figure). In fact, several of the observations of internal cracking documented by Stutzman (10) and also observed during this study, indicated significant branching of the surface cracks as they penetrated into the concrete cores (e.g., see Figures 32 and 43 from [10]). This observation,

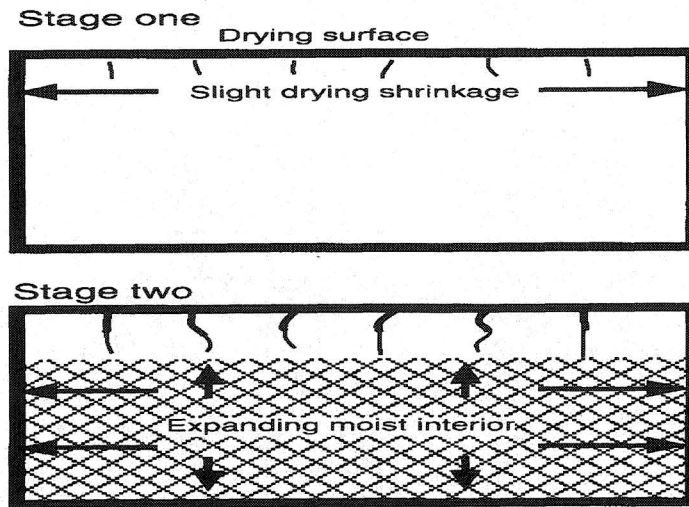


Figure 23 Model for concrete deterioration (adapted from Farny and Kosmatka [12]).

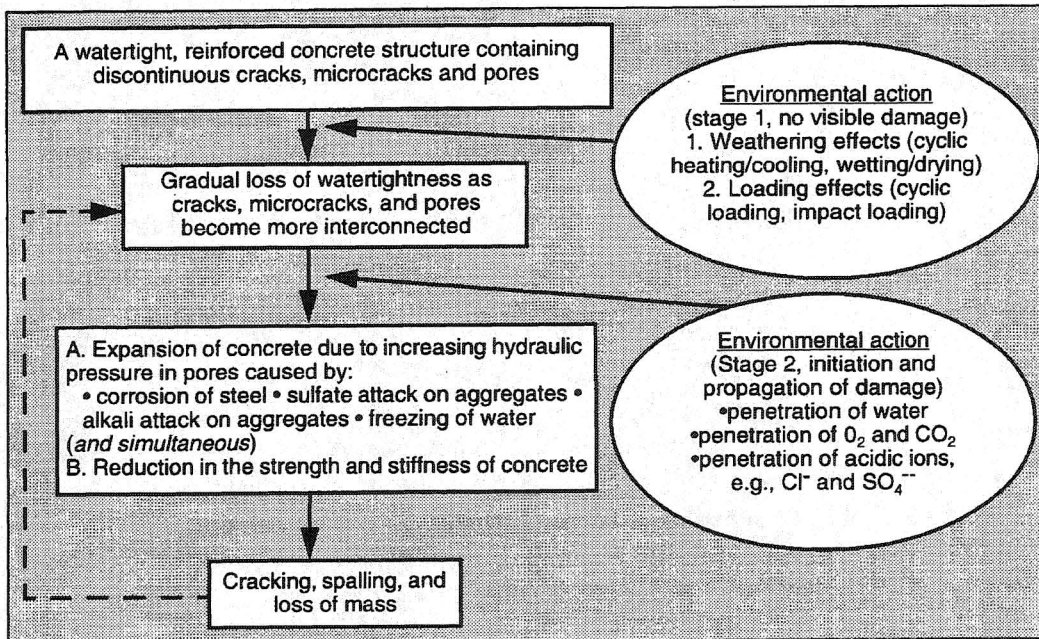


Figure 24 Holistic model for concrete deterioration (extracted from Mehta [13]).

coupled with the very poor hardened air contents of many of the pavements investigated in this study, provide strong support for the freeze-thaw deterioration argument.

The model proposed by Mehta (13) gives a holistic approach to concrete deterioration. The model applies to all modes of distress and clearly indicates the importance of the “loss of watertightness” in allowing environmental factors to propagate the damage. The model also avoids the reductionist approach of associating only a single cause for any observation of distress. This is in much better agreement with real field situations where it is extremely common to observe several deterioration mechanisms acting concurrently on concrete from any given site. It also helps to emphasize the role of water in the deterioration of concrete.

Recommendations

This research program has again indicated that many discrepancies exist between the concrete pavements that are placed in the field and the laboratory concrete specimens that are normally used to assess the strength and durability characteristics of any given mix design. Most of these differences arise from the fact that the laboratory mixing, placement, and curing procedures are of an ideal nature; and hence, they represent an upper bound to the properties that can be expected from the concrete. The recommendations stated below were drafted in an attempt to minimize or eliminate these discrepancies.

- Homogeneous and plastic concrete must reach the paver. For central plant concrete mixers, this can normally be accomplished by optimizing the mixing time needed for the materials used at each specific project. Note that field conditions (e.g., temperature, relative humidity, wind speed) and the potential for cement or cement-admixture problems can cause problems. Hence, minimum and maximum mixing cycles need to be set and they need to be strictly adhered to. If field conditions or cement/admixtures change then the mixing cycle needs to be re-evaluated (and adjusted if necessary). The goal of the mixing cycle is to produce well-mixed, plastic concrete that contains the proper volume of well-dispersed entrained-air voids.
- Paving operations should proceed in a manner that minimizes segregation and maximizes the retention of the entrained-air voids. This indicates that the vibrator frequency and track speed of the paver need to be constrained within specific operating limits. Again, the limits need to be set based on prior experience, field conditions, and materials constraints. The paver should not be used to compensate for mixing problems or premature stiffening problems because this leads to durability problems.
- The shrinkage characteristics of the cements used in this study indicate that changes in mix design may provide improvements in concrete durability. The changes in mix design would include both refinement of the aggregate grading plus the use of admixtures. Obviously, there will be a balance between workability and shrinkage—it will be a major task to maximize the first property while minimizing the other. However, it seems unlikely that the cement industry will reformulate cement composition or decrease fineness to meet the needs of the paving industry.

- Base drainage should be improved. Several of the pavement sites evaluated in this study indicated that they were deteriorating because of a saturated base. Water is the real culprit in these instances and it is simplest to drain the water away from the pavement structure.

Recommendations for Further Research

There were several items noted during the research project that would benefit from further investigation. They include the following:

1. Improvement of the SEM entrained-air void measurements by incorporating an estimate of the paste content of the section being analyzed. This would help to calculate better global estimates of the spacing factor of the concrete sections. With a modest investment of research time, one could also probably obtain an estimate of the water-cement ratio of the concrete section. Both of these estimates would be useful when attempting to diagnose the reason for poor field performance. This would fit nicely into a research program extending the durability testing that was originally conducted under research project HR-396. That project illustrated the potential of using apparent air void distribution curves to document (and predict) the performance of laboratory concrete, rather than the traditional global estimates such as spacing factor. However, HR-396 failed to create test specimens in the range that was critical to the study of many of the core specimens that were observed in this study.
2. Restrained shrinkage tests tended to separate the cements into groups that roughly agreed with the field observations of deterioration problems. However, these shrinkage tests were conducted on paste specimens that bear little resemblance to field concrete. Hence, it would be wise to repeat the restrained shrinkage tests using mortar or concrete specimens to validate the results of the paste tests. A curing study should be run concurrently with this project because of the potential to misinterpret the influence of curing on the observed test response. The research program should also attempt to clarify the role of different types of shrinkage (i.e., plastic shrinkage, autogenous shrinkage, and drying shrinkage) on the durability of common Iowa DOT concrete mixes. The results of this study suggest that water sorption would be an adequate technique for monitoring the “durability” of test specimens because of the close link between saturation and poor field performance.
3. The interaction between bassanite and the water reducer was noted earlier in this report. The reason for this interaction, and its relationship to premature stiffening, needs to be evaluated in more detail. This is important because bassanite is often one of the major sulfate phases present in Iowa cements.

ACKNOWLEDGMENTS

I would like to thank all of the many people who have made significant contributions to this project. Special thanks go to the Iowa Highway Research Board and the Center for Transportation Research and Education for their support of this project. I sincerely apologize for the time delays in producing this final report; however, they simply could not be avoided in this instance. Special thanks to the Iowa Department of Transportation personnel who contributed to this project by providing concrete cores and the other materials needed over the duration of this research project. I would also like to thank the CTRE and MARL staff who put forth great efforts in helping to create test data or finalize this report.

REFERENCES

1. Concrete and Aggregates. *Annual Book of ASTM Standards, Vol. 4.02*. American Society for Testing and Materials, West Conshohocken, Pa., 1998.
2. Schlorholtz, S. Image Analysis for Evaluating the Air Void Parameters of Concrete. Final Report HR-396. Iowa State University, Ames, Iowa, 1996.
3. Cement, Lime and Gypsum. *Annual Book of ASTM Standards, Vol. 4.01*. American Society for Testing and Materials, West Conshohocken, Pa., 1998.
4. Burrows, R. W. The Visible and Invisible Cracking of Concrete. Burrows, Lakewood, Colo., 1997.
5. Blaine, R. L., H. T. Arni, D. H. Evans, M. R. Defore, J. R. Clifton, and R. G. Methey. Part 4, Shrinkage of Neat Portland Cement Pastes and Concretes. *Interrelations between Cement and Concrete Properties*. Building Science Series 15. National Bureau of Standards, Washington, D.C., 1969.
6. Klieger, P. Effect of Entrained Air on Strength and Durability of Concrete with Various Size Aggregates. *Highway Research Board Bulletin 128*, 1956, p. 19.
7. Whiting, D., and M. A. Nagi. *Manual on Control of Air Content in Concrete*. Report EB116.01T. Portland Cement Association, Skokie, Ill., 1998.
8. Schlorholtz, S., and J. Amenson. *Evaluation of Microcracking and Chemical Deterioration in Concrete Pavements*. Final Report HR-358. Iowa State University, Ames, Iowa, 1995.
9. *Test Sections by Mileposts, Primary*. Office of Materials, Iowa Department of Transportation, Ames, Iowa, 1997.
10. Stutzman, P. *Deterioration of Iowa Highway Concrete Pavements: A Petrographic Study*. NISTIR 6399. National Institute of Standards and Technology, Gaithersburg, Md., 1999.
11. Bergeson, K., and S. Schlorholtz. *Rational Characterization of Iowa Fly Ashes*. Final Report HR-286. Iowa State University, Ames, Iowa, 1987.
12. Farny, J. A., and S. H. Kosmatka. *Diagnosis and Control of Alkali-Aggregate Reactions in Concrete*. Report IS413. Portland Cement Association, Skokie, Ill., 1998.
13. Mehta, P. K. Durability—Critical Issues for the Future. *Concrete International*, July 1997, pp. 27–33.

APPENDIX A: MODIFIED ASTM C 359 TEST METHOD AND TEST RESULTS

Early Stiffening of Portland Cement

ASTM C451 (Paste Method) and ASTM C359 (Mortar Method) have been used to detect early stiffening of portland cement. However, in instances where the mix cycle is less than 90 seconds (concrete mobiles and precast plants) it has been found that the regular ASTM tests do not identify or account for the rapid stiffening observed in the field. Thus, ASTM C359 (Mortar Method) has been modified by changing the mix cycle as indicated below. The correlation with field experience has been excellent.

ASTM C359 Modified

Mixing of Mortar--The mixing shall be done in the mechanical mixer as follows:

Place the sand and cement in the dry bowl, and mix the dry materials for a few seconds with the spoon.

Place the bowl in the mixer, set the paddle in place, and mix the dry materials for 10 s at slow speed.

With the mixer operating at slow speed, add the entire quantity of mixing water within 5 s, and continue mixing at slow speed for 1 min, timing from the first addition of water.

Immediately after completion of the mixing, remove the bowl and fill the container. Release the plunger 2 min after the beginning of the wet mixing and record, as the initial penetration.

The remaining penetration times should be reduced by one min since one min has been deleted from the original testing procedure.

The report shall show the depths of the penetrations as follows:

Initial penetration	-----	mm
4-min penetration	-----	mm
7-min penetration	-----	mm
10-min penetration	-----	mm
Remix penetration	-----	mm

Champ: Here are the results of "Early Stiffening of Portland Cement". The testing was done using the standard ASTM C-359 mixing method and also modified mixing method.

<u>Lab. No.</u>	<u>Cement Source</u>	<u>*Std. C-359</u>	<u>Fineness</u>	<u>**Modified C-359</u>
AC3-38	Lafarge	Init. pen. 50 mm 4 min. pen. 50 mm 7 min. pen. 48 mm 10 min. pen. 46 mm Remix pen. 50 mm	352	Init. pen. 45 mm 4 min. pen. 35 mm 7 min. pen. 12 mm 10 min. pen. 9 mm Remix pen. 50 mm
ACV3-6	Continental	Init. pen. 8 mm 4 min. pen. 7 mm 7 min. pen. 6 mm 10 min. pen. 5 mm Remix pen. 49 mm	374	Init. pen. 9 mm 4 min. pen. 3 mm 7 min. pen. 3 mm 10 min. pen. 3 mm Remix pen. 44 mm
ACV3-9	Lehigh	Init. pen. 10 mm 4 min. pen. 11 mm 7 min. pen. 10 mm 10 min. pen. 7 mm Remix pen. 8 mm	359	Init. pen. 12 mm 4 min. pen. 8 mm 7 min. pen. 7 mm 10 min. pen. 6 mm Remix pen. 12 mm
AC3-43	Holnam	Init. pen. 50 mm 4 min. pen. 50 mm 7 min. pen. 46 mm 10 min. pen. 47 mm Remix pen. 50 mm	374	Init. pen. 48 mm 4 min. pen. 35 mm 7 min. pen. 14 mm 10 min. pen. 10 mm Remix pen. 48 mm
AC3-49	Lehigh	Init. pen. 9 mm 4 min. pen. 6 mm 7 min. pen. 7 mm 10 min. pen. 6 mm Remix pen. 10 mm	360	Init. pen. 5 mm 4 min. pen. 7 mm 7 min. pen. 3 mm 10 min. pen. 3 mm Remix pen. 7 mm
AC3-50	Ash Grove	Init. pen. 49 mm 4 min. pen. 47 mm 7 min. pen. 46 mm 10 min. pen. 28 mm Remix pen. 50 mm	359	Init. pen. 44 mm 4 min. pen. 15 mm 7 min. pen. 8 mm 10 min. pen. 7 mm Remix pen. 44 mm

* All mixing was done according to ASTM C-359.

** All mixing was done according to modified mixing.
Instructions with mixer operating at slow speed for 1 minute timing from first addition of water.

Results of Premature Stiffening Tests

Test	Cement type	Cement (g)	Fly Ash (g)	Plast 161 Admixture (g)	Water (g)	Total Water (g) (w/admix)	Penetrations after Remix													
							Penetration 1	Penetration 2	Penetration 3	Penetration 4	Penetration 5	Penetration 2	Penetration 5	Penetration 7	Penetration 10	Penetration 14	Penetration 20	Penetration 21		
Modified	HOL	480	120	12	188	200	50	4	3	2	50	50	50	50	50	50	50	50	50	50
Standard	HOL	480	120	12	188	200	50	50	50	50	50	50	50	50	50	50	50	50	50	50
Modified	HOL	600		12	188	200	50	4	1	1	50	50	50	50	50	50	50	50	50	50
Standard	HOL	600		12	188	200	50	50	3	2	50	50	50	50	50	50	50	50	50	50
Modified	HOL	600			216	216	50	3	1	1	50	50	50	50	50	50	50	50	50	50
Standard	HOL	600			216	216	50	50	48	48	50	50	50	50	50	50	50	50	50	50
Modified	HOL	600			180	180	9	1	1	1	50	50	50	50	50	50	50	50	50	50
Standard	HOL	600			180	180	4	2	1	2	50	50	50	50	50	50	50	50	50	50
Modified	HOL	600			180	180	38	2	1	1	50	50	50	50	50	50	50	50	50	50
Standard	HOL	600			180	180	3	2	1	1	50	50	50	50	50	50	50	50	50	50
Standard	KAI	600		18	180	198	41	50	18	4	50	50	50	50	50	50	50	50	50	50
Standard	KAI	600		24	188	212	50	50	50	50	50	50	50	50	50	50	50	50	50	50
Standard	KAI	480	120	12	188	200	50	50	50	49	50	50	50	50	50	50	50	50	50	50
Standard	KAI	480	120	12	200	212	50	50	50	50	50	50	50	50	50	50	50	50	50	50
Modified	KAI	480	120	12	188	200	50	50	48	4	50	50	50	50	50	50	50	50	50	50
Standard	KAI	480	120	12	188	200	50	50	50	50	45	50	50	50	50	50	50	50	50	50
Standard	KAI	480	120	12	188	200	50	50	50	50	34	50	50	50	50	50	50	50	50	50
Standard	KAI	600		12	188	200	50	50	4	1	50	50	50	50	50	50	50	50	50	50
Modified	KAI	600			225	225	50	41	1	1	50	50	50	50	50	50	50	50	50	50
Standard	KAI	600			225	225	50	45	2	1	50	50	50	50	50	50	50	50	50	50
Modified	KAI	600			216	216	50	6	1	0	50	50	50	50	50	50	50	50	50	50
Standard	KAI	600			216	216	50	48	2	1	50	50	50	50	50	50	50	50	50	50
Modified	KAI	600			198	198	49	3	1	0	50	50	50	50	50	50	50	50	50	50
Standard	KAI	600			198	198	50	3	1	0	50	50	50	50	50	50	50	50	50	50
Standard	KAI	600			198	198	50	50	1	0	50	50	50	50	50	50	50	50	50	50
Modified	KAI	600			180	180	4	1	1	1	50	50	50	50	50	50	50	50	50	50
Standard	KAI	600			180	180	4	1	1	1	50	50	50	50	50	50	50	50	50	50
Standard	DIX	600		18	180	198	50	50	49	45	50	50	50	50	50	50	50	50	50	50
Standard	DIX	600			198	198	50	47	49	49	44	50	50	50	50	50	50	50	50	50
Standard	DIX	480	120	12	188	200	50	50	50	50	50	50	50	50	50	50	50	50	50	50
Standard	DIX	600		12	188	200	50	50	46	45	50	50	50	50	50	50	50	50	50	50
Modified	DIX	480	120		200	200	50	50	50	50	6	50	50	50	50	50	50	50	50	50

APPENDIX B: CORE LOGS

Table of Core Locations—TR-406

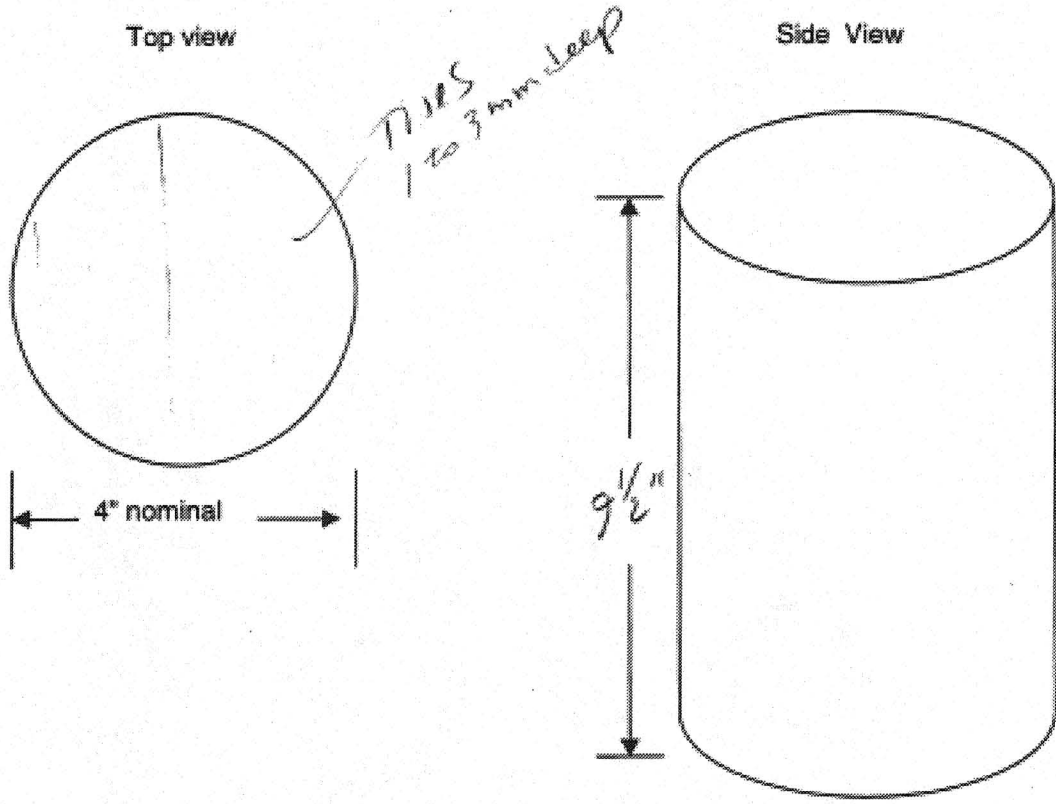
Site	County	Road	Approximate Mile Post	Station No.	Number of Cores
1	Webster	US 20 westbound	127.55	2002, passing lane	2 @ joint, 1 @ midpanel, 1 @ exit lane,
2	Hamilton	US 20 westbound	135.4	near station 49, passing lane	2 @ joint, 1 @ midpanel
3	Webster	Hwy 169 southbound		near station 2002, passing lane	2 @ joint
4	Hamilton	IA 175	156.2	143, westbound lane	2 @ joint, 1 @ midpanel
5	Hamilton	IA 175	157.5	191, eastbound lane	2 @ joint, 1 @ midpanel
6	Hamilton	IA 175	158.3	244, eastbound lane	2 @ joint, 1 @ midpanel
7	Marshall	IA 330 northbound	6.8	74+58, 74+76, 74+86	1 @ joint, 1 @ joint, 1 @ midpanel
8	Iowa	I-80 eastbound driving lane	210.36	298	2 @ joint, 1 @ midpanel, driving lane
9	Dallas	I-80 Van Meter	107.55 eastbound	509, driving lane	2 @ joint, 1 @ midpanel
10	Dallas	I-80 Van Meter	113.25 eastbound	810+40, driving lane	2 @ joint, 1 @ midpanel
11	Dallas	I-80 Van Meter	116.2 eastbound	966+20, driving lane	2 @ joint, 1 @ midpanel
12	Cass	I-80 by Anita	68 westbound	About 1019, driving lane	2 @ joint, 1 @ midpanel
13	Freemont	IA-2 Nebraska City exit I-29	2.6 westbound	1499, driving lane	2 @ joint, 1 @ midpanel
14	Polk	IA-160 stub	Not known eastbound	362, driving lane	2 @ joint, 1 @ midpanel
15	Johnson	US-218 southbound passing lane	near 95 (? 95.45)	1658	1 @ joint, 1 @ midpanel
16	Johnson	US-218 northbound passing lane	91.96	near 1498	2 @ joint, 1 @ midpanel
17	Scott	US-61 northbound driving lane	near 125	524+90, 525+20, 525+50	1 @ joint, 1 @ midpanel, 1 @ joint

TR-406 - Concrete Core Log-In Form

Sample Identification: 520 WB G 127.55
JL G STA 2002

General Observations:
Dimensions: See below
Surface conditions: looked good
Bottom: smooth
Reinforcement: None
Cracks, comments: No cracks evident
Some white material evident on
surface of core.

Diagram of core:



TR-406 - Concrete Core Log-In Form

Sample Identification: US 520 WB @ MP/27.55
STA 2002 Mid panel

General Observations:

Dimensions: see below

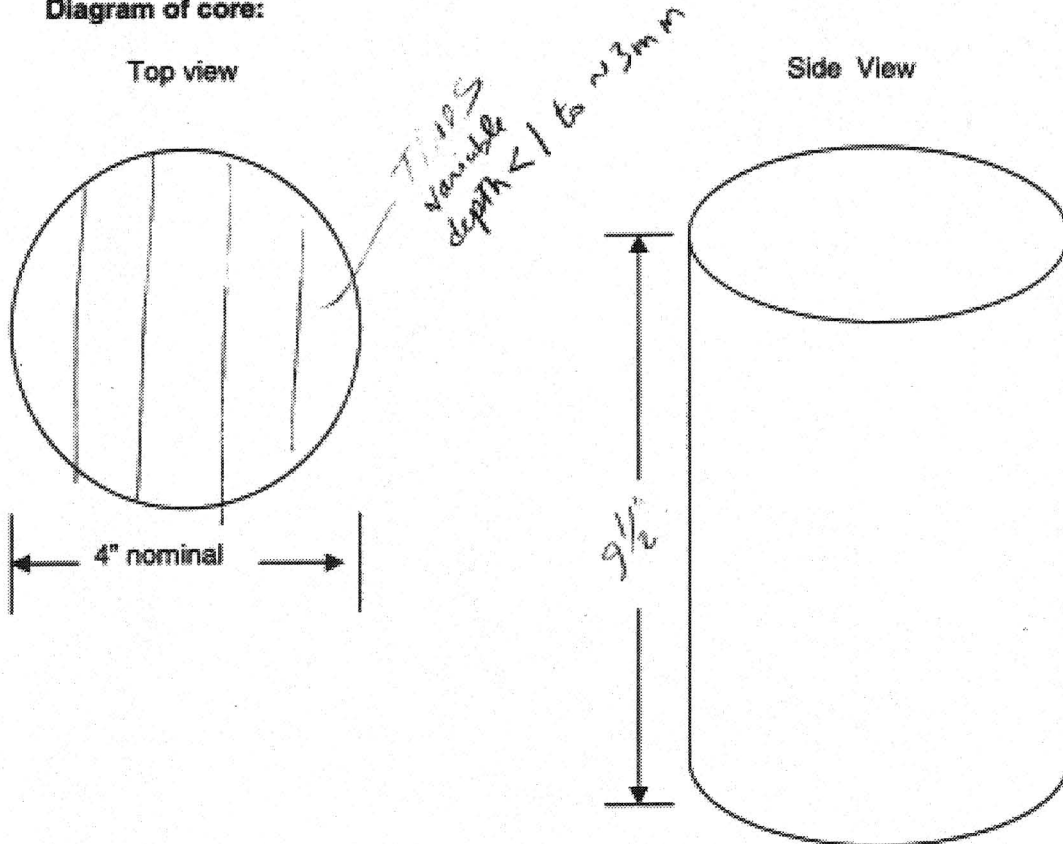
Surface conditions: looked ok

Bottom: smooth

Reinforcement: NONE

Cracks, comments: No cracks evident on core
some white residue was present
on inner of core

Diagram of core:



TR-406 - Concrete Core Log-In Form

Sample Identification: 520 WB m P 135.4
(Transverse Joint Near Longitudinal Joint)

General Observations: see below

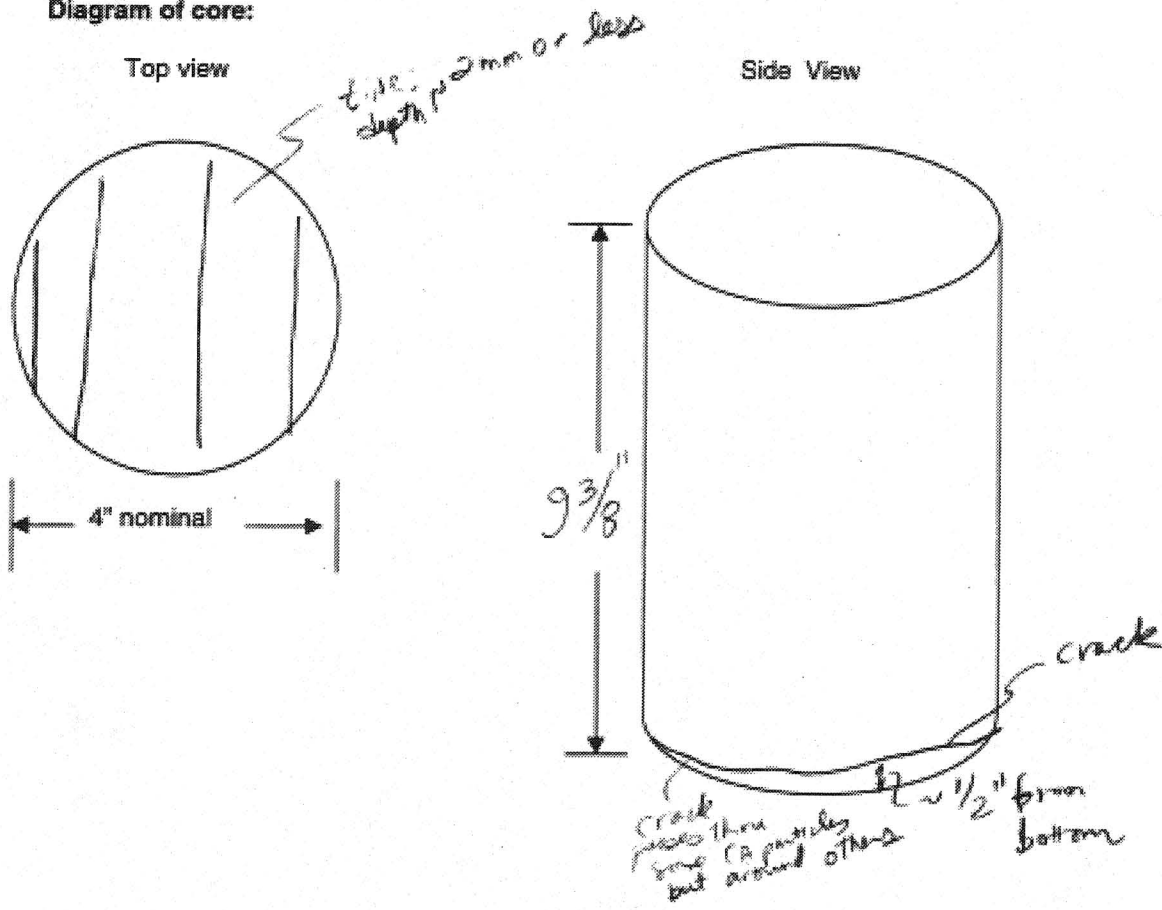
Surface conditions: ASR popouts from shale noted - some entrapped voids 1/4" dia

Bottom: smooth, paved on econcrete?

Reinforcement: NONE

Cracks, comments: severe crack at bottom of core -
difficult to say why - cracked -
some evidence of paste bond between
paste & aggregate.

Diagram of core:



TR-406 - Concrete Core Log-In Form

Sample Identification: 520 WB MP 135.4
of Trans Joint near shoulder

General Observations:

Dimensions: see below

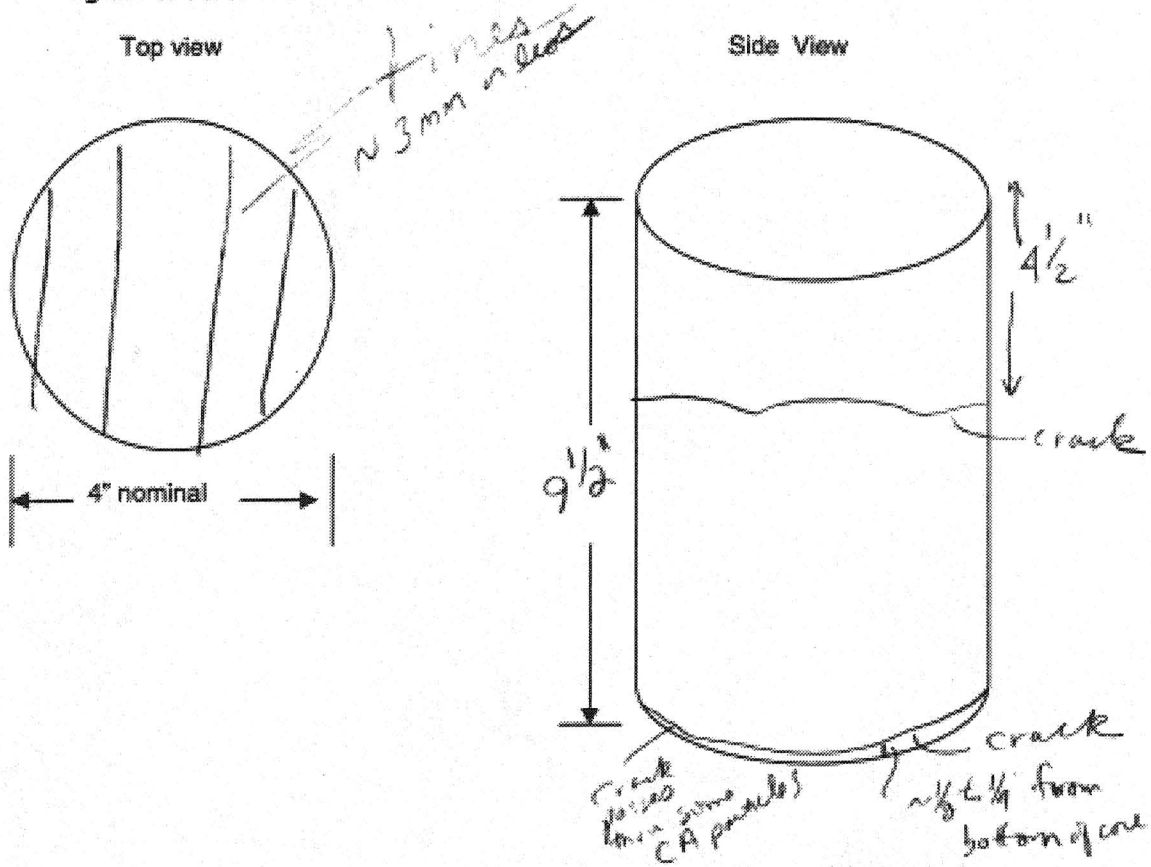
Surface conditions: Shale popouts common

Bottom: Smooth

Reinforcement: NONE

Cracks, comments: core cracked all way thru @ ~4 1/2"
Some shale noted on failure plane
again a crack ran around the
circumference of the bottom of the core

Diagram of core:



TR-406 - Concrete Core Log-In Form

Sample Identification: 520 WB MP 135.4
Q mid Panel

General Observations:

Dimensions: _____

Surface conditions: Shale popouts common

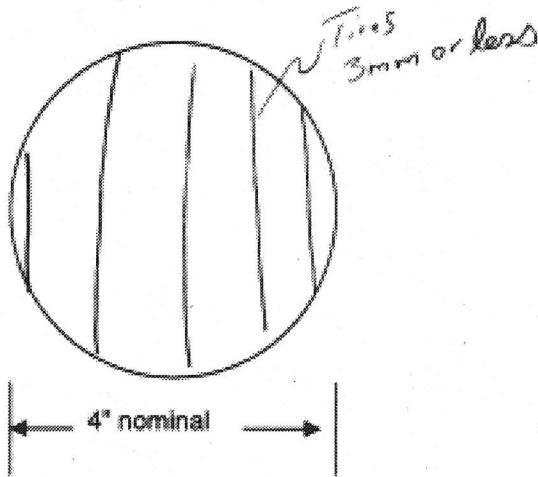
Bottom: smooth - no concrete base

Reinforcement: None

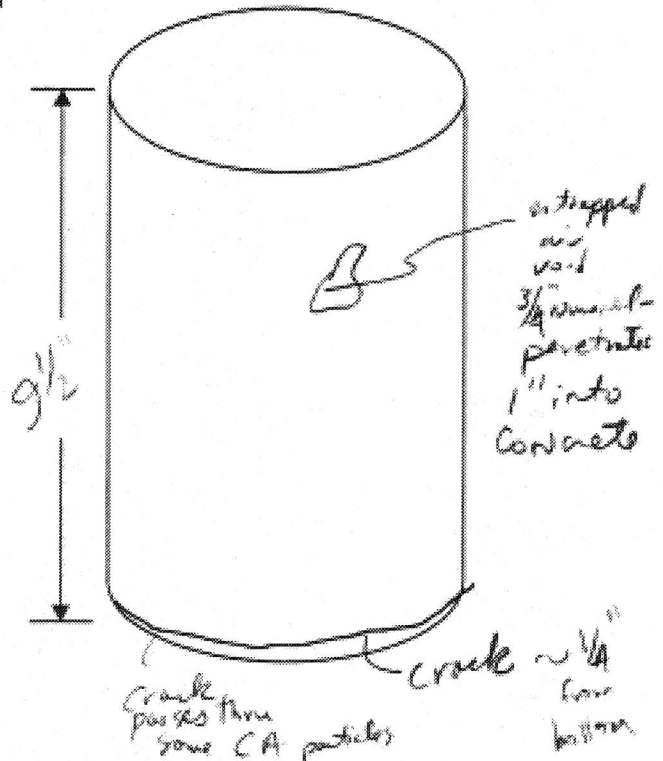
Cracks, comments: Crack at base of core - traverses
base of core

Diagram of core:

Top view



Side View



TR-406 - Concrete Core Log-In Form

Sample Identification: US-169 Webster SB
 Core 1 (Just north of JET 520) Joint in paving line 6' ctr of pavement

General Observations:
 Dimensions: see below - core broken @ 4 to 6"

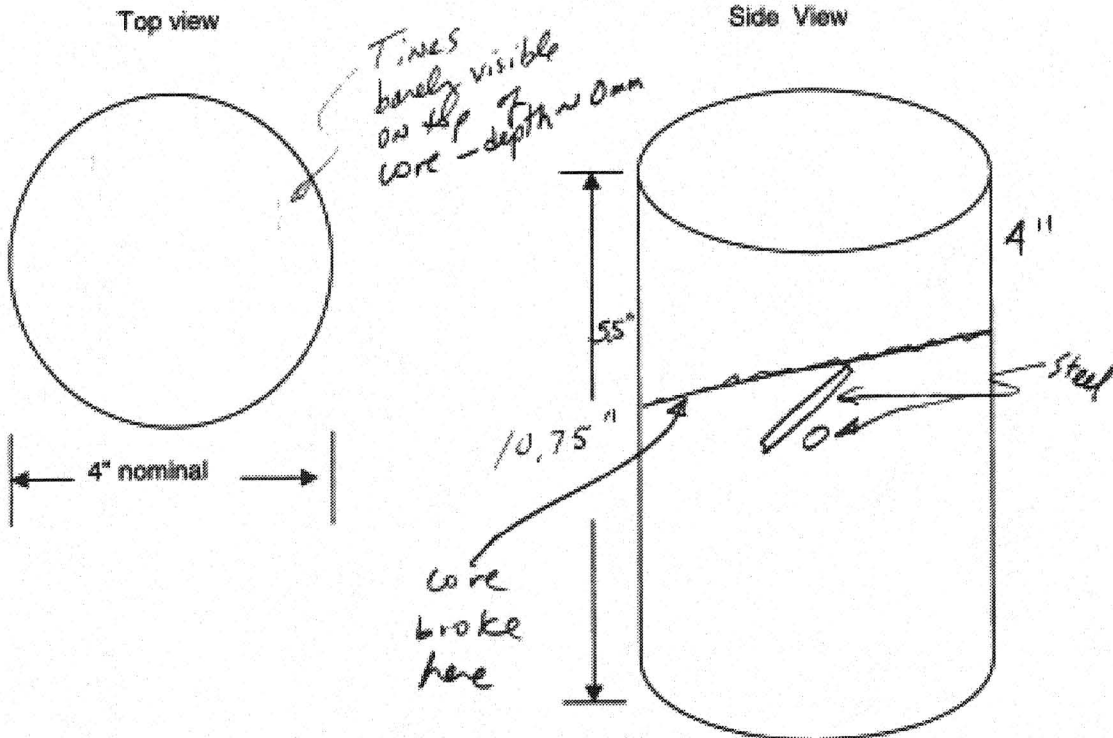
Surface conditions: Some popouts evident

Bottom: _____

Reinforcement: steel about 6" from top of core

Cracks, comments: Several clayey type of particles evident on top surface of core and in fracture surface - some were surrounded by white residue
Subparallel cracks noted at depth of 2" and 4" that ran through core.

Diagram of core:



TR-406 - Concrete Core Log-In Form

Sample Identification: US 169 - Webster - SB
Core 2
Just north of JCT 520 - Joint @ the intersection
of Lanes - Traverse points
of passing lane

General Observations:
 Dimensions: see below - core broken @ about 6" depth

Surface conditions: popouts on sides of core

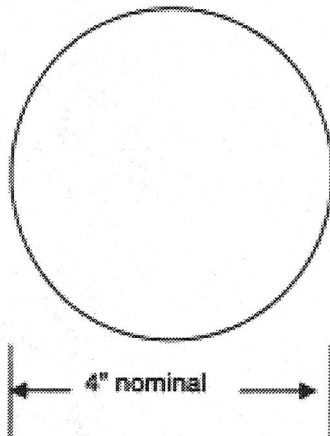
Bottom: _____

Reinforcement: NONE

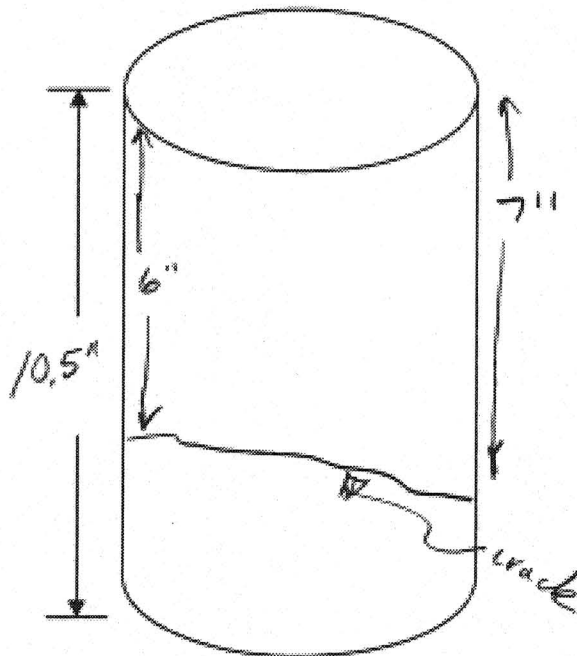
Cracks, comments: Core broken off at about
6 to 7" depth - material on
fracture surface highly variable, some
looks like clay or soft
Some popouts on fracture surface
with white material (? gel).

Diagram of core:

Top view



Side View



TR-406 - Concrete Core Log-In Form

Sample Identification: HWY 175 WB MP 156.2
midpanel

General Observations:

Dimensions: _____

Surface conditions: some large entrapped voids @ mid core

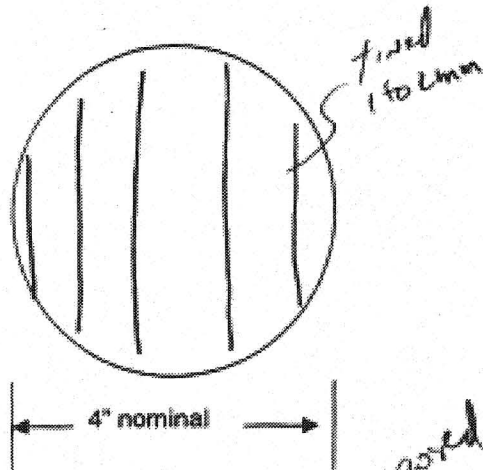
Bottom: rough but ? Ecocrete or Flyash

Reinforcement: None

Cracks, comments: some staining around shale particles
no cracks evident

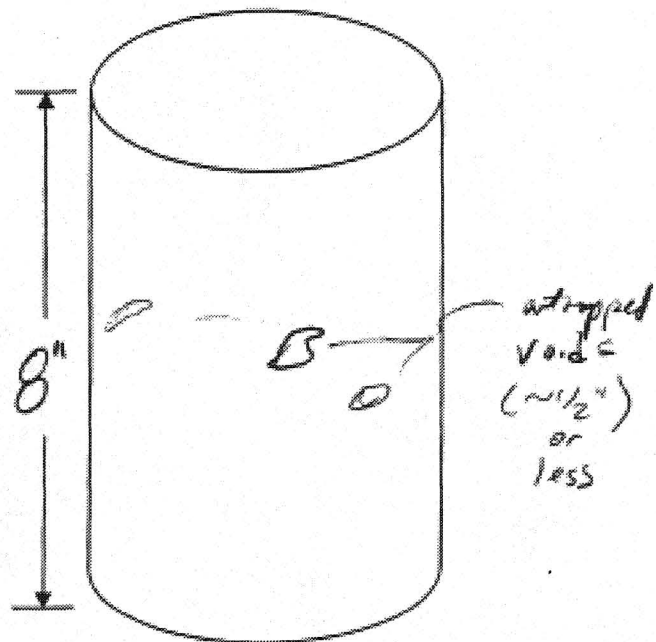
Diagram of core:

Top view



Some agg. exposed on wear surface

Side View



TR-406 - Concrete Core Log-In Form

Sample Identification: HWY 175 WB G n.l.c Post 156.2
(9 Inside Joint)

General Observations:

Dimensions: _____

Surface conditions: Many entrapped voids over whole core length

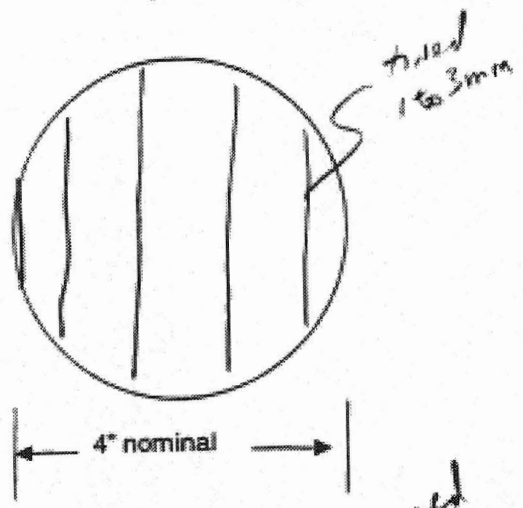
Bottom: Rough but could be re-concrete or fly ash base

Reinforcement: NONE

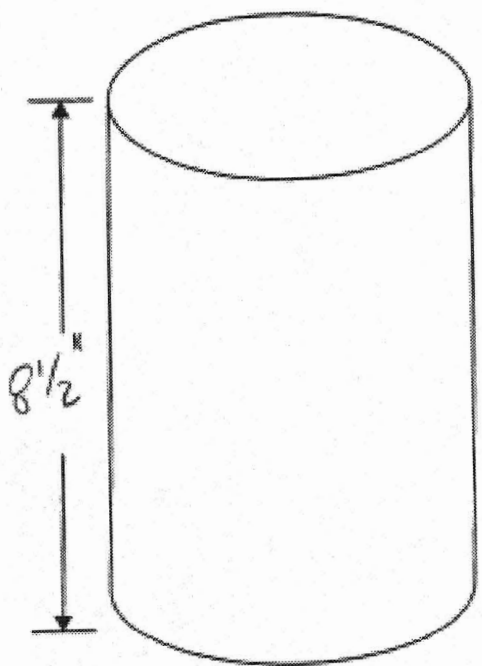
Cracks, comments: NONE

Diagram of core:

Top view



Side View



Some agg. exposed on lower surface

TR-406 - Concrete Core Log-In Form

Sample Identification: HWY 175^{EB} MP 157.5
TRANS. JOINT INSIDE

General Observations:

Dimensions: _____

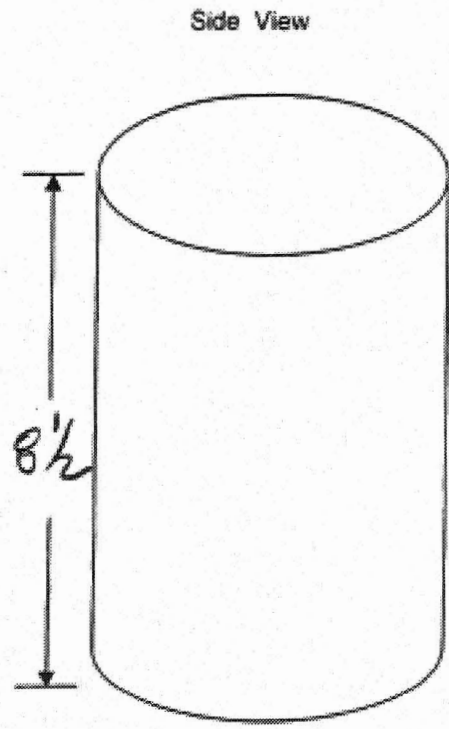
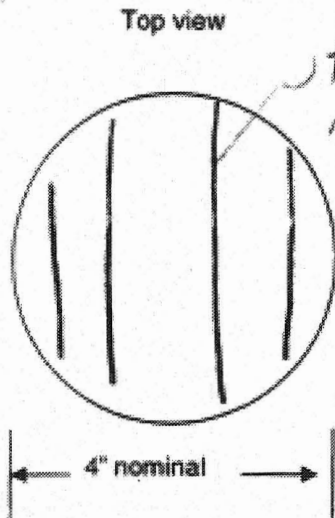
Surface conditions: Many shale particles evident, white material surrounds shale

Bottom: Rough

Reinforcement: NONE

Cracks, comments: NONE
some CA exposed @ top surface

Diagram of core:



TR-406 - Concrete Core Log-In Form

Sample Identification: HWY 175 EB MP 157.5
Midpanel

General Observations:

Dimensions: _____

Surface conditions: Many shale particles noted + white efflorescence near

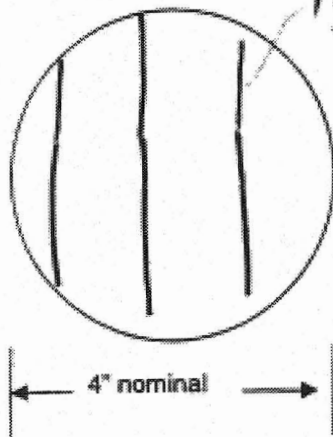
Bottom: Rough

Reinforcement: None

Cracks, comments: No cracks evident

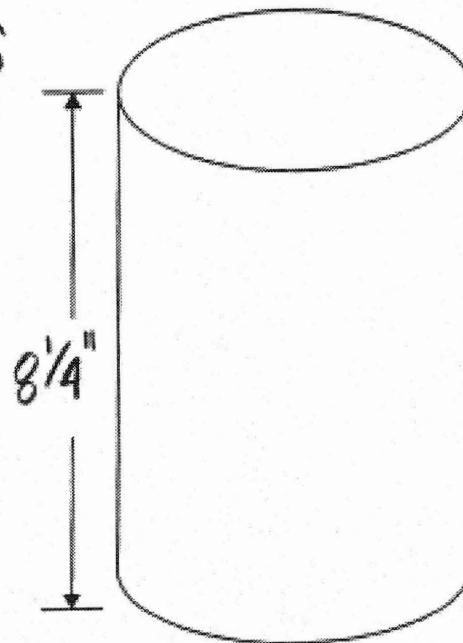
Diagram of core:

Top view



*Lines sloppy
very
2 to 5mm
deep*

Side View



TR-406 - Concrete Core Log-In Form

Sample Identification: HWY 175 EB @ MP 158.3
Midpanel

General Observations:

Dimensions: _____

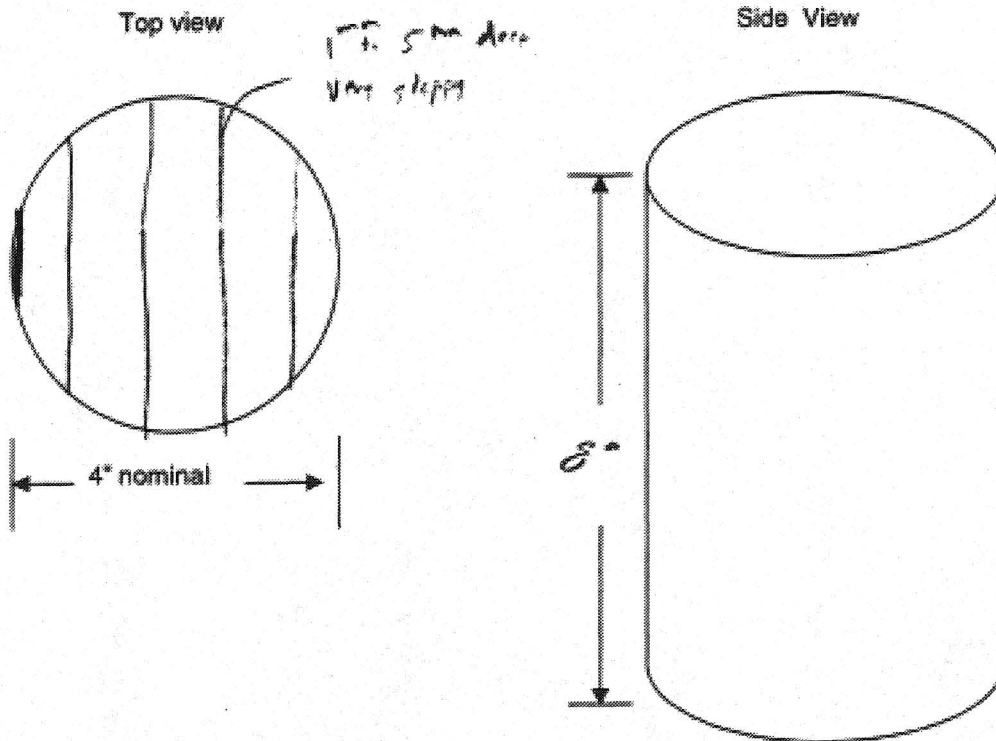
Surface conditions: _____

Bottom: Rough

Reinforcement: NONE

Cracks, comments: NO CRACKS EVIDENT

Diagram of core:



TR-406 - Concrete Core Log-In Form

Sample Identification: 175 EB@MP 158.3
Joint inside

General Observations:

Dimensions: _____

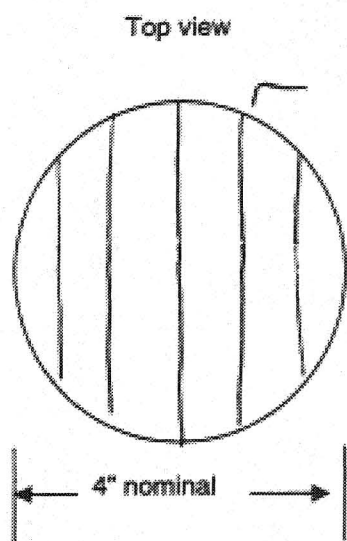
Surface conditions: small void

Bottom: ROUGH

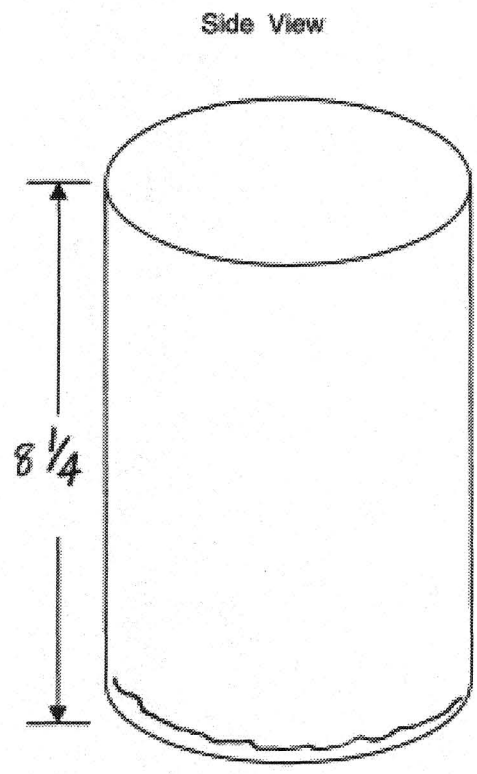
Reinforcement: NONE

Cracks, comments: 1 CRACK RUNNING HALF WAY AROUND BOTTOM

Diagram of core:



1 to 4"
very sloppy



TR-406 - Concrete Core Log-In Form

Sample Identification: IA 330 Marshall Co.
A-panel G MP 6.8 North

General Observations:

Dimensions: _____

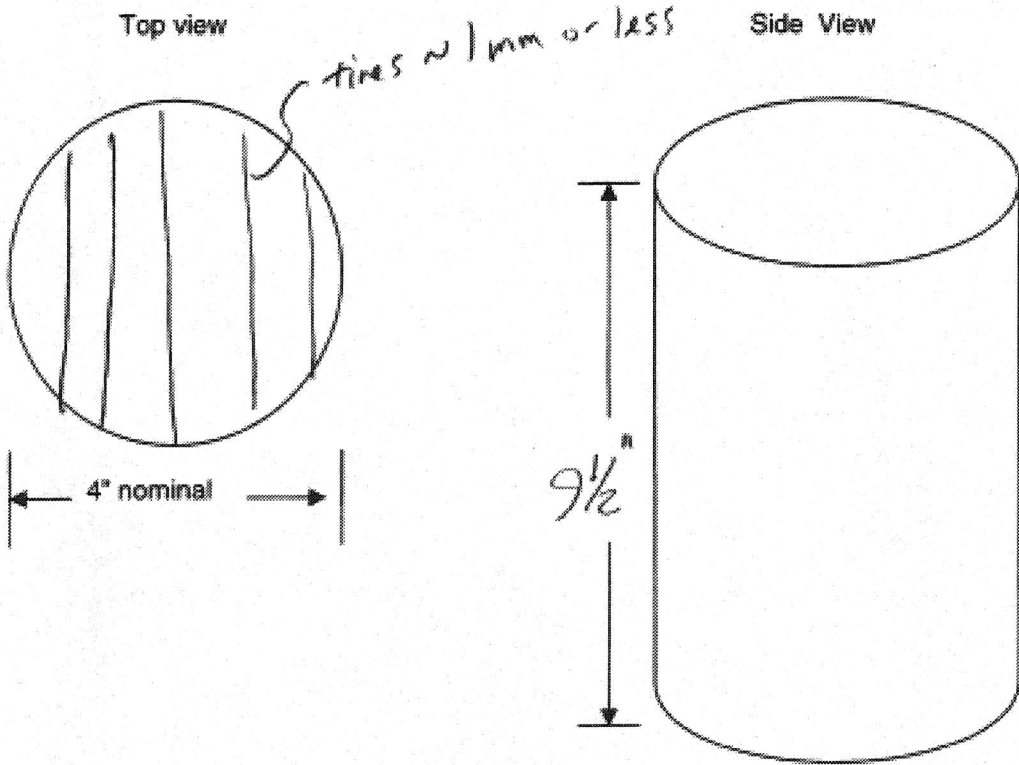
Surface conditions: Some white residue evident

Bottom: Rough

Reinforcement: NONE

Cracks, comments: None evident
Gravel coarse Aggregate

Diagram of core:



TR-406 - Concrete Core Log-In Form

Sample Identification: IT 330 Marshall
St B @ G MP 6.8

General Observations:

Dimensions: _____

Surface conditions: Gravel Agg.

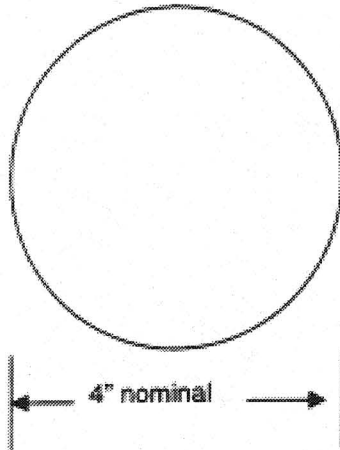
Bottom: ROUGH

Reinforcement: Steel @ 4 1/2"

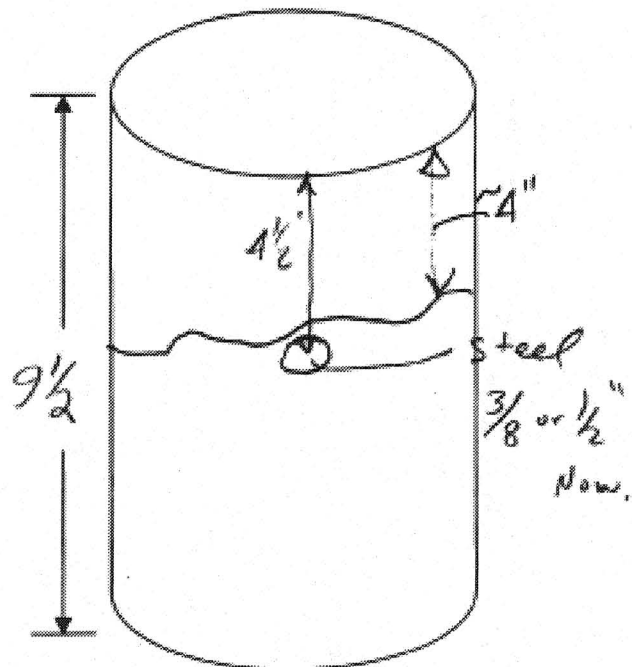
Cracks, comments: Steel was extensively corroded
Core broke at ~4" due to steel
Some cracked aggregates noted

Diagram of core:

Top view



Side View



TR-406 - Concrete Core Log-In Form

Sample Identification: I-80 EB Iowa Co. hwy 210.36
top 1/3 of extra core

General Observations:

Dimensions: _____

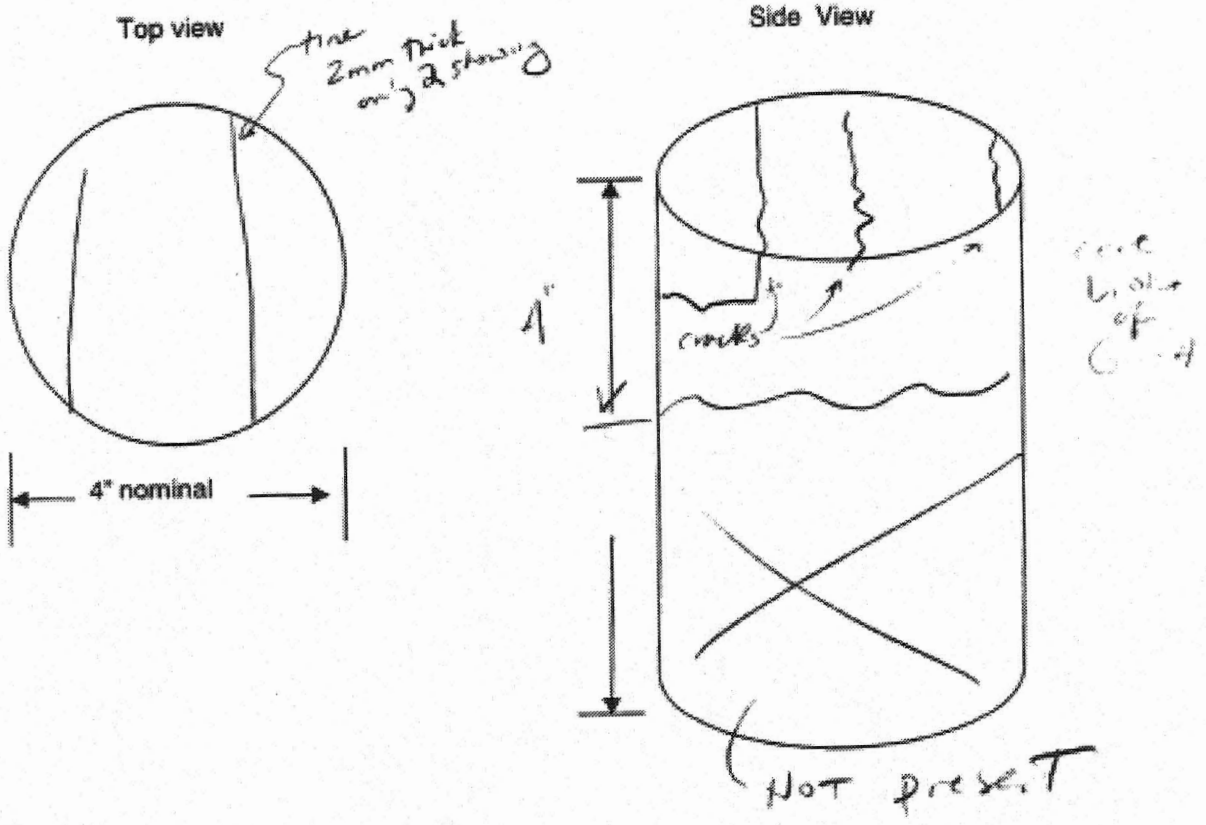
Surface conditions: Poor - surface cracks

Bottom: NOT present

Reinforcement: None

Cracks, comments: surface cracks prevalent

Diagram of core:



TR-406 - Concrete Core Log-In Form

Sample Identification: L80-EB Iowa County MP 210.36
Joint

General Observations:

Dimensions: _____

Surface conditions: many regions of patchy white material

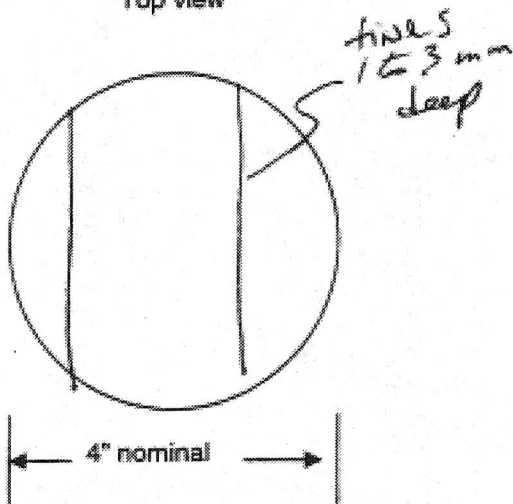
Bottom: smooth, concrete base

Reinforcement: None

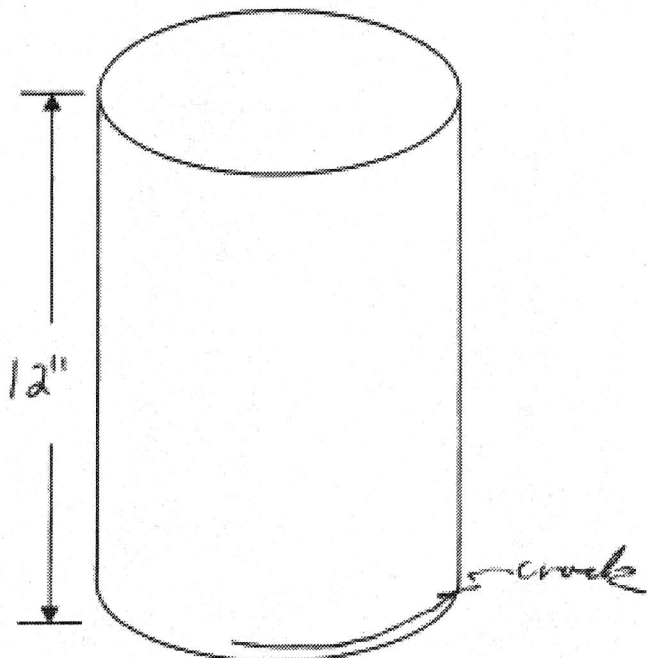
Cracks, comments: crack @ base (within 1/4" of
bottom of core) that
fractured several aggregate particles

Diagram of core:

Top view



Side View



TR-406 - Concrete Core Log-In Form

Sample Identification: I-80 EB Iowa County MP210.36
midpanel

General Observations:

Dimensions: _____

Surface conditions: large entrapped airvoids common

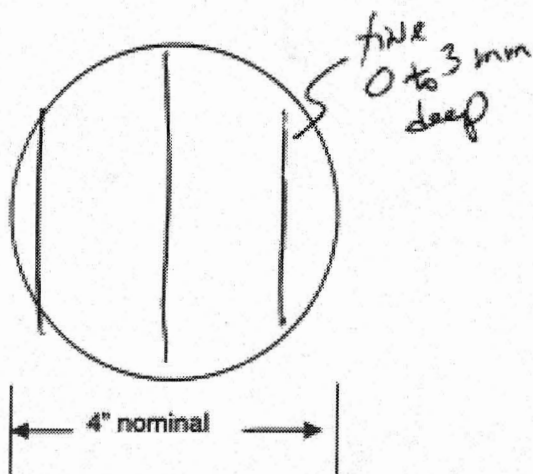
Bottom: 3 reconcrete base

Reinforcement: NONE

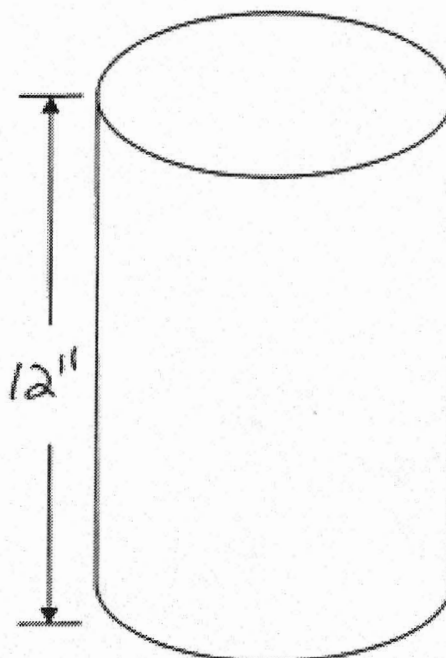
Cracks, comments: NONE evident

Diagram of core:

Top view



Side View



TR-406 - Concrete Core Log-In Form

Sample Identification: ISO DALLAS STA 509
It Near $\frac{1}{2}$

General Observations:

Dimensions: _____

Surface conditions: _____

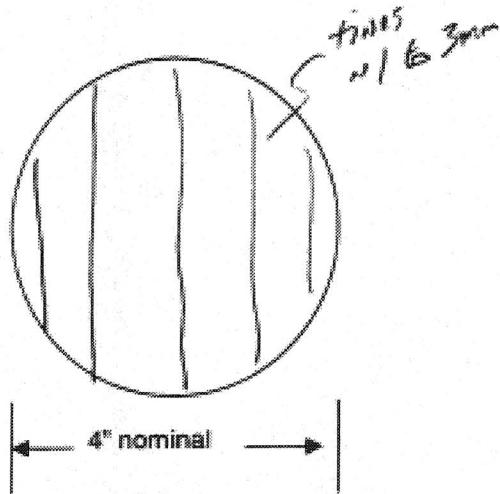
Bottom: Level

Reinforcement: Steel @ $6\frac{1}{2}$ " Also impression of steel @ bottom of core

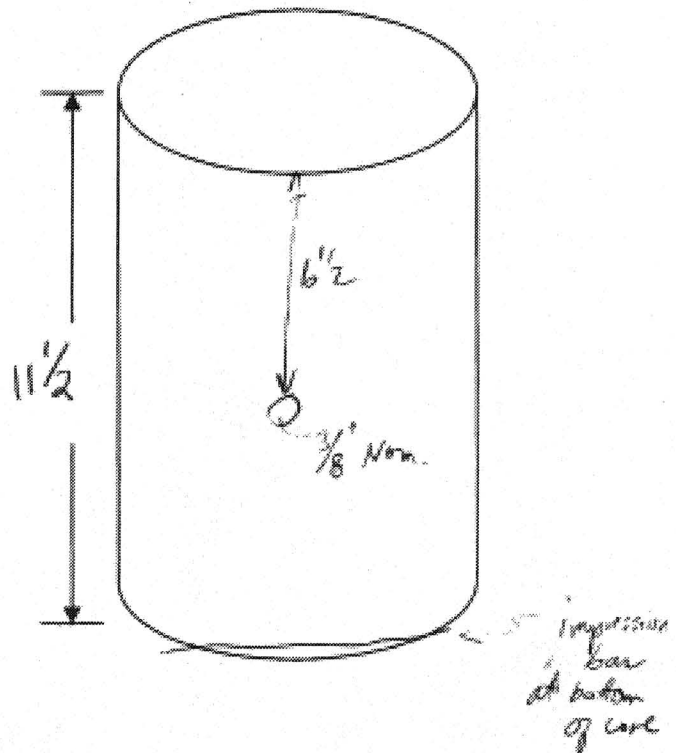
Cracks, comments: Shale particles common - No white residue evident
No cracks

Diagram of core:

Top view



Side View



TR-406 - Concrete Core Log-In Form

Sample Identification: IA-80 DALLAS STA 509
midpanel

General Observations:

Dimensions: _____

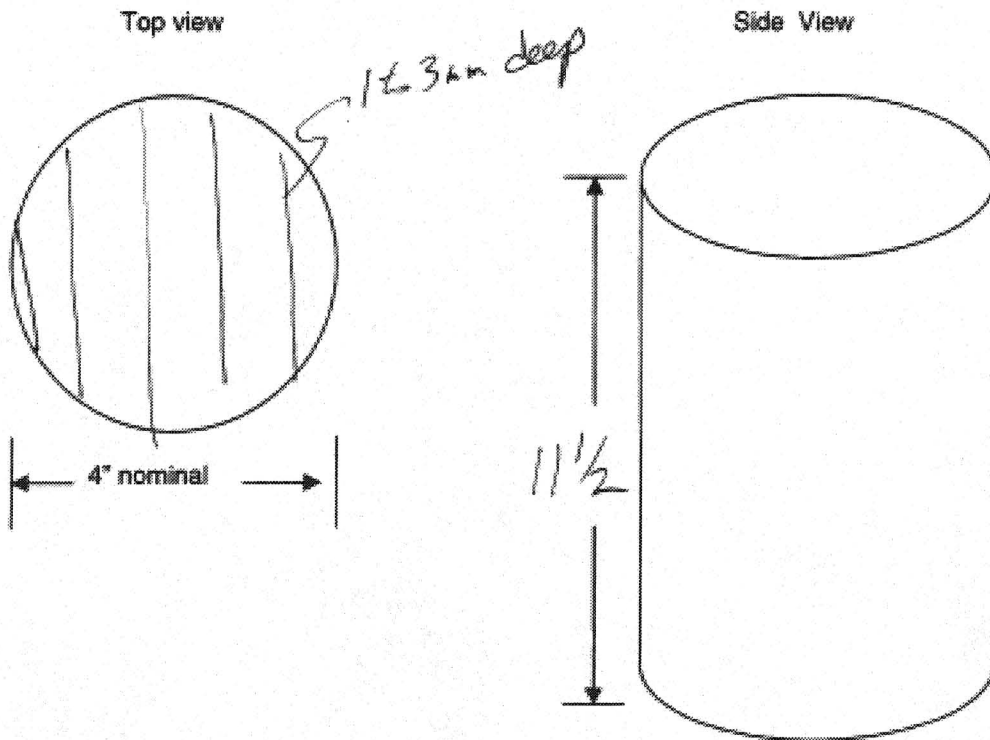
Surface conditions: _____

Bottom: Rough - crushed agg base

Reinforcement: None

Cracks, comments: No cracks evident
Shale particles common - some with
white residue near them (? ASR gel)

Diagram of core:



TR-406 - Concrete Core Log-In Form

Sample Identification: I-80 DALLAS Sta 810+40
Joint outside

General Observations: Dimensions: 4 x 12 1/4

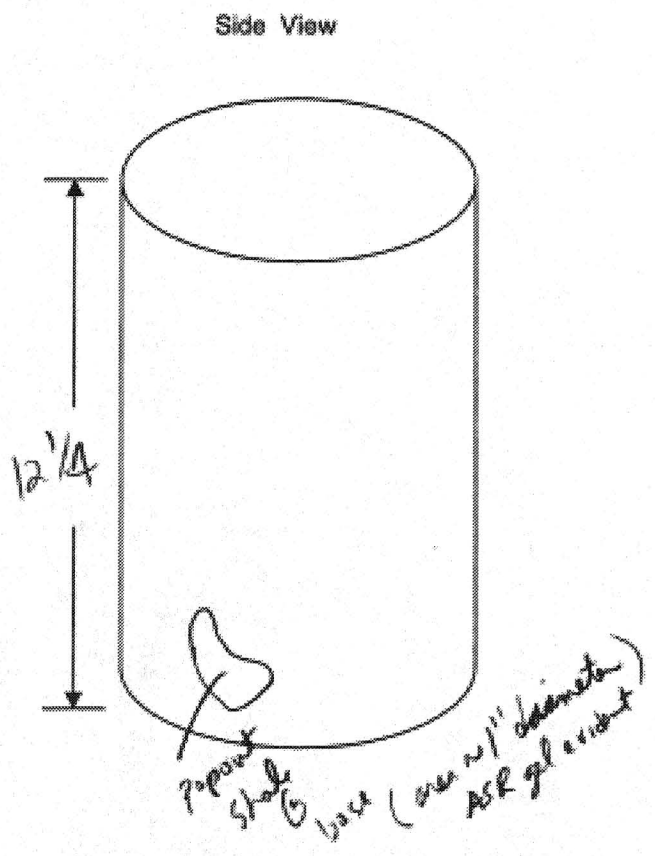
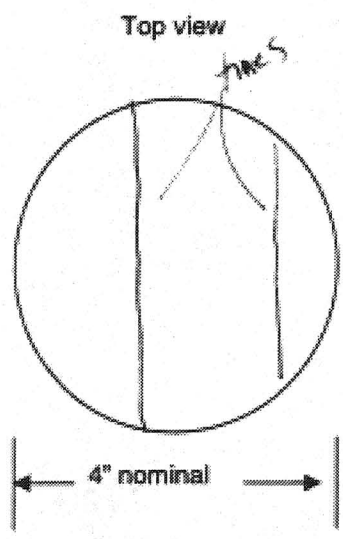
Surface conditions: Irregular fines

Bottom: Cracked Ang Base

Reinforcement: None evident

Cracks, comments: some popouts evident due to scale
entrapped air voids common by
typical < 5mm diam.
Dried uniformly

Diagram of core:



TR-406 - Concrete Core Log-In Form

Sample Identification: I 80 Dallas Sta 810 + 40
Midpanel

General Observations:

Dimensions: 4 x 12 1/4 Nom

Surface conditions: Irregular finish ~ 1 to 2 mm deep

Bottom: crushed agg base

Reinforcement: None evident

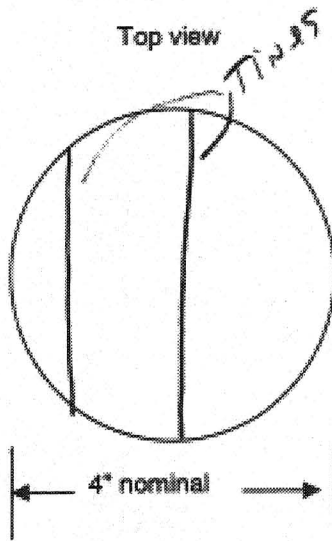
Cracks, comments: some chipping staining water

some shell popouts on sides of core

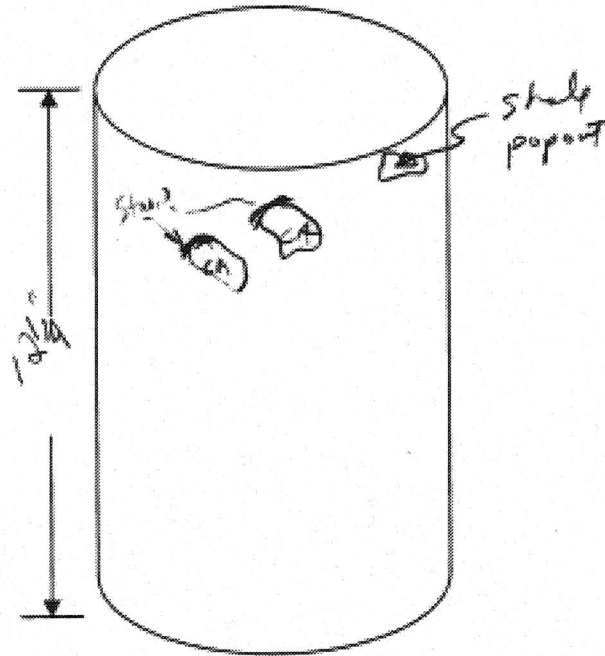
entrapped air voids common but not > 5 mm
diameter

Dried uniformly

Diagram of core:



Side View



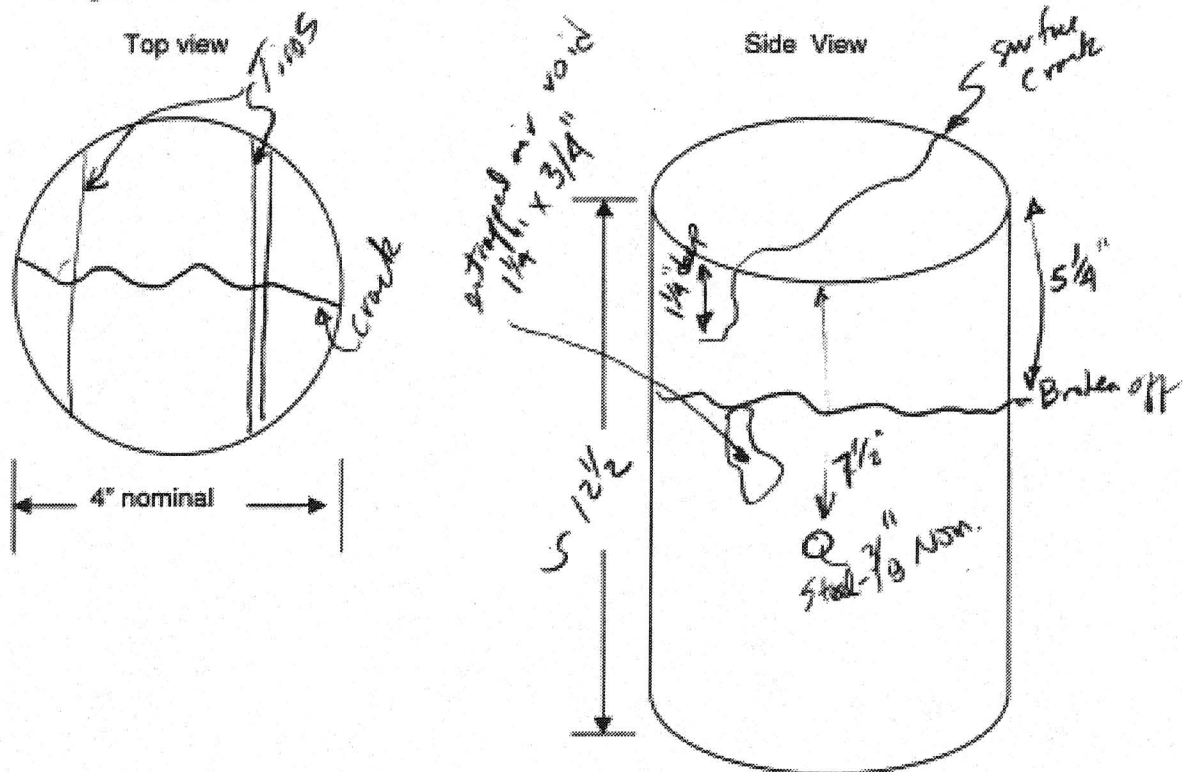
TR-406 - Concrete Core Log-In Form

Sample Identification: I-80 DALLAS Sta B10 + 40
JT Near E

General Observations:
 Dimensions: 4 x ~12 1/2
 Surface conditions: Tiny irogelaw (only 3 tubes show on core)
 Bottom: crush egg base
 Reinforcement: steel @ 7 1/2"
 Cracks, comments: cracked extensively - surface crack across core
core. core broken off @ 5 1/4" from top
some white residue noted on surface
of core; scale particles present + pop outs,
some CA staining

Dried pretty uniformly

Diagram of core:



TR-406 - Concrete Core Log-In Form

Sample Identification: IA-80 DALLAS Sta 966+20
Joint outside

General Observations:

Dimensions: 1 1/2 x 4

Surface conditions: TINES barely cut surface < 1 or 2 mm deep

Bottom: Agg base

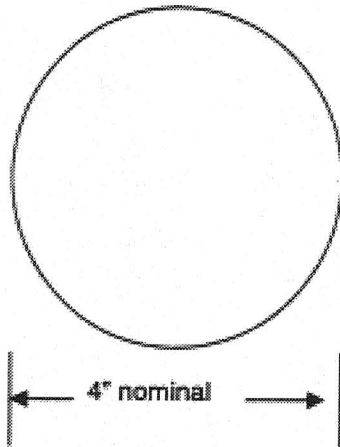
Reinforcement: None evident

Cracks, comments: some finer diameter voids
noted @ mid core - some agg staining (CA)

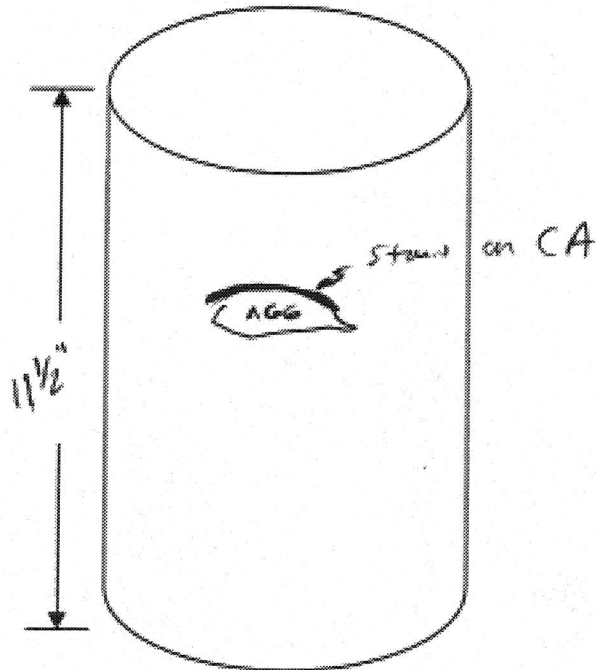
Dried uniformly except for entrapped air voids

Diagram of core:

Top view



Side View



TR-406 - Concrete Core Log-In Form

Sample Identification: IA 30 - DALLAS sta 966+20
mid panel

General Observations:
Dimensions: 4 x 11 1/2

Surface conditions: Tines cut surface to depth of ~2mm

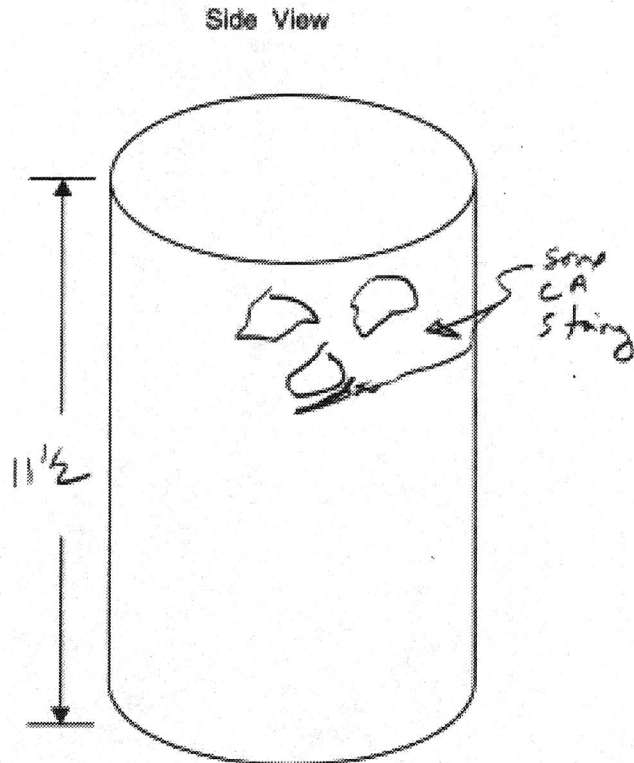
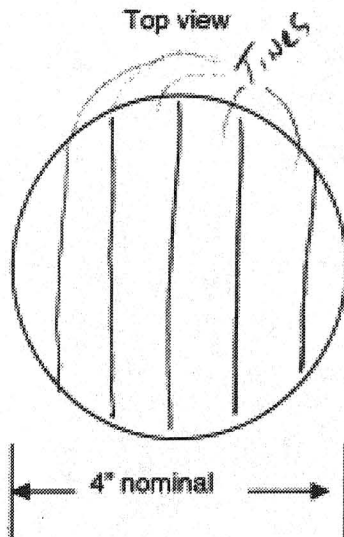
Bottom: crushed aggr base

Reinforcement: None visible

Cracks, comments: some staining on 3 coarse
aggr particles near top of
core - did not wash off

Dried uniformly except for entrapped air voids
- some white residue noted near top of specimen

Diagram of core:



TR-406 - Concrete Core Log-In Form

Sample Identification: I-80 DALLAS Sta 966+20
It Near Q

General Observations:
Dimensions: 4 x 1 1/2

Surface conditions: Tined ~ 1 to 2mm deep

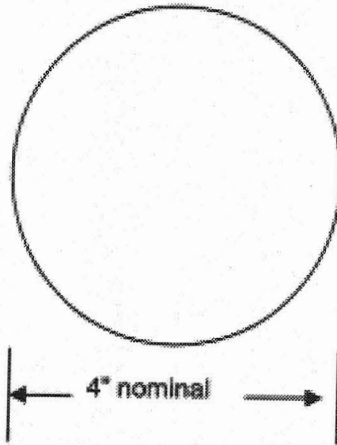
Bottom: Crusted Agg base

Reinforcement: steel @ - 11" - 11 1/4"

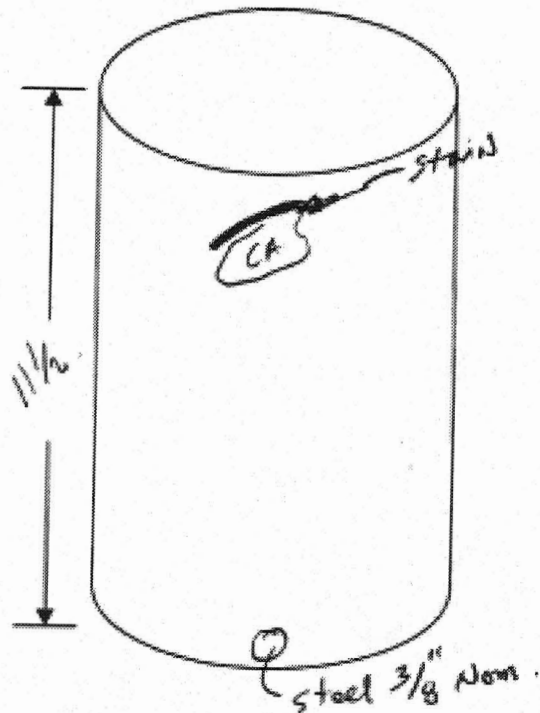
Cracks, comments: Some CA staining that doesn't wash off
Dried uniformly except for entrapped voids

Diagram of core:

Top view



Side View



TR-406 - Concrete Core Log-In Form

Sample Identification: I80 WB Cass Co.
about 4' from G

General Observations:

Dimensions: _____

Surface conditions: looked good ^{few} ~~no~~ entrapped air voids

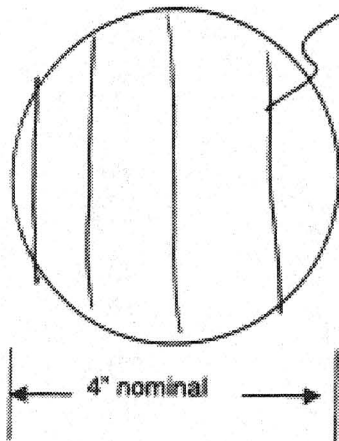
Bottom: Rough

Reinforcement: None

Cracks, comments: No cracks observed (except
for some marks at interface of
base & concrete)

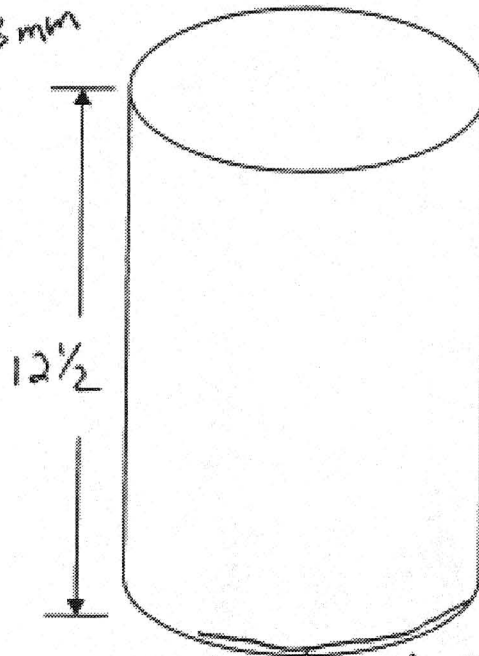
Diagram of core:

Top view



lines
vary from
0 to 3mm

Side View



slight crack withing
1/4" of base

TR-406 - Concrete Core Log-In Form

Sample Identification: I-80 WB - CASS
12-panel

General Observations:

Dimensions: _____

Surface conditions: Entrapped Air voids common (~0.5")

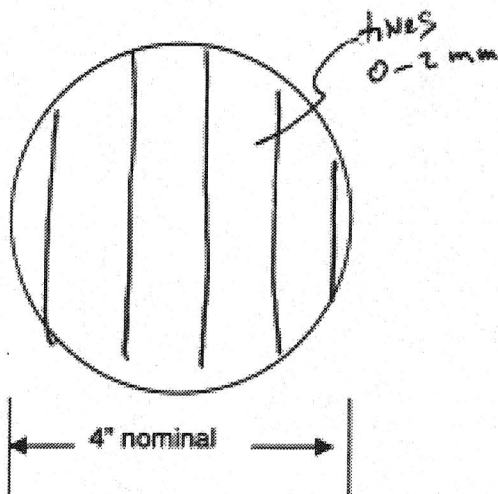
Bottom: Rough

Reinforcement: NONE

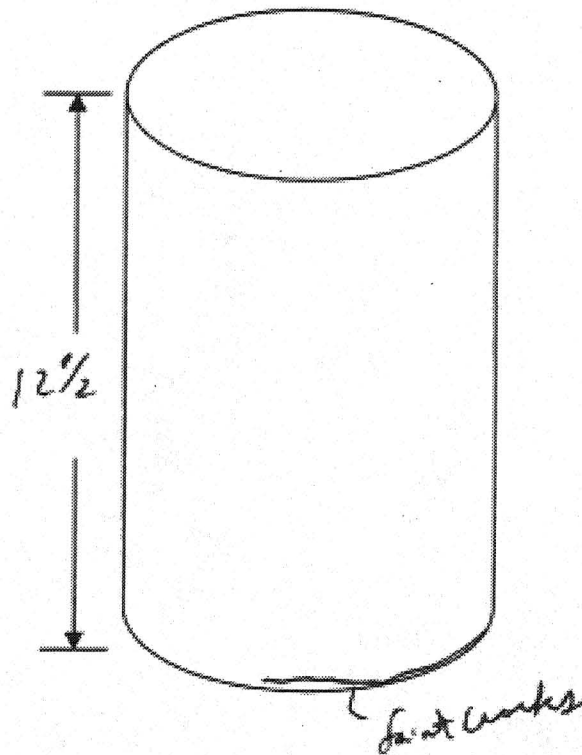
Cracks, comments: No cracks evident (except
some questionable ones at very base)

Diagram of core:

Top view



Side View



TR-406 - Concrete Core Log-In Form

Sample Identification: I-80 WB Cass Co.
Joint

General Observations:

Dimensions: _____

Surface conditions: looked good

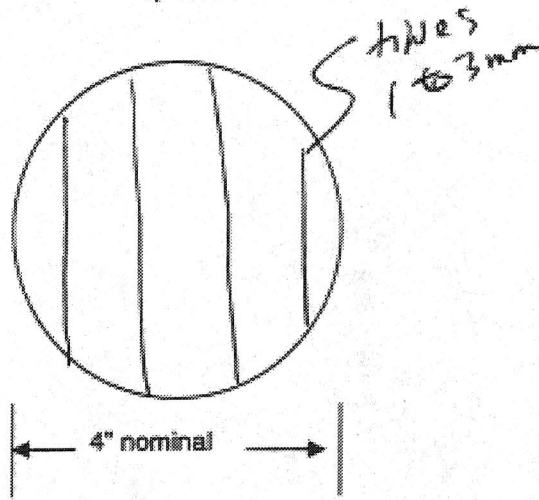
Bottom: rough

Reinforcement: Yes 3/8" diam.

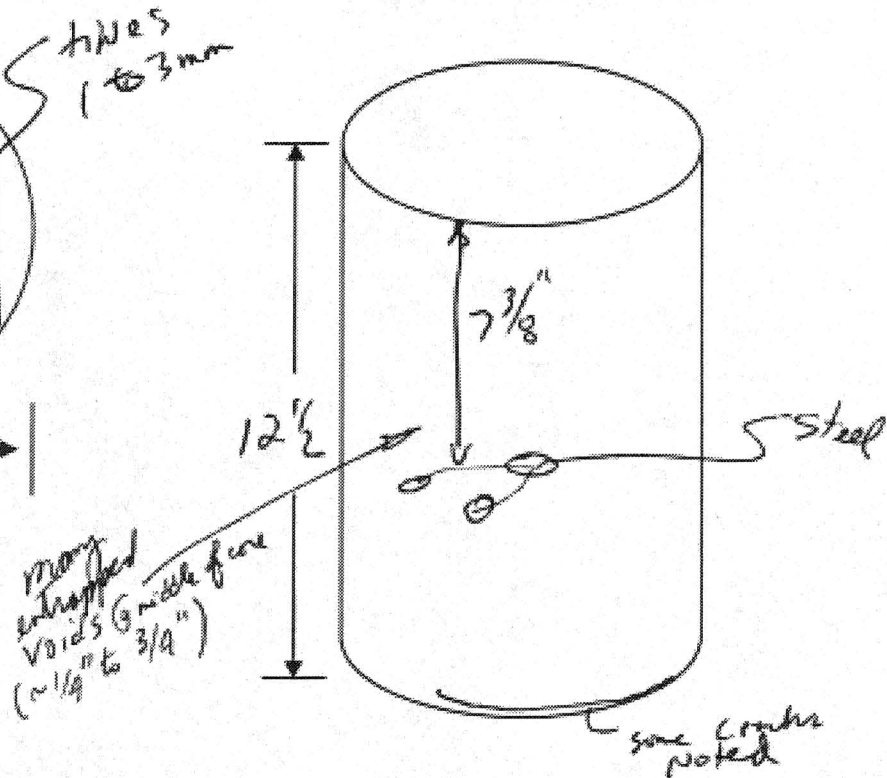
Cracks, comments: Some cracking noted @ bottom of core

Diagram of core:

Top view



Side View



TR-406 - Concrete Core Log-In Form

Sample Identification: IA-2 MP2.6 WB
STA 1498+95 JOINT

General Observations:

Dimensions: see below

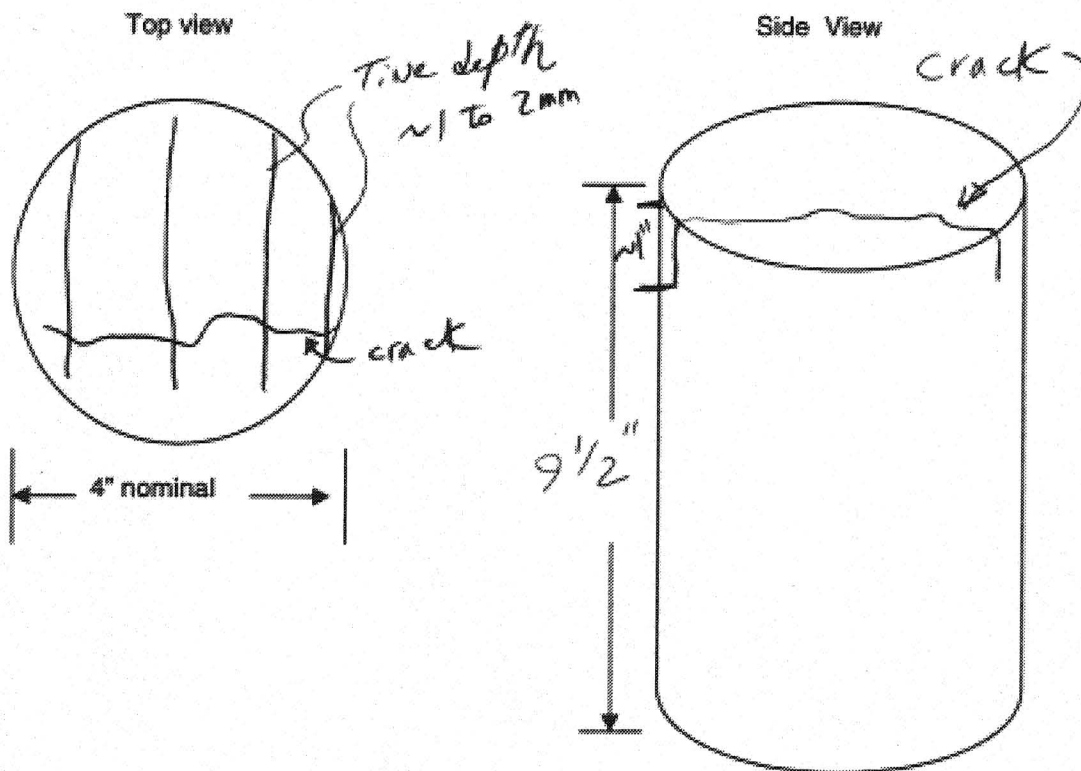
Surface conditions: _____

Bottom: ? Econocrete BASE

Reinforcement: NONE

Cracks, comments: Crack on Top surface of core,
penetrates about 1" below top surface
No material filled the crack
Some damp spots dried to leave white material

Diagram of core:



TR-406 - Concrete Core Log-In Form

Sample Identification: IA-2 MP 2.6 WB
STA 1498+85 Midpanel

General Observations:

Dimensions: see Below

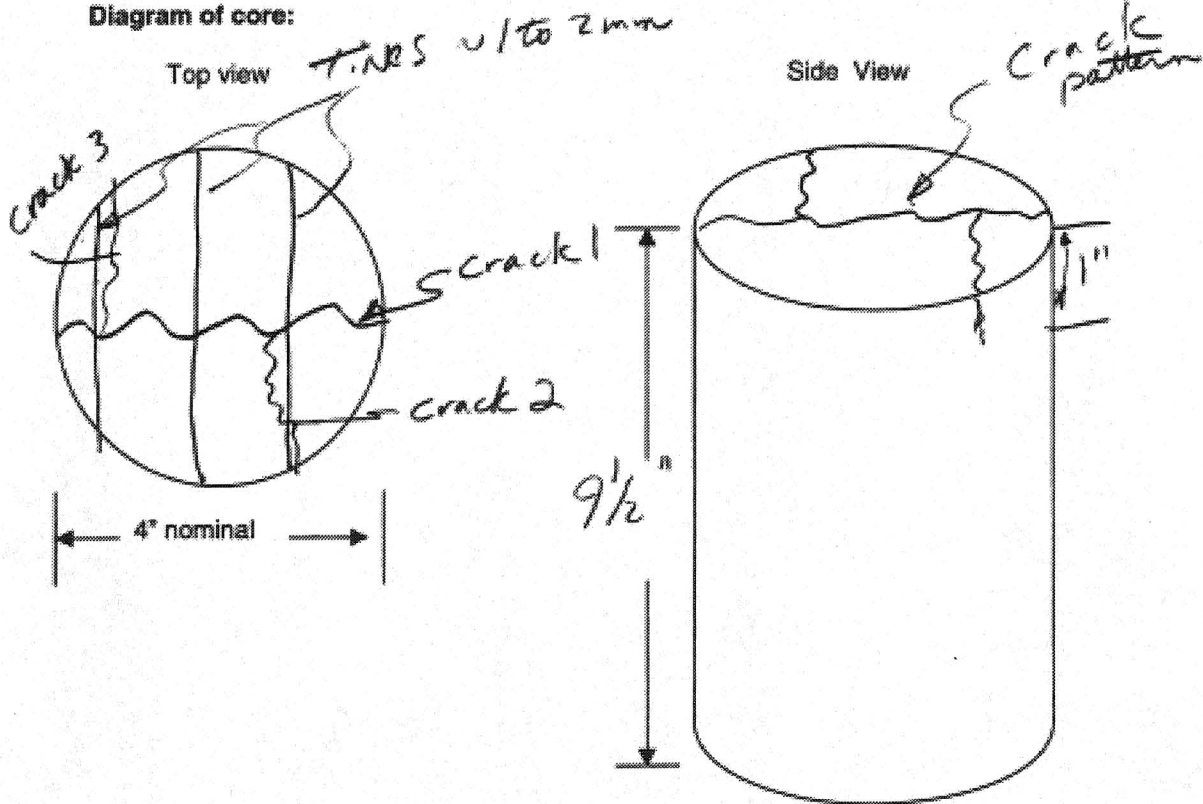
Surface conditions: cracking noted on top surface

Bottom: 2 concrete base

Reinforcement: NONE

Cracks, comments: Cracks evident on top surface - random
from main crack - The cracks
penetrated about 1" into core. No
material found in cracks. One shell
particle popout noted.

Diagram of core:



TR-406 - Concrete Core Log-In Form

Sample Identification: IA - 2 WB
STA 1499 ? Joint or Midpanel

General Observations:

Dimensions: see below

Surface conditions: No cracks & voids

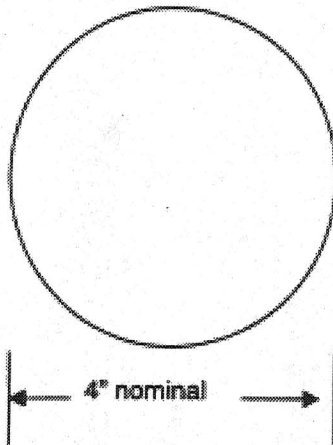
Bottom: ? concrete base

Reinforcement: NONE

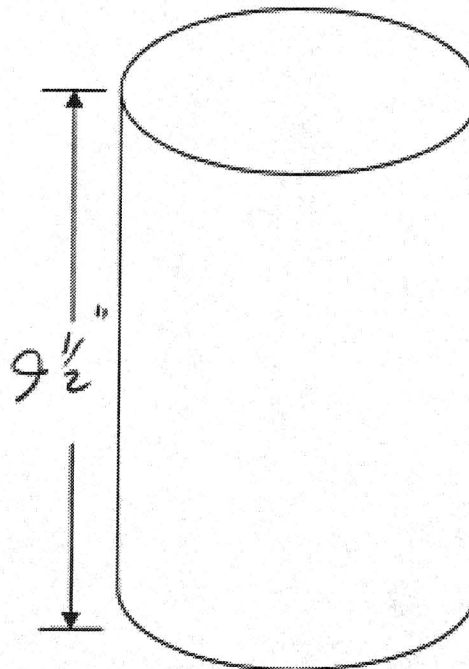
Cracks, comments: No cracks
some areas dried to leave a
white residue

Diagram of core:

Top view



Side View



TR-406 - Concrete Core Log-In Form

Sample Identification: IA - No 0 EB STA 362
mid panel

General Observations:

Dimensions: _____

Surface conditions: Some spotty white deposits noted near shale particles

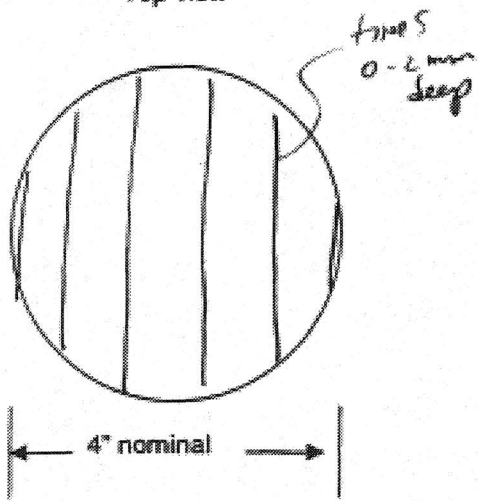
Bottom: Rough

Reinforcement: NONE

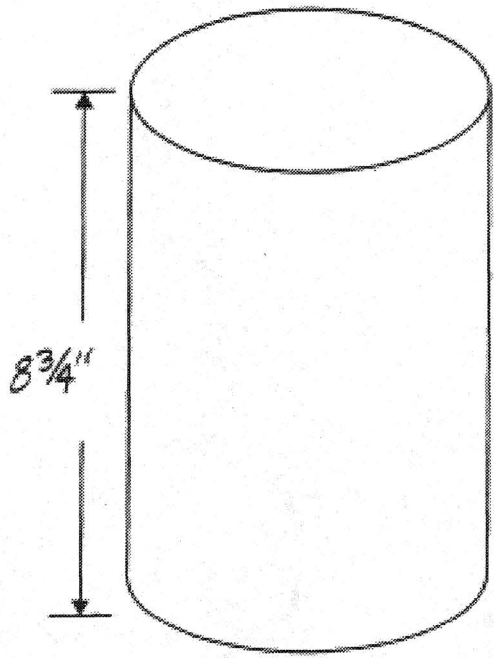
Cracks, comments: NONE evident on core

Diagram of core:

Top view



Side View



TR-406 - Concrete Core Log-In Form

Sample Identification: IA - 160 EB STA 362
Joint 4' from G

General Observations:

Dimensions: _____

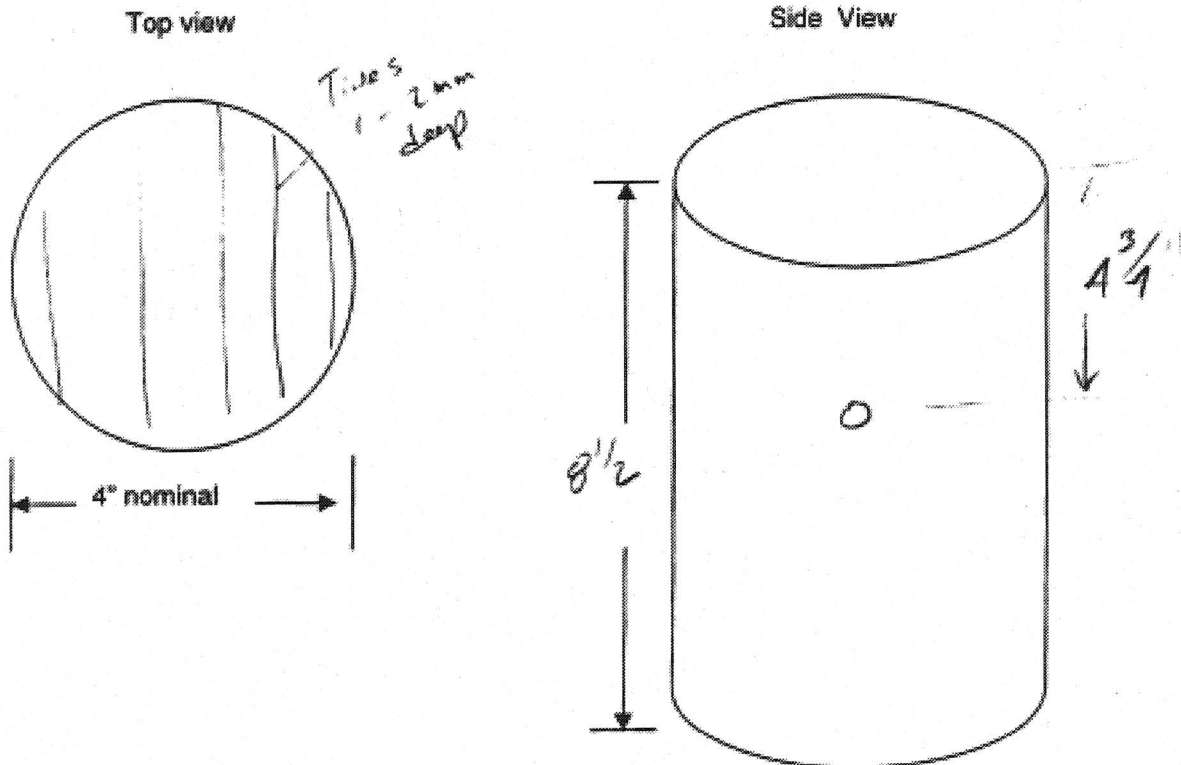
Surface conditions: Note - some reactive shale particles

Bottom: rough - ? gravel base

Reinforcement: Steel G ϕ 4 3/4"

Cracks, comments: Note some reactive shale particles
on outside of core - no real
cracking was evident

Diagram of core:



TR-406 - Concrete Core Log-In Form

Sample Identification: US 218 SB
CA JOINT 6 MP95

General Observations:

Dimensions: _____

Surface conditions: some large entrapped voids in top 6" of core

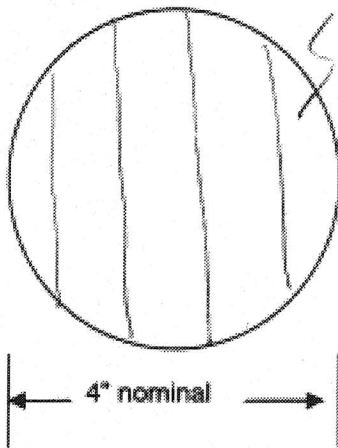
Bottom: SMOOTH

Reinforcement: NONE

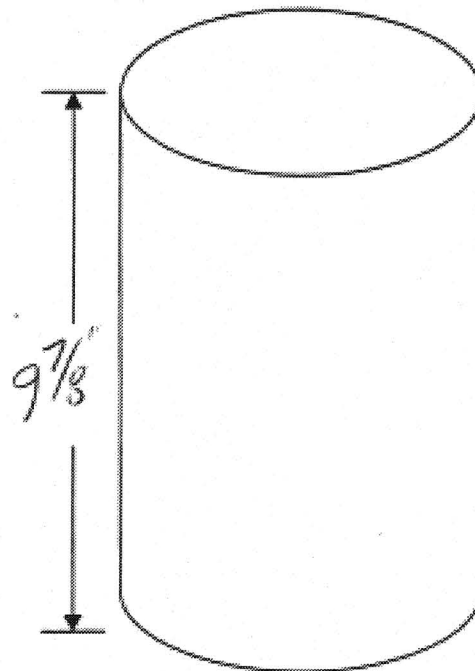
Cracks, comments: No cracks evident
White residue sometimes evident
near fine aggregate particles
Core did not feel very slick when wet

Diagram of core:

Top view



Side View



TR-406 - Concrete Core Log-In Form

Sample Identification: US 21B SB (Passing lane)
mid panel CA MP 25

General Observations:

Dimensions: _____

Surface conditions: Many entrapped air voids noted in top 6" of core

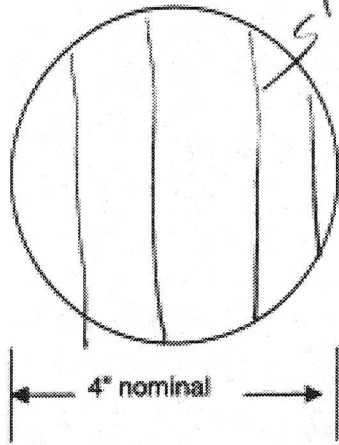
Bottom: Smooth Bottom

Reinforcement: NONE

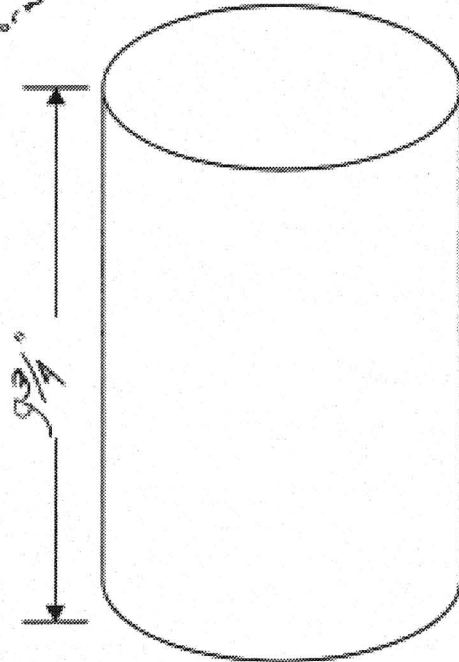
Cracks, comments: No cracks evident
little white residue as noted compared
to NB cores

Diagram of core:

Top view



Side View



*STIPES
~2 or 3 mm
deep
fully uniform*

TR-406 - Concrete Core Log-In Form

Sample Identification: US 218 NB
MP 91.96 Co Joint

General Observations:

Dimensions: _____

Surface conditions: one top crack evident, fixed ~2mm deep

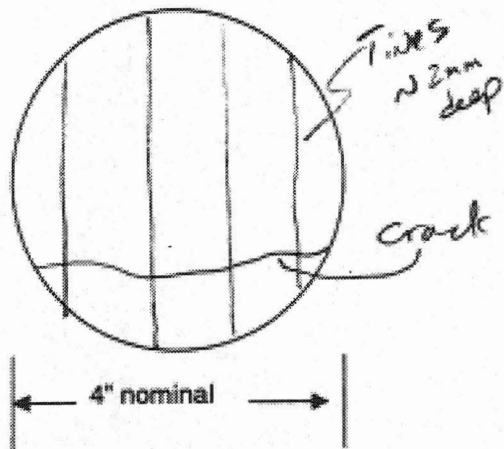
Bottom: ? concrete base

Reinforcement: None evident

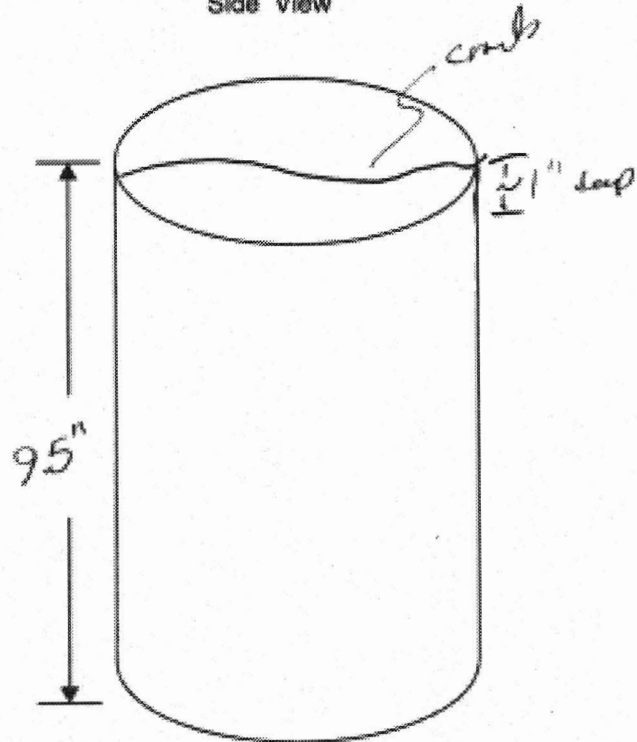
Cracks, comments: Much white residue on side of
core associated with fine aggregate
particles - some shale + some dirt
top surface crack penetrated ~1" into core

Diagram of core:

Top view



Side View



TR-406 - Concrete Core Log-In Form

Sample Identification: US 218 NB
NB - MP 91.96 (9 dia of long + 7 cov) 0.15

General Observations:

Dimensions: _____

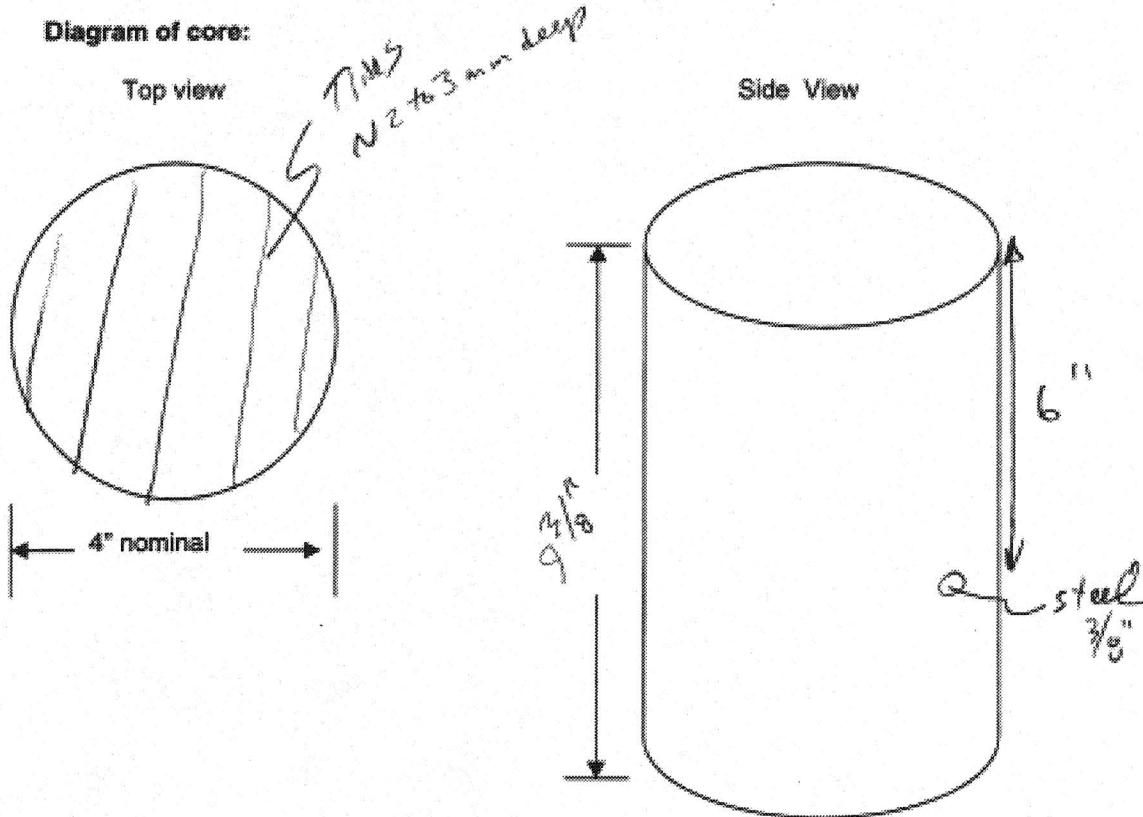
Surface conditions: Good - fines ~ uniform - no cracking

Bottom: Smooth - ? re concrete base

Reinforcement: Yes, 3/8" bars @ 6" from top

Cracks, comments: much white surface staining on sides of core
some shade; clast particles
Surface feels slick when wet - perhaps
white residue is Ca(OH)₂

Diagram of core:



TR-406 - Concrete Core Log-In Form

Sample Identification: US 218 NB
Mid panel @ MP 91.76

General Observations:

Dimensions: _____

Surface conditions: Good - No cracks evident

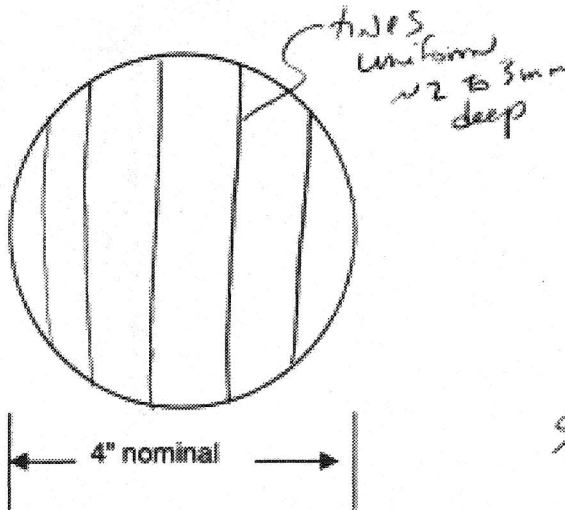
Bottom: Smooth - ? concrete layer

Reinforcement: None

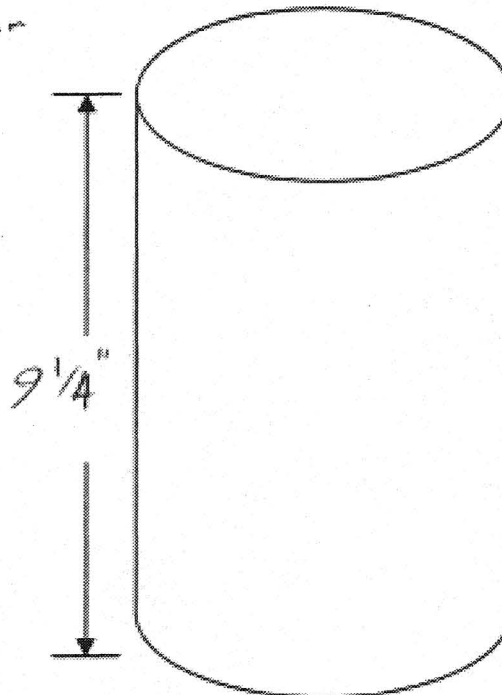
Cracks, comments: Sides feel slick when wet
and less white residue on sides as
compared to joint specimens

Diagram of core:

Top view



Side View



TR-406 - Concrete Core Log-In Form

Sample Identification: HWJ61 Near MP 125
C JOINT

General Observations:

Dimensions: _____

Surface conditions: TINES uniform but shallow

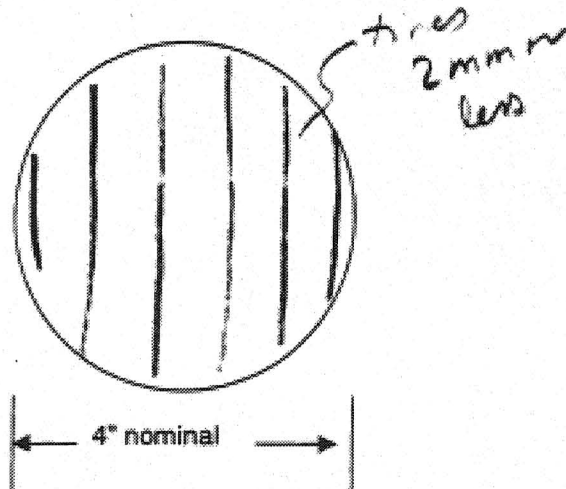
Bottom: NOT Present

Reinforcement: NOSE EVIDENT

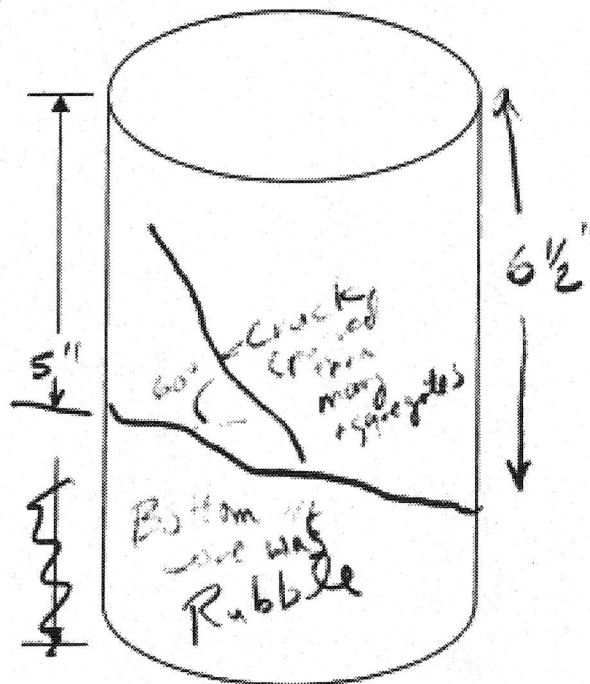
Cracks, comments: Bottom 1/3 of core was rubble
Some cracked as shown in drawing
Some white efflorescence on portions
of the core

Diagram of core:

Top view



Side View



TR-406 - Concrete Core Log-In Form

Sample Identification: HWY 61 North Near MP 125
Hole Near joint

General Observations:

Dimensions: _____

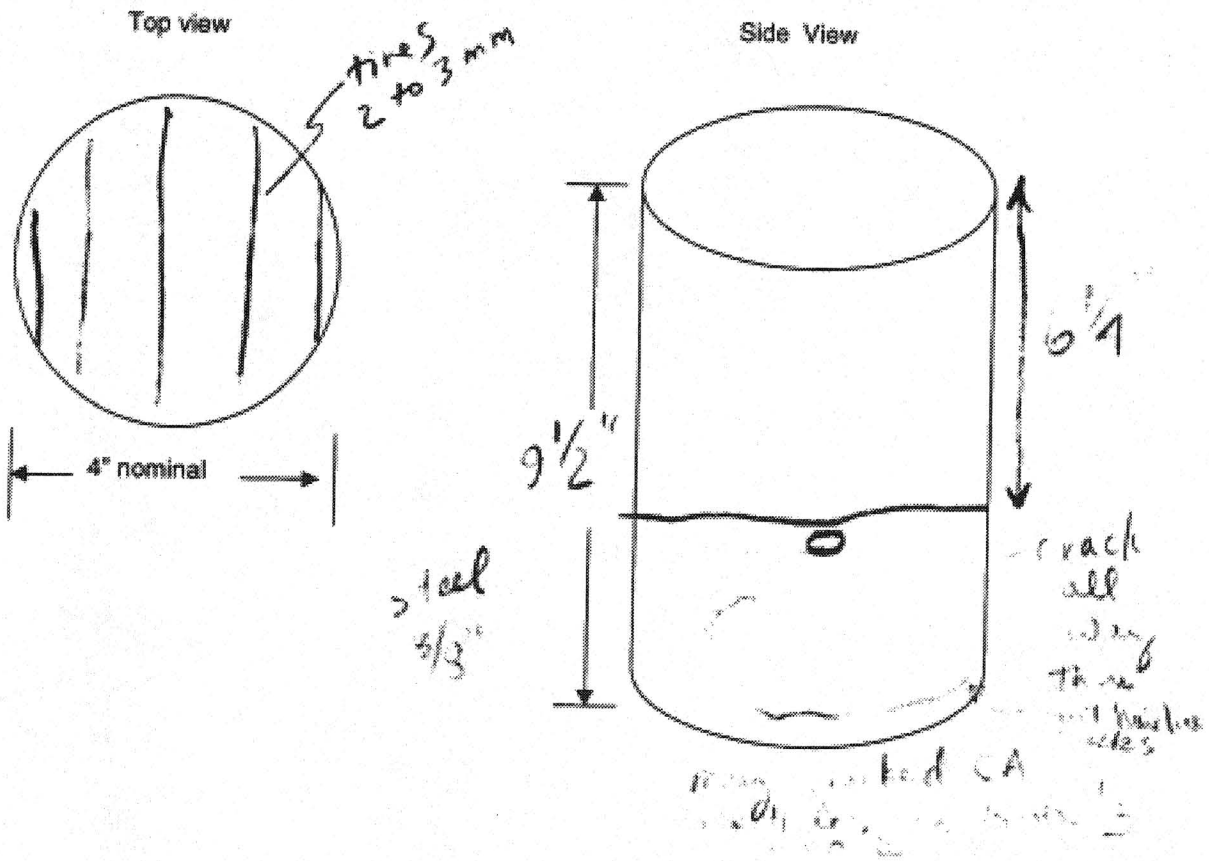
Surface conditions: fair uniform

Bottom: rough -

Reinforcement: 3/8" dia. 6 @ 1/2"

Cracks, comments: Cracking of CA common below
steel reinforcement. None noted
above steel.

Diagram of core:



TR-406 - Concrete Core Log-In Form

Sample Identification: HWY 61
1' from JOINT

General Observations:

Dimensions: _____

Surface conditions: Tined

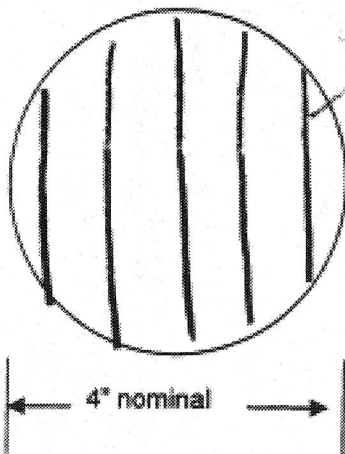
Bottom: Rough

Reinforcement: NONE

Cracks, comments: Bottom of core (last 1/2")
shows fine hairline cracks
thin paste & CA - many
CA particles are cracked

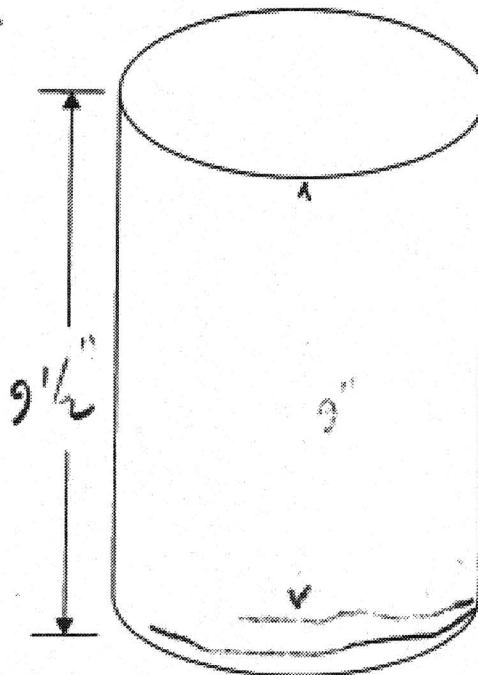
Diagram of core:

Top view



*7 mil
1000 mm
uniform*

Side View



*fine cracks
some
thin
paste &
CA*

TR-406 - Concrete Core Log-In Form

Sample Identification: HWY 61 MP 125
mid panel

General Observations:

Dimensions: _____

Surface conditions: Tined surface

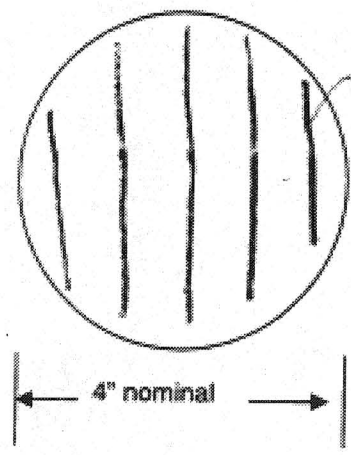
Bottom: Rough base

Reinforcement: NONE

Cracks, comments: severe cracking @ base of
core

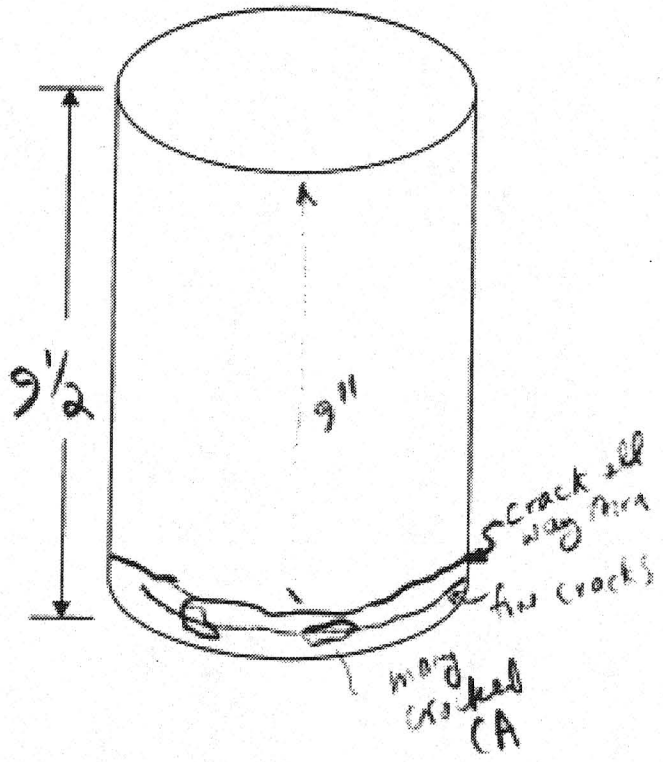
Diagram of core:

Top view



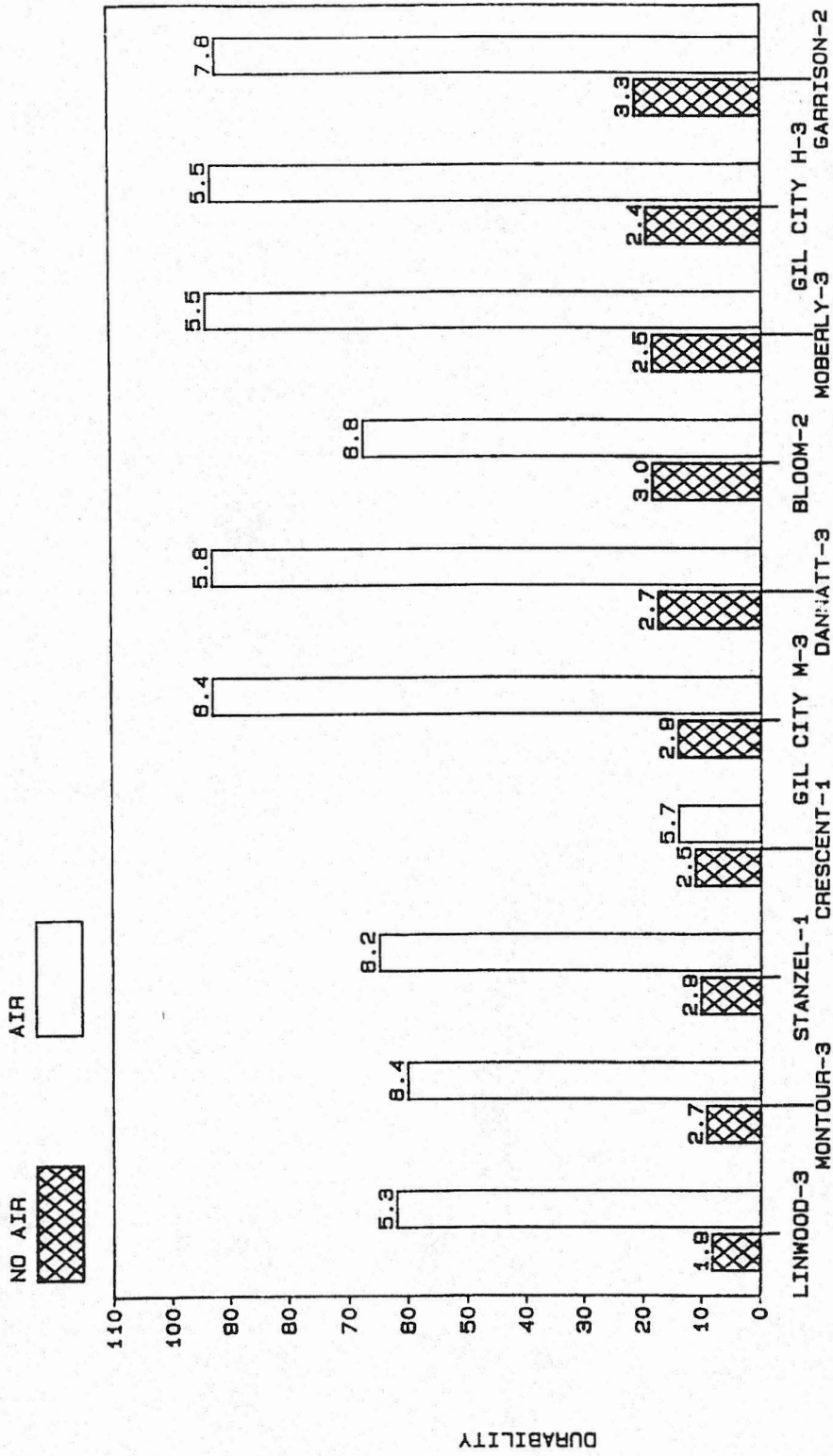
*rebar's uniform
2 to 3 mm*

Side View



APPENDIX C: IOWA DOT ASTM C 666 DATA

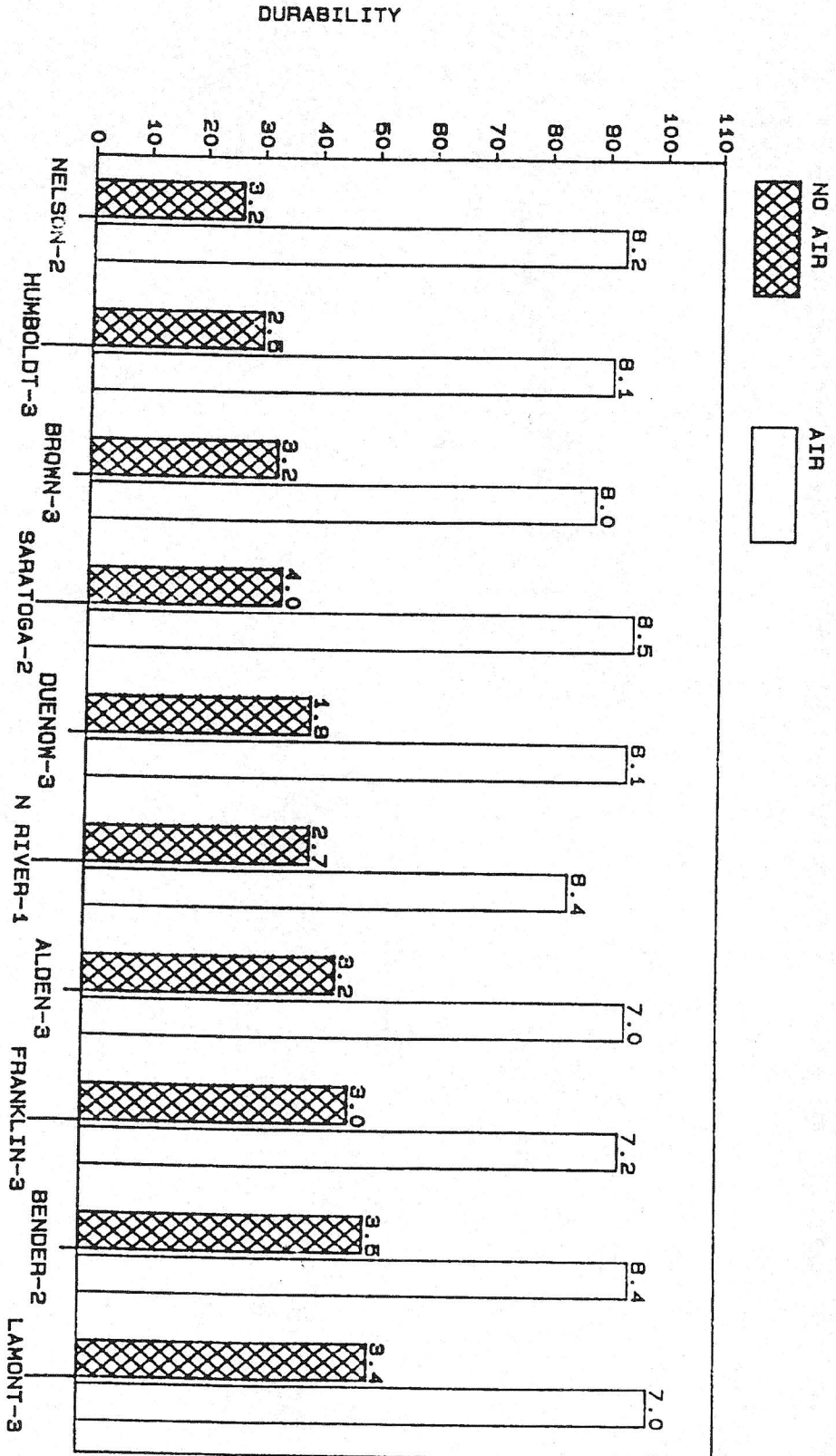
DURABILITY FACTORS
AIR ENTRAINMENT VS NO AIR ENTRAINMENT



AGG SOURCE AND CLASS

IOWA DOT JANUARY 1985
GEOLOGY SECTION
1-515-238-1204

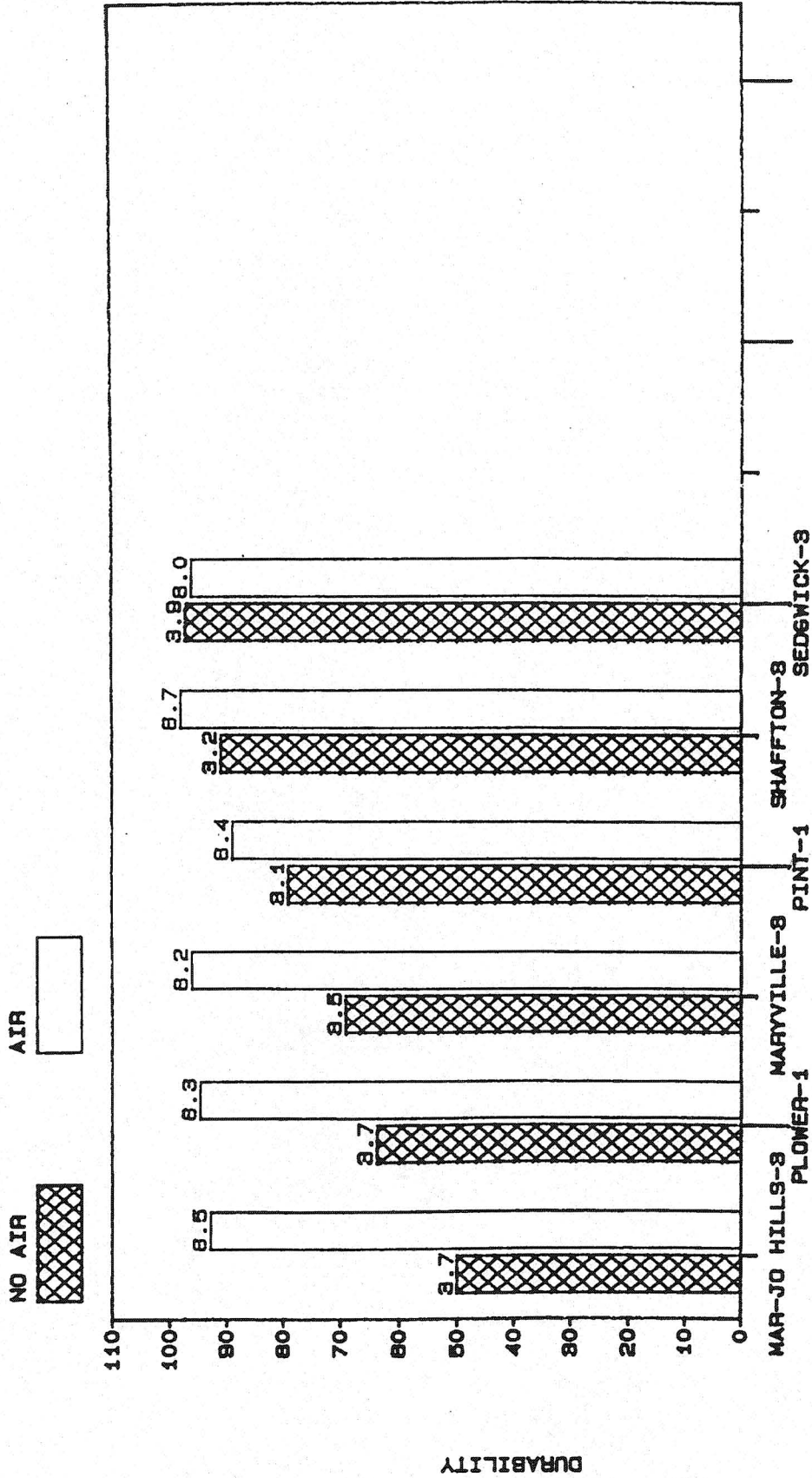
DURABILITY FACTORS AIR ENTRAINMENT VS NO AIR ENTRAINMENT



TOWA DOT JANUARY 1985
GEOLOGY SECTION
1-515-239-1204

AGG SOURCE AND CLASS

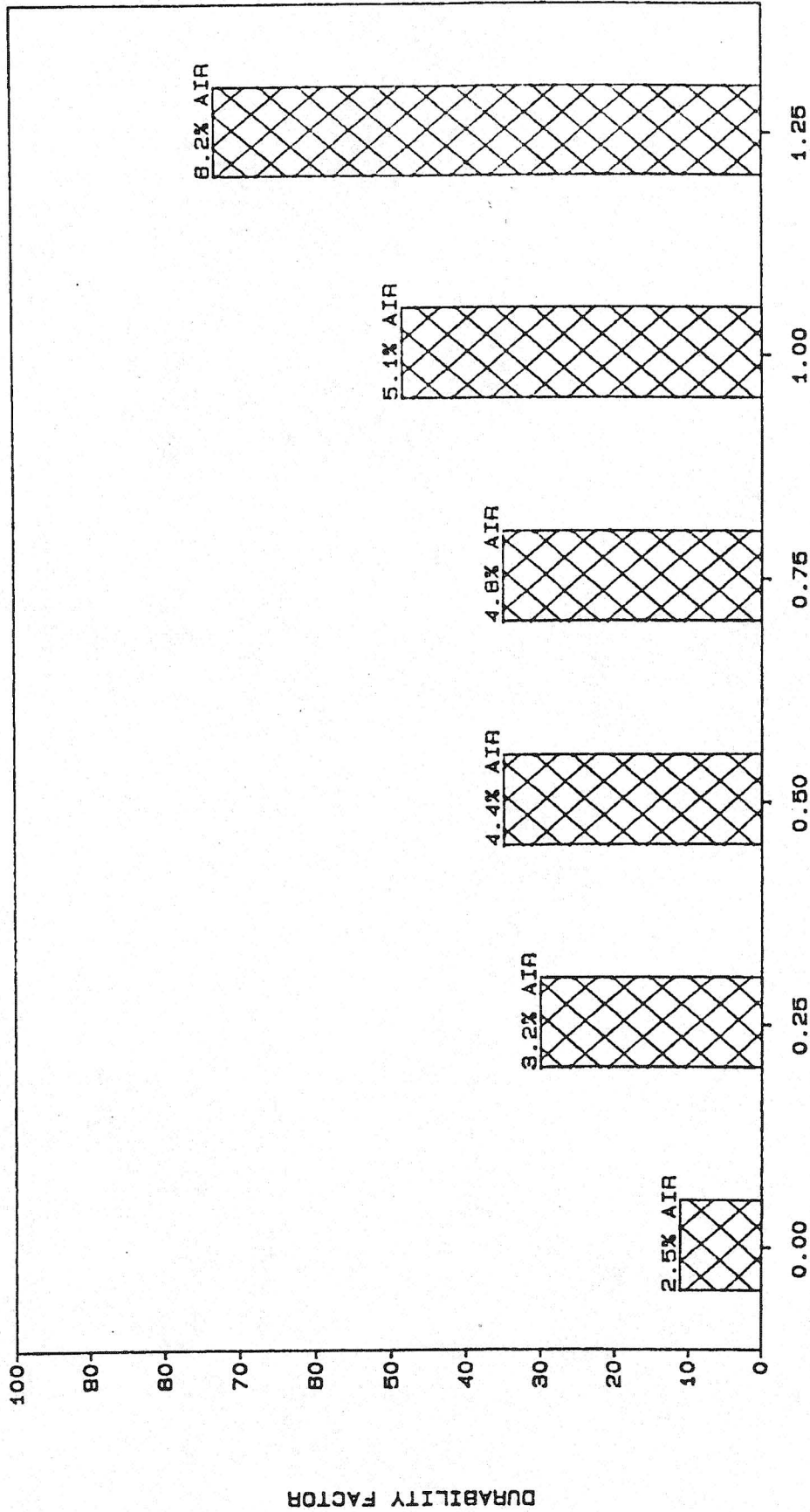
DURABILITY FACTORS AIR ENTRAINMENT VS NO AIR ENTRAINMENT



AGG SOURCE AND CLASS

IOWA DOT JANUARY 1985
GEOLOGY SECTION
1-515-239-1204

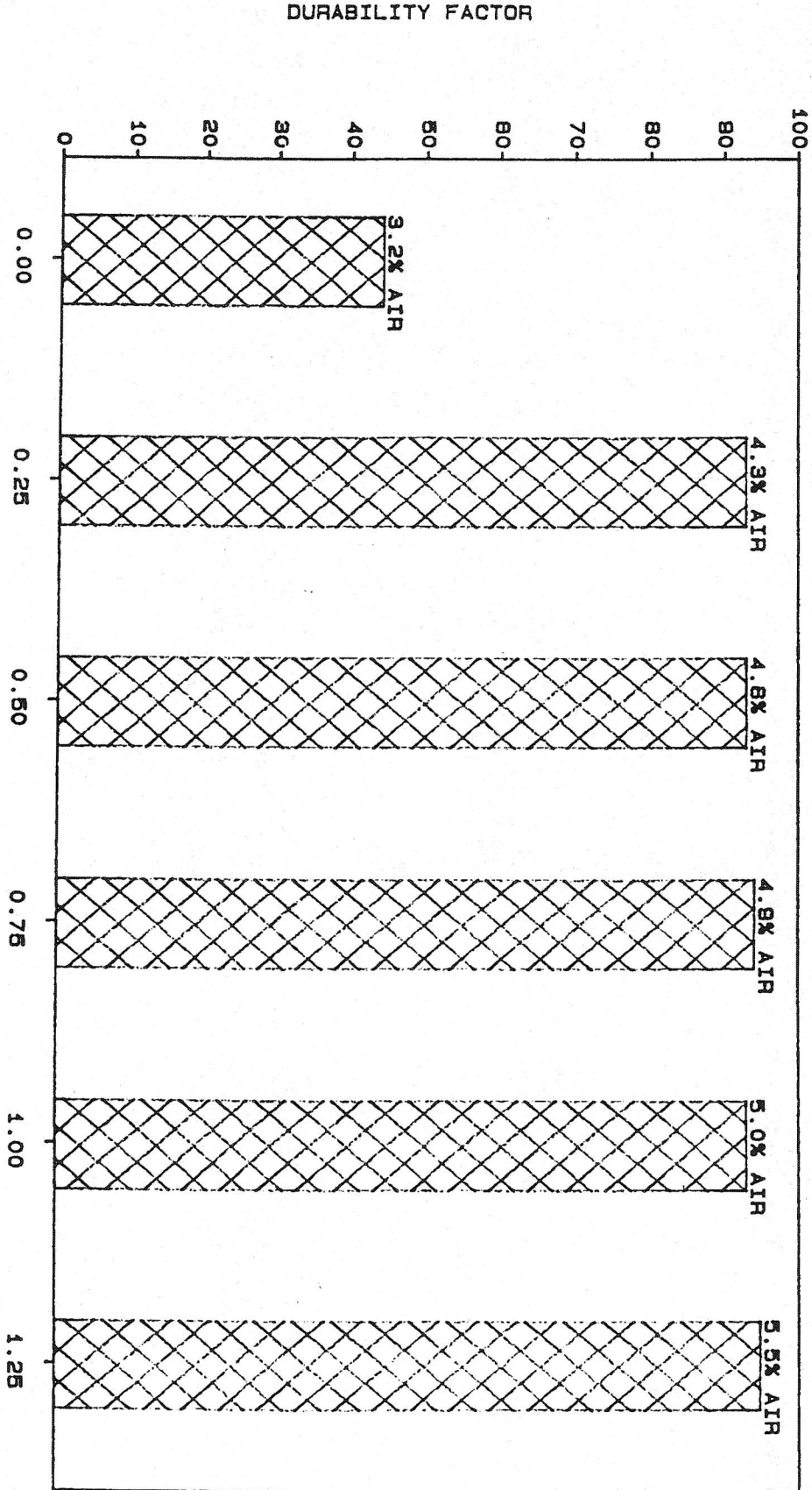
EFFECT OF AIR CONTENT ON DURABILITY FACTOR CRESCENT QUARRY



OUNCES OF AD-AIRE

IOWA DOT JANUARY 1986
GEOLOGY SECTION
1-515-238-1204

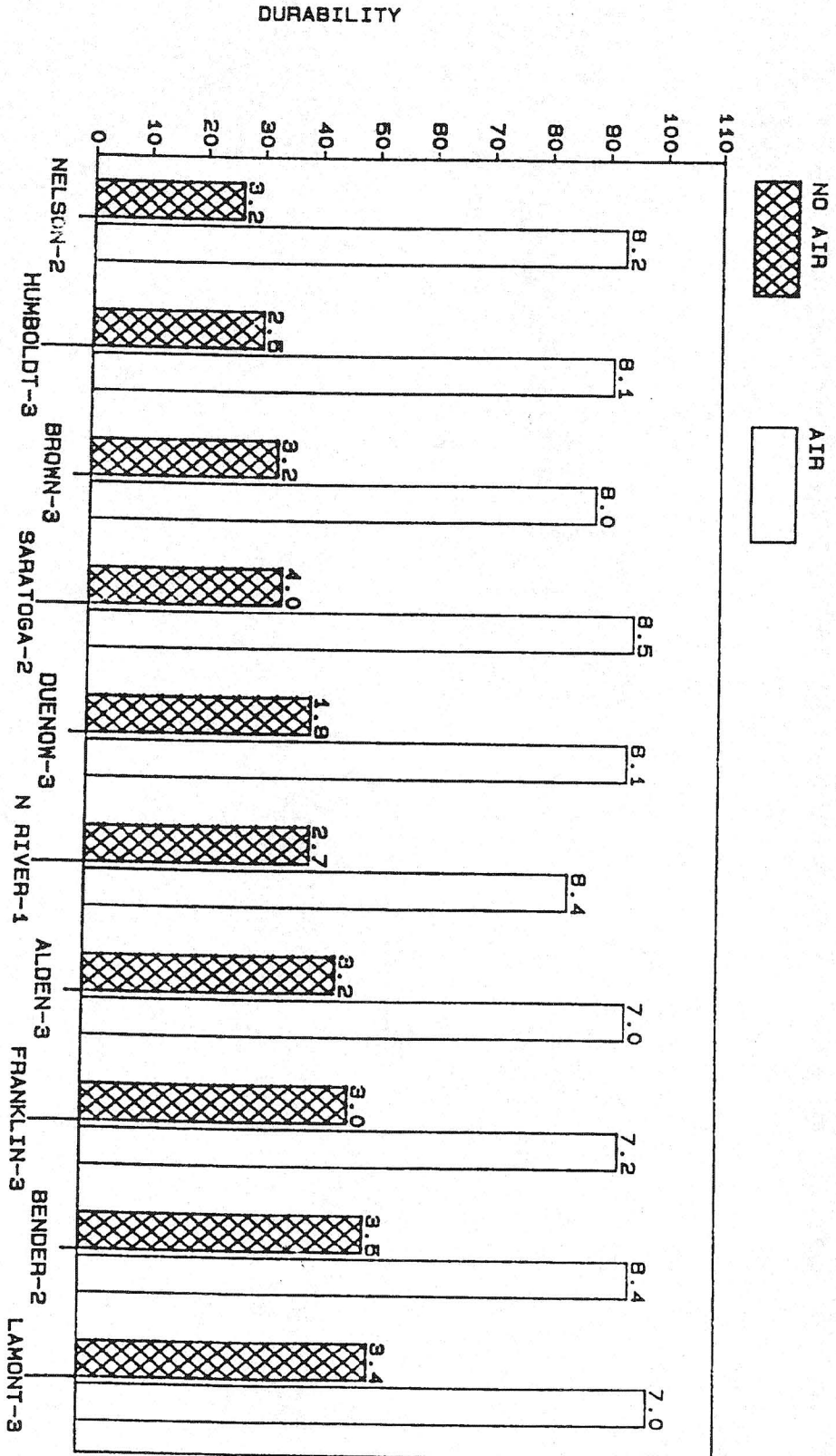
EFFECT OF AIR CONTENT ON DURABILITY FACTOR ALDEN QUARRY



IOWA DOT JANUARY 1988
GEOLOGY SECTION
1-515-239-1204

OUNCES OF AD-AIRE / per sack

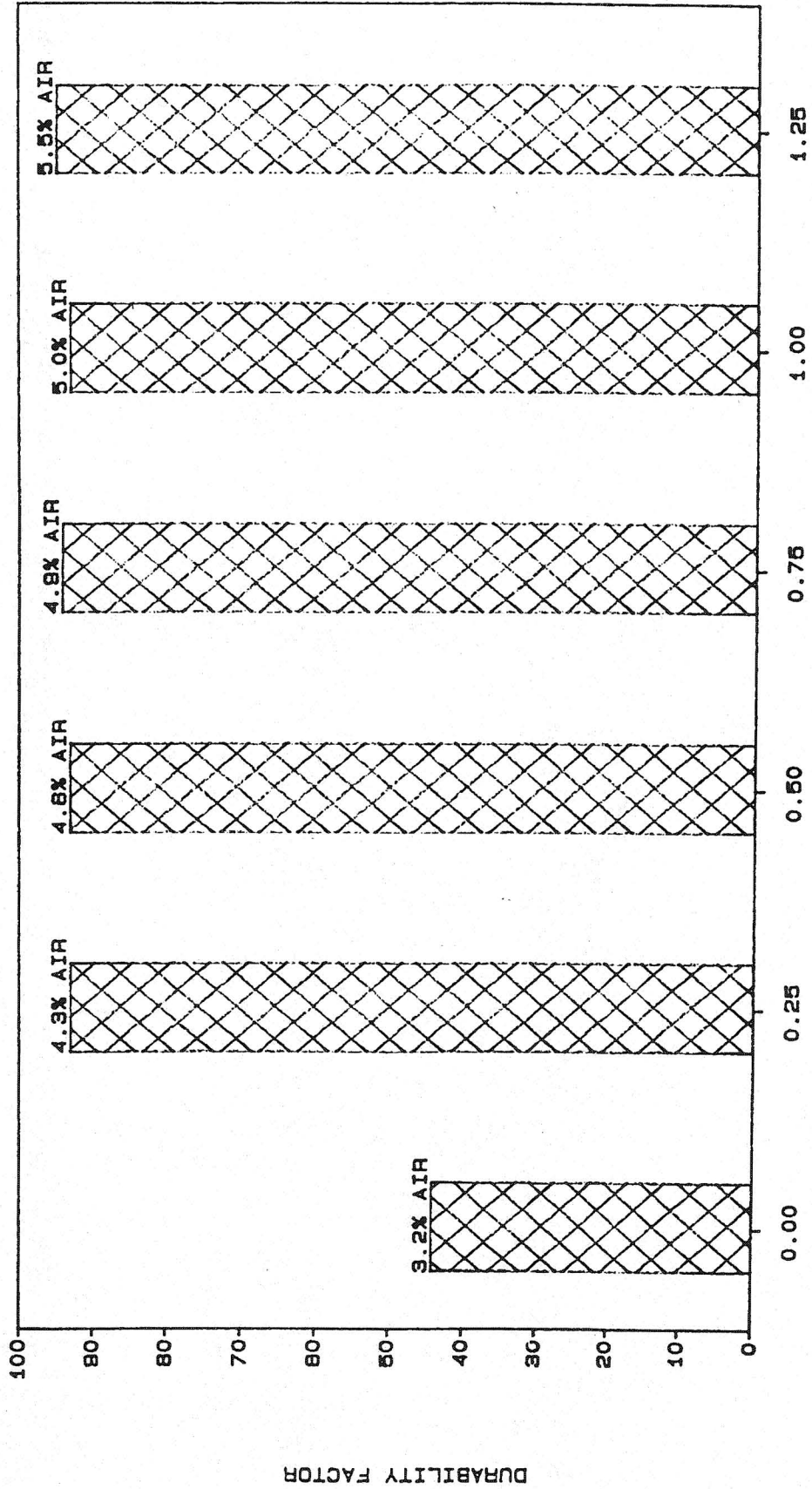
DURABILITY FACTORS AIR ENTRAINMENT VS NO AIR ENTRAINMENT



TOWA DOT JANUARY 1985
GEOLOGY SECTION
1-515-239-1204

AGG SOURCE AND CLASS

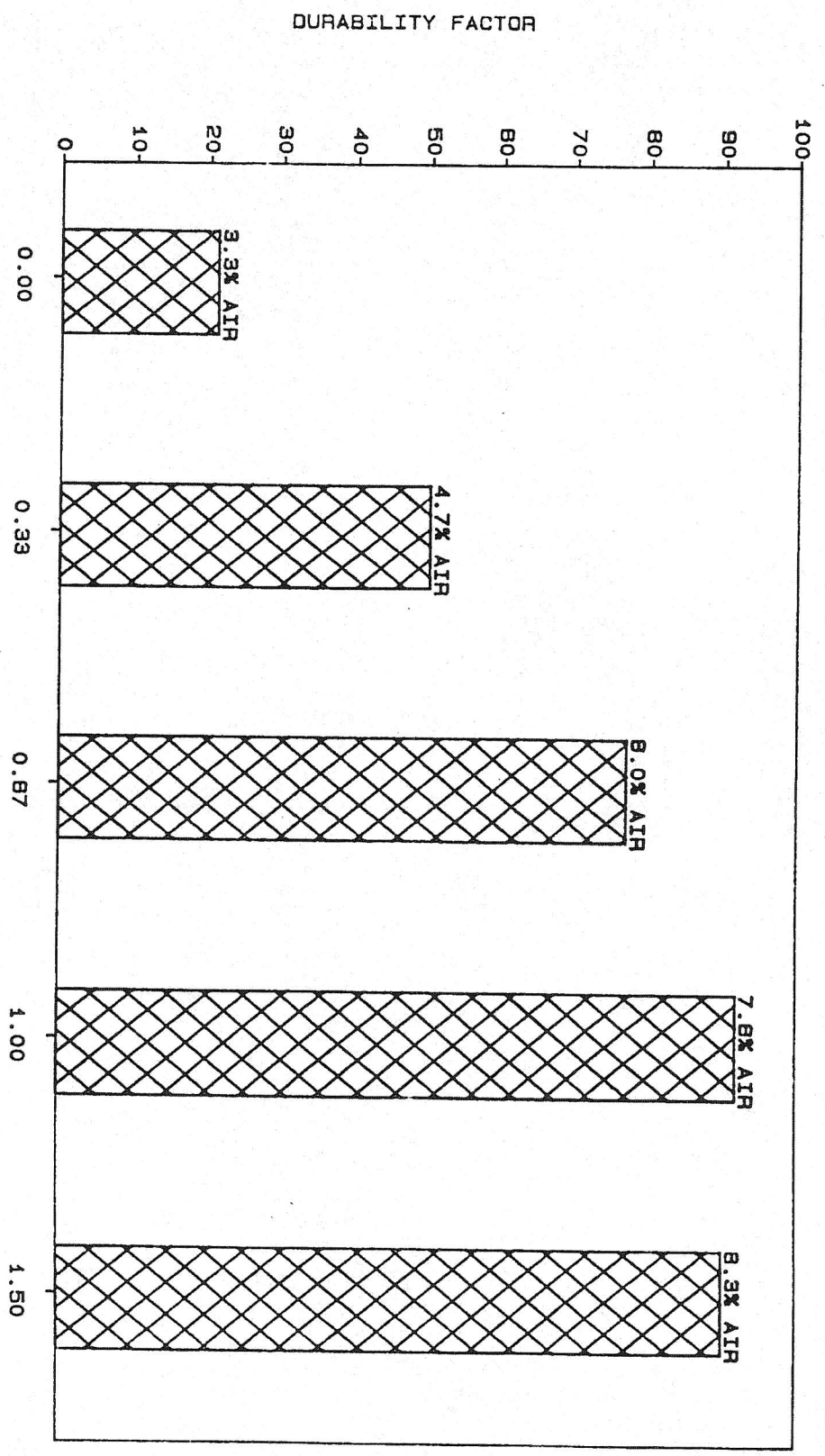
EFFECT OF AIR CONTENT ON DURABILITY FACTOR ALDEN QUARRY



OUNCES OF AD-AIRE / per sack

IOWA DOT JANUARY 1985
GEOLOGY SECTION
1-515-239-1204

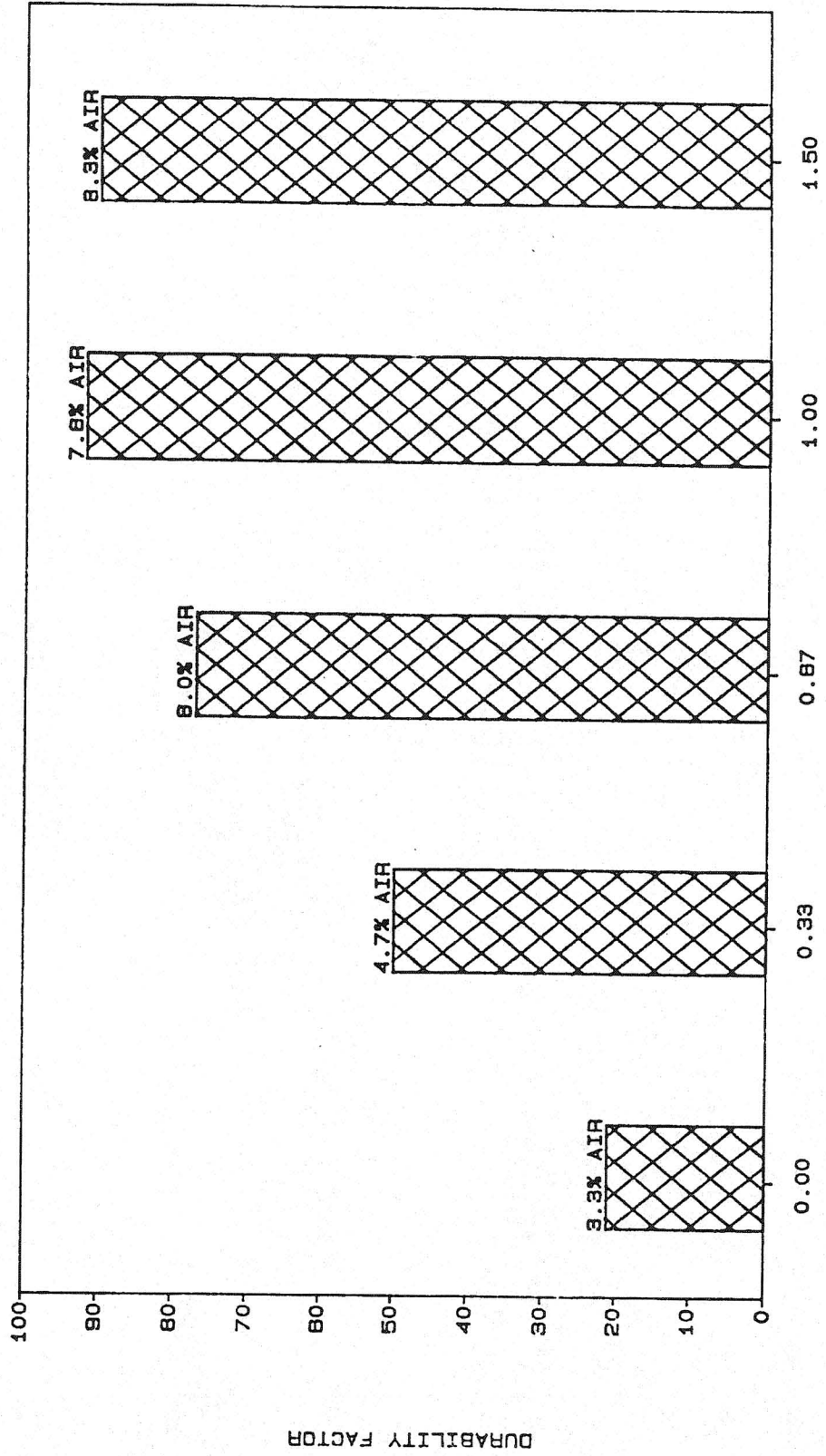
EFFECT OF AIR CONTENT ON DURABILITY FACTOR GARRISON QUARRY



IOWA DOT JANUARY 1985
GEOLOGY SECTION
1-515-239-1204

OUNCES OF AD-AIRE

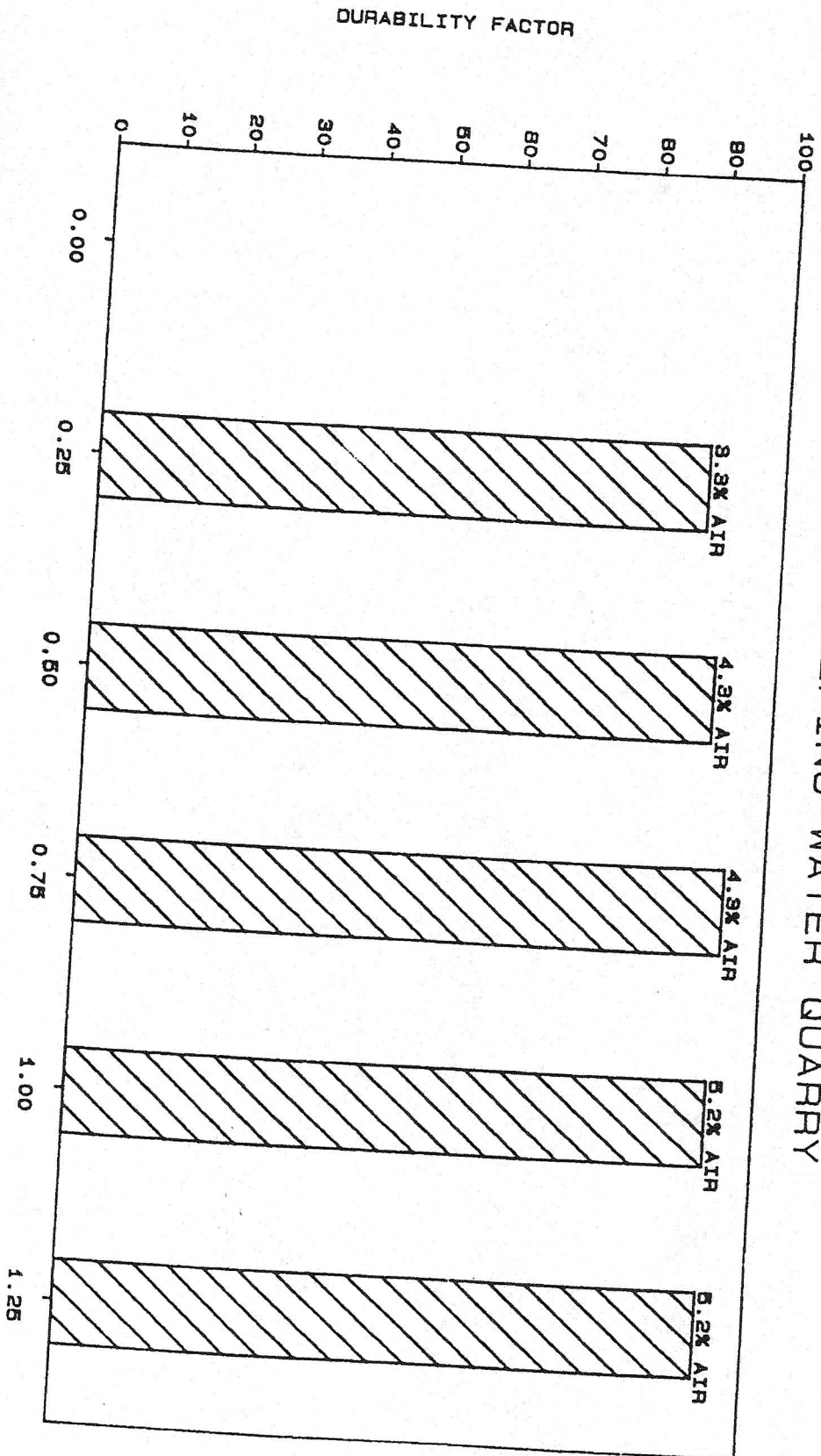
EFFECT OF AIR CONTENT ON DURABILITY FACTOR GARRISON QUARRY



OUNCES OF AD-AIR

IOWA DOT JANUARY 1985
GEOLOGY SECTION
1-515-239-1204

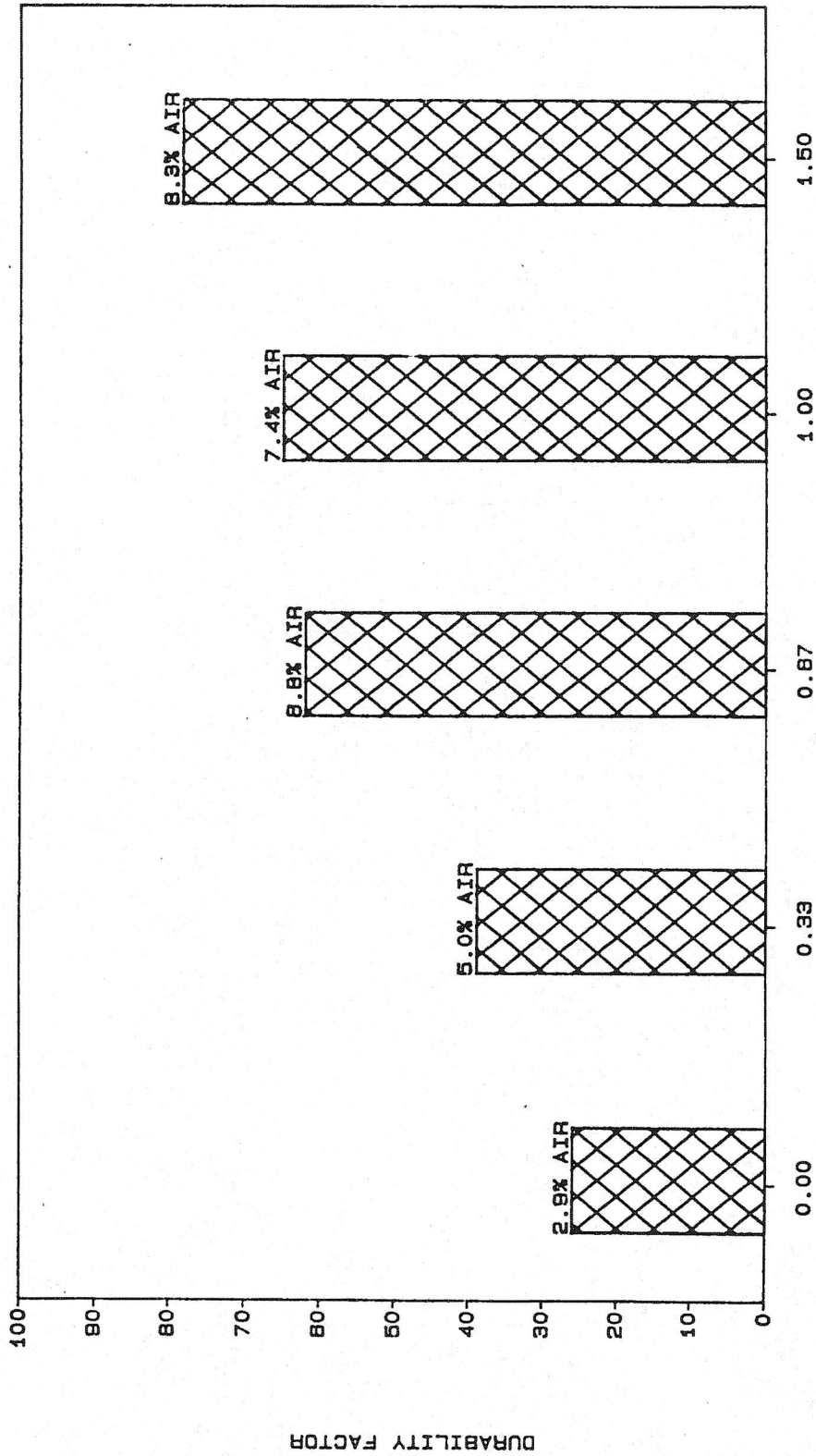
EFFECT OF AIR CONTENT ON DURABILITY FACTOR KERFORD WEEPING WATER QUARRY



IOWA DOT JANUARY 1985
GEOLOGY SECTION
1-818-238-1204

OUNCES OF AD-AIR

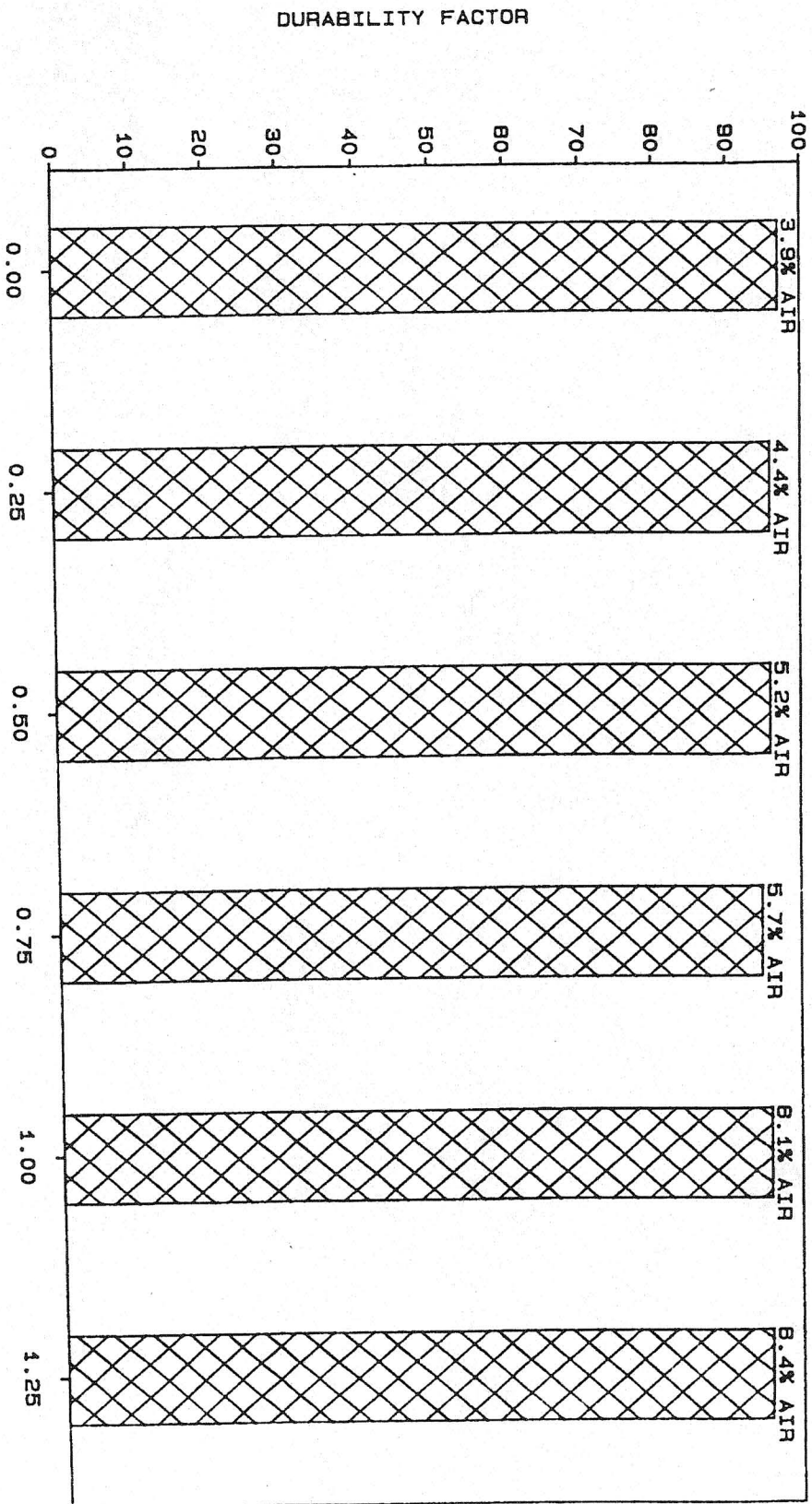
EFFECT OF AIR CONTENT ON DURABILITY FACTOR MONTOUR QUARRY



OUNCES OF AD-AIRE

IOWA DOT JANUARY 1985
GEOLOGY SECTION
1-515-239-1204

EFFECT OF AIR CONTENT ON DURABILITY FACTOR SEDGWICK QUARRY



IOWA DOT JANUARY 1985
GEOLOGY SECTION
1-515-238-1204

DUNCES OF AD-AIR

APPENDIX D: PETROGRAPHIC SUMMARIES AND SITE INFORMATION

Site	Road/County	Premature distress	Cement source	Aggregates Coarse/Fine	Fly Ash source/%	water reducer	Curing method
1	US 20/Webster	No	Lehigh	Ft. Dodge/Croft	None	Plastocrete 161	White cure
2	US 20/Hamilton	Yes	Lehigh	Ft. Dodge/Yates	Port Neal 4/15	None	White cure
3	Hwy 169/Webster	Yes	Lehigh	Ft. Dodge/Croft	None	Plastocrete 161	White cure
4	Hwy 175/Hamilton	No	Penn Dixie	Moberly Mine/Hallet	Port Neal 3/15	None	White cure
5	Hwy 175/Hamilton	No	Penn Dixie	Moberly Mine/Hallet	Council Bluffs/15	None	White cure
6	Hwy 175/Hamilton	No	Penn Dixie	Moberly Mine/Hallet	None	None	White cure
7	Hwy 330/Marshall	Yes	Davenport	? Hallets pit ? let as Ferguson/Clemons	None	WRDA Hycol	White cure
8	I-80/Iowa	Yes	Davenport	Conklin/Kimmich	Louisa/15	Plastocrete 161	White cure
9	I-80/Dallas	No	Davenport	Shaffton/Van Meter	Council Bluffs/15	SIKA 161	White cure
10	I-80/Dallas	Yes	Davenport	Alden/Van Meter	Council Bluffs/15	SIKA 161	White cure
11	I-80/Dallas	No	Ash Grove	Alden/Van Meter	Council Bluffs/15	SIKA 161	White cure
12	I-80/Cass	No	Ash Grove	Shaffton/Finley	Council Bluffs/15	Plastocrete 161	White cure
13	Hwy 2/Fremont	Yes	Ash Grove	Weeping Water/Oreapolis	None	Plastocrete 161	White cure
14	Hwy160/Polk	Yes	?	Ames Mine/?	None	?	?
15	US 218/Johnson	Yes	Davenport	Conklin/Stevens	None	Plastocrete 161	White cure
16	US 218/Johnson	Yes	Davenport	Conklin/Stevens	None	Plastocrete 161	White cure
17	US 61/Scott	No	Lehigh	McCausland/McCausland Pit	None	Plastocrete 161	White cure

Site	Road/County	Location	Premature distress	la DOT mix design	Water/cement ratio	Paving dates	Contractor
1	US 20/Webster	WB, MP 127.55, sta 2002	No	C-3WR	0.40	10/23/1986	Carlson
2	US 20/Hamilton	WB, MP 135.4, sta 49	Yes	C-3C	0.48	05/20/1986	Carlson
3	Hwy 169/Webster	SB, near sta 2002	Yes	C-3WR	0.49	10/10/90 to 10/30/90	Carlson
4	Hwy 175/Hamilton	WB lane, MP 156.2, sta 143	No	A-3-F		05/07 to 05/27/80	Quad City Construction Co.
5	Hwy 175/Hamilton	EB lane, MP 157.5, sta 191	No	A-3-C	0.49	05/07 to 05/27/80	Quad City Construction Co.
6	Hwy 175/Hamilton	EB lane, MP 158.3, sta 244	No	A-3		05/07 to 05/27/80	Quad City Construction Co.
7	Hwy 330/Marshall	NB lane, MP 6.8, sta 74	Yes	C-5WR	0.46	08/15/1983	Carlson
8	I-80/Iowa	EB, MP 210.36, sta 298	Yes	C-3WR-C	0.38	08/24 to 09/25/87	Jensen
9	I-80/Dallas	EB, MP 107.55, sta 509	No	C-4WR-C		05/13/1988	Jensen
10	I-80/Dallas	EB, MP 113.25, sta 810	Yes	C-4WR-C		08/31/1989	Carlson
11	I-80/Dallas	EB, MP 116.2, sta 966	No	C-4WR-C		06/02/1989	Jensen
12	I-80/Cass	WB, MP 68, sta 1019	No	C-4WR-C		04/12 to 08/15/98	Carlson
13	Hwy 2/Fremont	WB, MP 2.6, sta 1499	Yes	47-B Class V	0.45	07/01/86 through 04/28/1987	Godberson/Smith
14	Hwy 160/Polk	EB, near sta 362	Yes	Unknown	?	?	U.S Army Corp.
15	US 218/Johnson	SB, MP 95.45, sta 1658	Yes	C-3WR	0.43	08/21/1984	McCarthy
16	US 218/Johnson	NB, MP 91.96, sta 1498	Yes	C-3WR	0.43	10/23/1984	McCarthy
17	US 61/Scott	NB, MP 125, sta 525	No	C-3WR	0.42 max.	Not on card	Quad City Construction Co.

Highway: US 20/Webster.WB, MP 127.55, sta 2002

Mix details: C-3WR

Coarse Aggregate: Ft. Dodge Limestone
 Fine Aggregate : Croft sand
 Cement : Lehigh
 Fly Ash : None

Observations: Visual inspection and light microscopy

Core Location & Details	Aggregates	Voids	Cracks	Comments
Trans. Joint Section A	Limestone sound Sand contains shale	Few evident	None, except for cracked shale	Gradation OK, some segregation noted
Trans. Joint Section B	Limestone sound Sand contains shale	Entrapped voids normally < 5mm diam.	None, except for cracked shale	Good gradation, few cracked shale particles
Midpanel Section A	Limestone sound Sand contains shale	Some distorted entrapped voids	None, except for cracked shale	Good gradation
Midpanel Section B	Limestone sound Sand contains shale	Some distorted entrapped voids	None, except for cracked shale	Slight segregation noted

Observations: scanning electron microscopy

Location & Details	Air Content, % (mortar basis)	Area Weighted Mean Diameter. (microns)	Comments
Trans. Joint Section A	7.9	298	Some voids lined, few filled
Trans. Joint Section B	4.9	210	Some voids lined, few filled
Midpanel Section A	8.5	251	
Midpanel Section B	6.4	210	

Highway: US 20/Hamilton WB, MP 135.4, sta 49

Mix details: C-3WR-C

Coarse Aggregate: Ft. Dodge Limestone

Fine Aggregate : Yates sand

Cement : Lehigh

Fly Ash : Port Neal 4, @15% replacement

Observations: Visual inspection and light microscopy

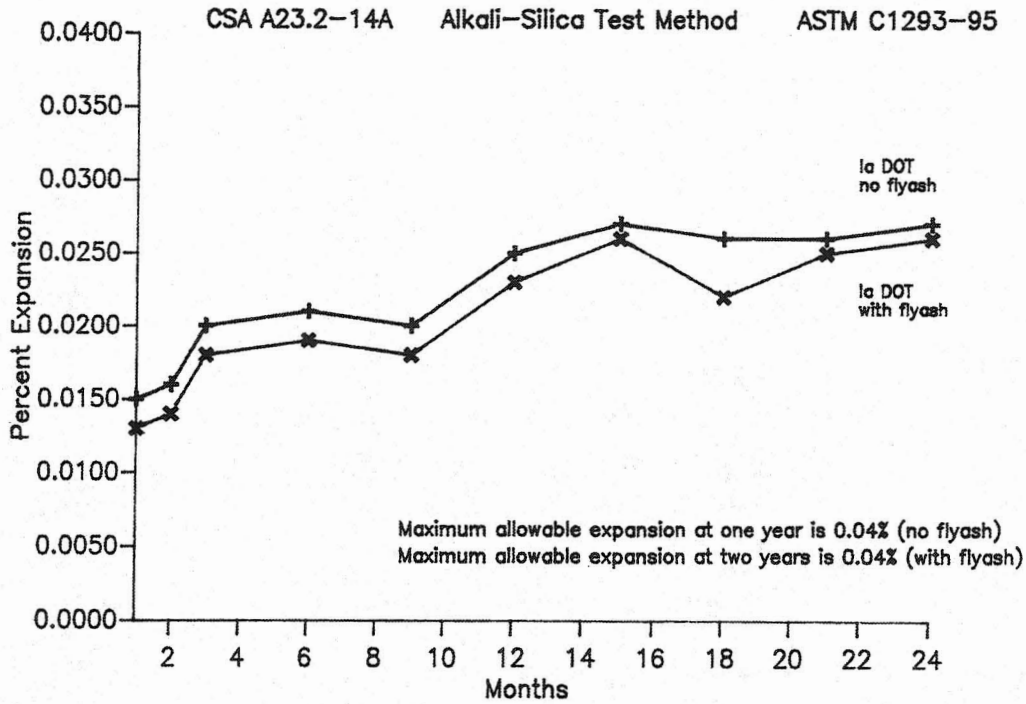
Core Location & Details	Aggregates	Voids	Cracks	Comments
Trans. Joint Section A	Limestone sound Sand contains shale	Distorted, many filled	Severe, open- often near entrapped voids	Segregation common
Trans. Joint Section C	Limestone sound Sand contains shale	Look better than the top sections	None, except for cracked shale	Segregation common ? Gap graded
Midpanel Section A	Limestone sound Sand contains shale	Some distorted entrapped voids	One fine crack noted from top surface into core	Good gradation
Midpanel Section B	Limestone sound Sand contains shale	Some distorted entrapped voids	Few cracks except for shale	Slight segregation noted
Jt @ Center line Section A	Limestone sound Sand contains shale	Distorted, many filled	Severe, open Fine cracks from top of core	Major cracks subparallel to the top of the core, segregation common in the cores
Jt @ Center line Section B	Limestone sound Sand contains shale	Distorted, many filled	? section dropped	Aggregate appears to be gap graded

Observations: scanning electron microscopy

Location & Details	Air Content, % (mortar basis)	Area Weighted Mean Diameter. (microns)	Comments
Trans. Joint Section A			Coarse aggregate particles often show poor interfacial transition zones on the bottom side of the coarse aggregate particles.
Trans. Joint Section C	6.2	260	Many small voids completely filled
Midpanel Section A	3.9	197	Many small voids completely filled
Midpanel Section B	5.3	302	Many small voids completely filled
Jt @ Center line Section A	4.7	263	Many small voids completely filled
Jt @ Center line Section B			Many small voids completely filled

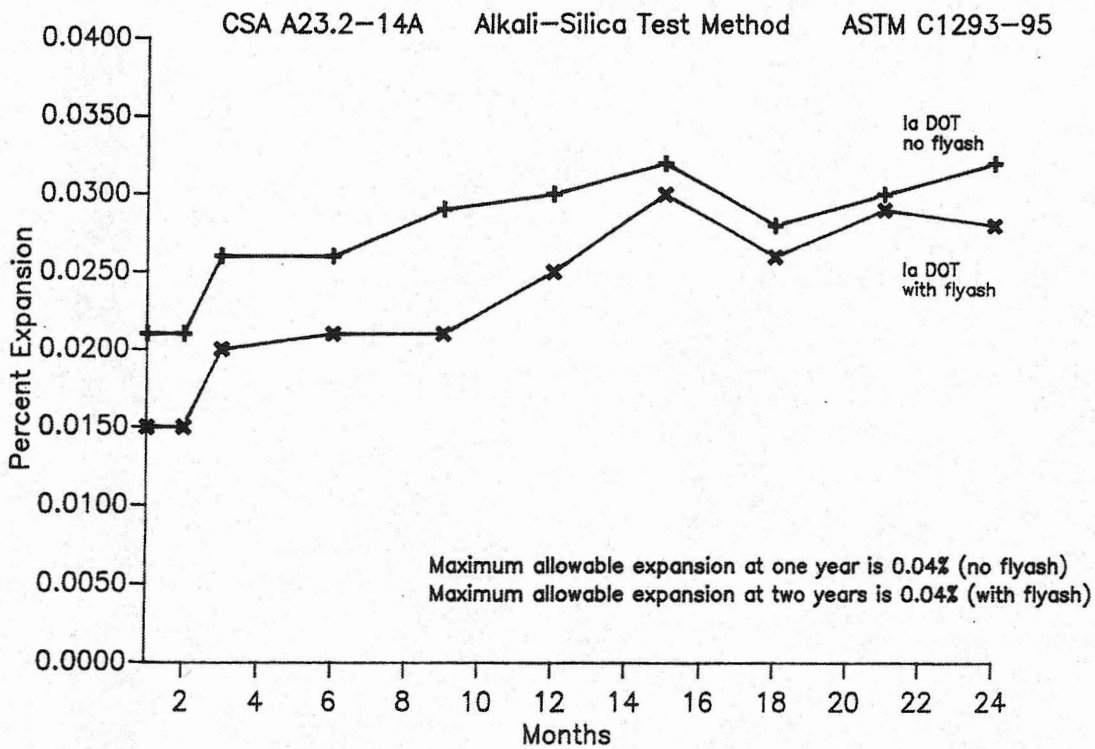
**CONCRETE PRISM TEST RESULTS ON CROFT SAND FROM WEBSTER COUNTY
IOWA DOT TEST RESULTS**

JAN 04, 1998



**CONCRETE PRISM TEST RESULTS ON YATES SAND FROM WEBSTER COUNTY
IOWA DOT TEST RESULTS**

JAN 04, 1998



Highway: Hwy 169/Webster SB, near sta 2002

Mix details: C-3WR
 Coarse Aggregate: Ft. Dodge Limestone
 Fine Aggregate : sand
 Cement : Lehigh
 Fly Ash : None

Observations: Visual inspection and light microscopy

Core Location & Details	Aggregates	Voids	Cracks	Comments
Trans. Joint Section A	Limestone sound Sand contains shale and some chert	Many distorted voids	Moderate, open most commonly subparallel	Segregation common in cores, some areas very rich in mortar and devoid of coarse agg.
Trans. Joint Section B	Limestone sound Sand contains shale	Many distorted voids, some voids 25mm diameter	Moderate, open most commonly subparallel	Segregation common.
Jt @ Center line Section A	Limestone sound Sand contains shale	Many distorted voids, many agglomerated voids	Severe, open most commonly subparallel	Segregation common.

Observations: scanning electron microscopy

Location & Details	Air Content, % (mortar basis)	Area Weighted Mean Diameter. (microns)	Comments
Trans. Joint Section A	7.0	248	Many filled voids
Trans. Joint Section B	9.6	280	Many filled voids
Jt @ Center line Section A	4.9	257	Many filled voids

Highway: Hwy 175/Hamilton WB lane, MP 156.2, sta 143

Mix details: A-3-F

Coarse Aggregate: Moberly Mine (Alden)
 Fine Aggregate : Hallet sand
 Cement : Penn Dixie
 Fly Ash : Port Neal 3, 17% by mass

Observations: Visual inspection and light microscopy

Core Location & Details	Aggregates	Voids	Cracks	Comments
Trans. Joint Section A	Limestone sound Sand contains shale	Some distorted entrapped voids	Shale, two coarse aggregate particles cracked near wear surface	Slight segregation noted
Trans. Joint Section B	Limestone sound Sand contains shale	Entrapped air voids <5mm diameter	Shale, one coarse aggregate particle cracked	
Trans. Joint Section C	Limestone sound Sand contains shale		Shale, one coarse aggregate particle cracked	
Midpanel Section A	Limestone sound Sand contains shale	Entrapped air voids <5mm diameter	None, except for cracked shale	One cracked chert particle noted
Midpanel Section B	Limestone sound Sand contains shale	Entrapped air voids <12mm diameter	None, except for cracked shale	

Observations: scanning electron microscopy

Location & Details	Air Content, % (mortar basis)	Area Weighted Mean Diameter. (microns)	Comments
Trans. Joint Section A	7.0	235	
Trans. Joint Section B	8.1	231	
Trans. Joint Section C	8.8	300	
Midpanel Section A	7.6	218	
Midpanel Section B	6.4	204	

Highway: Hwy 175/Hamilton EB lane, MP 157.5, sta 191

Mix details: A-3-C

Coarse Aggregate: Moberly Mine (Alden)
 Fine Aggregate : Hallet sand
 Cement : Penn Dixie
 Fly Ash : Council Bluffs, 15%

Observations: Visual inspection and light microscopy

Core Location & Details	Aggregates	Voids	Cracks	Comments
Trans. Joint Section A	Limestone sound Sand contains shale	Some distorted entrapped voids	None, except for cracked shale	No surface cracks
Trans. Joint Section B	Limestone sound Sand contains shale		None, except for cracked shale	
Midpanel Section A	Limestone sound Sand contains shale		None, except for cracked shale	
Midpanel Section B	Limestone sound Sand contains shale		None, except for cracked shale	

Observations: scanning electron microscopy

Location & Details	Air Content, % (mortar basis)	Area Weighted Mean Diameter. (microns)	Comments
Trans. Joint Section A	8.1	266	Some voids lined with ettringite, none filled.
Trans. Joint Section B	5.0	221	
Midpanel Section A	6.8	223	
Midpanel Section B	5.8	244	

Highway: Hwy 175/Hamilton EB lane, MP 158.3, sta 244

Mix details: A-3

Coarse Aggregate: Moberly Mine (Alden)
 Fine Aggregate : Hallet sand
 Cement : Penn Dixie
 Fly Ash : None

Observations: Visual inspection and light microscopy

Core Location & Details	Aggregates	Voids	Cracks	Comments
Trans. Joint Section A	Limestone sound Sand contains shale	Some voids lined with white material	None, except for cracked shale	No surface cracks
Trans. Joint Section B	Limestone sound Sand contains shale		None, except for cracked shale	
Midpanel Section A	Limestone sound Sand contains shale		None, except for cracked shale	
Midpanel Section B	Limestone sound Sand contains shale		None, except for cracked shale	

Observations: scanning electron microscopy

Location & Details	Air Content, % (mortar basis)	Area Weighted Mean Diameter. (microns)	Comments
Trans. Joint Section A	10.5	241	Some voids lined with ettringite, none filled.
Trans. Joint Section B	8.8	259	
Midpanel Section A	8.1	190	
Midpanel Section B	8.2	227	

Highway: Hwy 330/Marshall NB lane, MP 6.8, sta 74

Mix details: C-5WR

Coarse Aggregate: Gravel, source unknown (may be Hallets pit)
 Fine Aggregate : Sand, source unknown (may be Hallets pit)
 Cement : Davenport
 Fly Ash : None

Observations: Visual inspection and light microscopy

Core Location & Details	Aggregates	Voids	Cracks	Comments
Trans. Joint Section A	Gravel not sound Sand contains shale	Some distorted entrapped voids	Some cracked coarse aggregate particles, cracked shale	The coarse aggregate in this site should have been a crushed carbonate rock.
Trans. Joint Section C	Gravel not sound Sand contains shale	Some distorted entrapped voids	Many cracks evident, often associated with coarse aggregate particles	Some cracks were also subparallel to the top of the core
Midpanel Section A	Gravel not sound Sand contains shale	Some distorted entrapped voids	Some cracked coarse aggregate particles, cracked shale	Surface crack penetrates 10mm into the core
Midpanel Section B	Gravel not sound Sand contains shale	Some distorted entrapped voids	Cracked shale	Poor gradation noted

Observations: scanning electron microscopy

Location & Details	Air Content, % (mortar basis)	Area Weighted Mean Diameter. (microns)	Comments
Trans. Joint Section A	5.0	299	Very coarse air void system
Trans. Joint Section C	5.2	319	
Midpanel Section A	5.3	293	
Midpanel Section B	5.7	320	

Highway: I-80/Iowa EB, MP 210.36, sta 298

Mix details: C-3WR-C

Coarse Aggregate: Conklin
 Fine Aggregate : Kimmich
 Cement : Davenport
 Fly Ash : Louisa, 15%

Observations: Visual inspection and light microscopy

Core Location & Details	Aggregates	Voids	Cracks	Comments
Trans. Joint Section A	Limestone sound Sand sound	Entrapped voids as large as 20mm	Surface cracks penetrate about 10mm into core	
Trans. Joint Section B	Limestone questionable Sand questionable	Few entrapped voids	Occasional cracked coarse aggregate particle, some cracked fine agg	
Trans. Joint Section C	Limestone questionable Sand sound	Many voids appear filled	Occasional cracked coarse aggregate particle	
Midpanel Section A	Limestone questionable Sand sound	Entrapped voids as large as 20mm	Occasional cracked coarse aggregate particle	No surface cracks, coarse agg sometimes contains chert
Midpanel Section B	Limestone sound Sand sound	Entrapped voids as large as 15mm	None evident	Entrapped voids common and often are connected
Extra Core Section A	Limestone sound Sand questionable		Surface cracks common, may penetrate 20mm into core	Core broke off – moved over and drilled another hole

Observations: scanning electron microscopy

Location & Details	Air Content, % (mortar basis)	Area Weighted Mean Diameter. (microns)	Comments
Trans. Joint Section A	4.6	225	Filled voids common in all sections
Trans. Joint Section B	4.7	279	
Trans. Joint Section C	4.1	252	
Midpanel Section A	5.8	228	
Midpanel Section B	8.3	263	
Extra Core Section A	3.3	262	

Highway: I-80/Dallas EB, MP 107.55, sta 509

Mix details: C-4WR-C

Coarse Aggregate: Shaffton (dolomite)
 Fine Aggregate : Van Meter sand
 Cement : Davenport
 Fly Ash : Council Bluffs, 15%

Observations: Visual inspection and light microscopy

Core Location & Details	Aggregates	Voids	Cracks	Comments
Joint near CL Section A	Dolomite sound Sand contains shale	Few voids, few look filled	None, except for cracked shale	No surface cracks
Joint near CL Section B	Dolomite sound Sand contains shale	Few filled	None, except for cracked shale	Many shale particles in this section
Midpanel Section A	Dolomite sound Sand contains shale	Few voids, few look filled	One surface crack penetrates 8 mm into core	Cracked shale also noted
Midpanel Section B	Dolomite sound Sand contains shale	Entrapped voids as large as 15mm diam.	None, except for cracked shale	Fly ash present but it looks significantly less than 15% in this section

Observations: scanning electron microscopy

Location & Details	Air Content, % (mortar basis)	Area Weighted Mean Diameter. (microns)	Comments
Joint near CL Section A	5.2	248	
Joint near CL Section B	5.4	270	
Midpanel Section A	7.3	309	
Midpanel Section B	6.5	277	

Highway: I-80/Dallas EB, MP 113.25, sta 810

Mix details: C-4WR-C

Coarse Aggregate: Alden

Fine Aggregate : Van Meter sand

Cement : Davenport

Fly Ash : Council Bluffs, 15%

Observations: Visual inspection and light microscopy

Core Location & Details	Aggregates	Voids	Cracks	Comments
Trans. Joint Section A	Limestone sound Sand contains shale and iron colored particles	Few entrapped, often look filled	Severe, open – mostly subparallel to top of core	Segregation and poor gradation noted, one coal particle noted
Trans. Joint Section B	Limestone sound Sand contains shale	Entrapped voids as large as 15mm	Severe, open – mostly subparallel to top of core	Segregation and poor gradation noted
Joint near CL Section A	Limestone sound Sand contains shale		Severe, open – mostly subparallel to top of core	Surface crack penetrates 30mm into core, segregation noted
Joint near CL Section B	Limestone sound Sand contains shale		Severe, open – mostly subparallel to top of core	Core broken about 75mm from top
Midpanel Section A	Limestone sound Sand contains shale	Air voids look filled	One surface crack noted, also cracked shale	Some dark areas noted around coarse agg particles
Midpanel Section B	Limestone sound Sand contains shale and chert	Entrapped voids as large as 15mm	Cracked shale	Many entrapped and agglomerated air voids

Observations: scanning electron microscopy

Location & Details	Air Content, % (mortar basis)	Area Weighted Mean Diameter. (microns)	Comments
Trans. Joint Section A	4.6	205	Many voids filled with ettringite in all sections
Trans. Joint Section B	5.1	319	
Joint near CL Section A			
Joint near CL Section B			
Midpanel Section A	2.8	246	
Midpanel Section B	8.4	244	

Highway: I-80/Dallas EB, MP 116.2, sta 966

Mix details: C-4WR-C

Coarse Aggregate: Alden
 Fine Aggregate : Van Meter sand
 Cement : Ash Grove
 Fly Ash : Council Bluffs, 15%

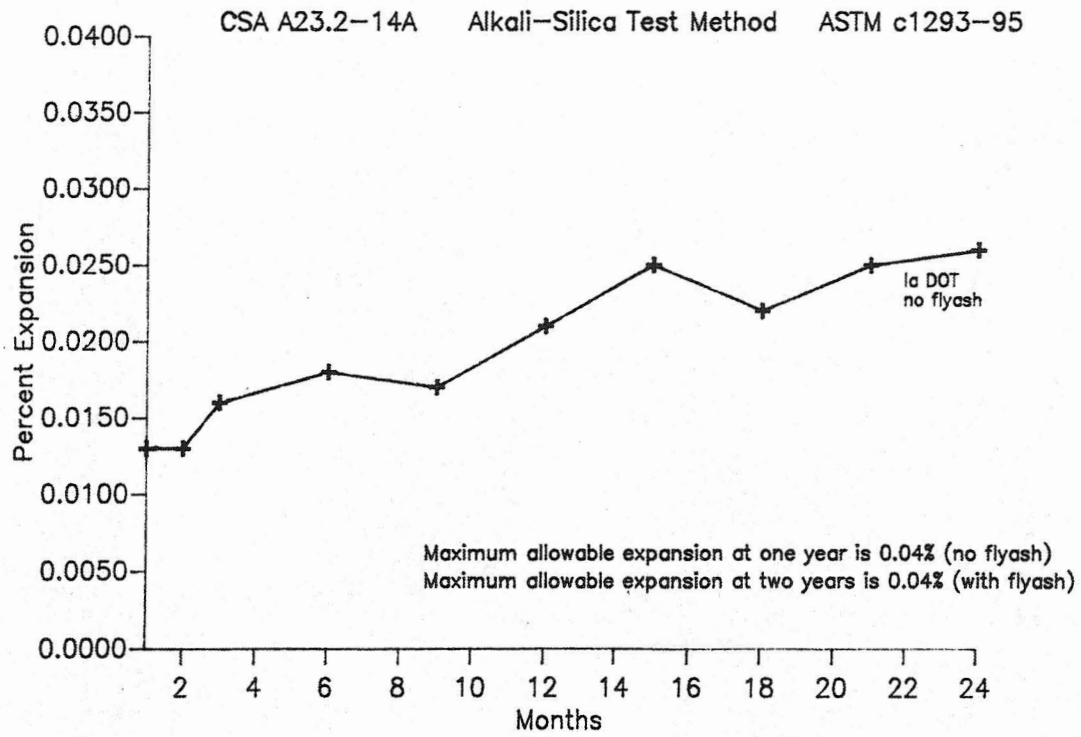
Observations: Visual inspection and light microscopy

Core Location & Details	Aggregates	Voids	Cracks	Comments
Joint near CL Section A	Limestone sound Sand sound	Agglomerated distorted voids	None evident	Very fine surface cracks
Joint near CL Section B	Limestone sound Sand contains some shale and chert	Entrapped voids as large as 8mm	None, except for cracked shale and chert	Many coarse agg particles aligned with the top of the core
Midpanel Section A	Limestone sound Sand contains some shale and chert	Distorted entrapped voids	None, except for cracked shale	Several chert particles noted but none were cracked
Midpanel Section B	Limestone sound Sand contains some shale and chert	Entrapped voids as large as 11mm	None evident	A couple of chert particles noted but none were cracked

Observations: scanning electron microscopy

Location & Details	Air Content, % (mortar basis)	Area Weighted Mean Diameter. (microns)	Comments
Joint near CL Section A	4.8	207	
Joint near CL Section B	3.9	160	
Midpanel Section A	6.4	192	
Midpanel Section B	5.3	245	

CONCRETE PRISM TEST RESULTS ON VAN METER SAND FROM DALLAS COUNTY
IOWA DOT TEST RESULTS
JAN 04, 1998



Highway: I-80/Cass WB, MP 68, sta 1019

Mix details: C-4WR-C

Coarse Aggregate: Shaffton (dolomite)

Fine Aggregate : Finley sand

Cement : Ash Grove

Fly Ash : Council Bluffs, 15%

Observations: Visual inspection and light microscopy

Core Location & Details	Aggregates	Voids	Cracks	Comments
Trans. Joint Section A	Dolomite sound Sand sound except for occasional chert	Irregular entrapped voids as large as 10mm	None evident	No surface cracks
Trans. Joint Section B	Dolomite sound Sand sound	Some filling noted in this section	None evident	Some light colored rims around coarse aggregate particles
Trans. Joint Section C	Dolomite not sound Sand sound	Many filled voids in this section	Active cracks in Dolomite coarse agg	
Midpanel Section A	Dolomite sound Sand sound	Distorted entrapped voids	None evident	Some light colored rims around coarse aggregate particles, fly ash noted
Midpanel Section B	Dolomite questionable Sand sound	Irregular entrapped voids as large as 17mm	Two cracked coarse agg particles	
Joint near CL Section A	Dolomite sound Sand sound		None evident	Some light colored rims around coarse aggregate particles, fly ash noted

Observations: scanning electron microscopy

Location & Details	Air Content, % (mortar basis)	Area Weighted Mean Diameter. (microns)	Comments
Trans. Joint Section A	10.9	231	Some voids lined with ettringite, none filled.
Trans. Joint Section B	9.0	206	
Trans. Joint Section C	8.6	228	
Midpanel Section A	8.0	211	
Midpanel Section B	9.2	284	
Joint near CL Section A			

Highway: Hwy 2/Fremont WB, MP 2.6, sta 1499

Mix details: 47-B Class V

Coarse Aggregate: Weeping Water
 Fine Aggregate : Oreapolis
 Cement : Ash Grove
 Fly Ash : None

Observations: Visual inspection and light microscopy

Core Location & Details	Aggregates	Voids	Cracks	Comments
Trans. Joint Section A	Limestone sound Sand sound	Few voids evident	Severe, open – mostly subparallel to top of core	Surface crack penetrates to about 8mm into core
Trans. Joint Section B	Limestone sound Sand sound	Coarse, voids often agglomerated	Severe, open – mostly subparallel to top of core	Cracks tend to go around aggregates
Midpanel Section A	Limestone sound Sand sound	Some voids filled	Severe, open – mostly subparallel to top of core	Surface crack penetrates to about 40mm into core
Midpanel Section B	Limestone sound Sand questionable	All small voids filled	Severe, open – mostly subparallel to top of core	Some fine aggregate particles are cracked
				Strange gradation noted in all cores – very rich in mortar

Observations: scanning electron microscopy

Location & Details	Air Content, % (mortar basis)	Area Weighted Mean Diameter. (microns)	Comments
Trans. Joint Section A	5.0	262	Small voids filled in most sections
Trans. Joint Section B	3.8	226	
Midpanel Section A	4.6	174	
Midpanel Section B	2.7	181	

Highway: Hwy160/Polk EB, near sta 362
Mix details: Unknown (US Army Corp. Project)
Coarse Aggregate: Ames Mine
Fine Aggregate : ? Hallet sand
Cement : Unknown
Fly Ash : None

Observations: Visual inspection and light microscopy

Core Location & Details	Aggregates	Voids	Cracks	Comments
Trans. Joint Section A	Coarse agg. sound Sand contains shale	Few entrapped voids	None, except for cracked shale	Mixed limestone+dolomite coarse aggregate exhibits poor gradation
Trans. Joint Section B	Coarse agg. sound Sand contains shale		None, except for cracked shale	
Midpanel Section A	Coarse agg. sound Sand contains shale	Few entrapped voids	Surface crack penetrates to 11 mm below top of core	All angular coarse aggregate particles oriented with top of slab
Midpanel Section B	Coarse agg. sound Sand contains shale	Few entrapped voids	None, except for cracked shale	

Observations: scanning electron microscopy

Location & Details	Air Content, % (mortar basis)	Area Weighted Mean Diameter. (microns)	Comments
Trans. Joint Section A	2.0	284	No fly ash observed
Trans. Joint Section B			
Midpanel Section A	2.2	161	No fly ash observed
Midpanel Section B	2.4	295	

Highway: US 218/Johnson SB, MP 95.45, sta 1658

Mix details: C-3WR

Coarse Aggregate: Conklin
 Fine Aggregate : Stevens
 Cement : Davenport
 Fly Ash : None

Observations: Visual inspection and light microscopy

Core Location & Details	Aggregates	Voids	Cracks	Comments
Trans. Joint Section A	Limestone sound Sand questionable, contains some chert	Many entrapped voids	Three surface cracks penetrate about 5 to 10mm into core	Poor consolidation, many visible gaps around particles, cracked chert
Trans. Joint Section B	Limestone sound Sand questionable, contains some chert	Many filled voids	Some cracks noted in fine aggregate particles	
Midpanel Section A	Limestone sound Sand questionable, contains some chert	Distorted agglomerated air voids	Some cracks noted in fine aggregate particles	Coarse aggregate particles often aligned with top of core
Midpanel Section B	Limestone sound Sand questionable		None, except for cracked shale	Very poor consolidation

Observations: scanning electron microscopy

Location & Details	Air Content, % (mortar basis)	Area Weighted Mean Diameter. (microns)	Comments
Trans. Joint Section A	5.0	253	No fly ash Small voids filled in most sections
Trans. Joint Section B	3.6	295	
Midpanel Section A	5.4	296	No fly ash
Midpanel Section B			

Highway: US 218/Johnson NB, MP 91.96, sta 1498

Mix details: C-3WR

Coarse Aggregate: Conklin
 Fine Aggregate : Stevens
 Cement : Davenport
 Fly Ash : None

Observations: Visual inspection and light microscopy

Core Location & Details	Aggregates	Voids	Cracks	Comments
Trans. Joint Section A	Limestone sound Sand contains chert	Coarse, agglomerated air voids	Surface crack penetrates 30mm into core	Few cracks subparallel to top of core, many branch off the surface crack, cracked chert
Trans. Joint Section B	Limestone questionable Sand contains chert	Many filled voids	Many cracks associated with fine aggregate	One coarse aggregate particle cracked, many fine aggregate particles cracked
Midpanel Section A	Limestone sound Sand contains chert	Distorted entrapped voids	Few cracks noted	Cracked chert particles noted
Joint at CL Section A	Limestone sound Sand contains chert	Coarse, agglomerated air voids	Few cracks noted	Poor consolidation noted, cracked chert particles noted
Joint at CL Section B	Limestone sound Sand contains chert	Many filled voids	Severe, open – often subparallel to top of core	Poor consolidation noted, cracked chert particles noted

Observations: scanning electron microscopy

Location & Details	Air Content, % (mortar basis)	Area Weighted Mean Diameter. (microns)	Comments
Trans. Joint Section A	4.9	205	No fly ash Small voids filled in most sections
Trans. Joint Section B	5.2	415	No fly ash
Midpanel Section A	7.8	301	No fly ash
Joint at CL Section A	6.0	207	
Joint at CL Section B	5.0	221	

Highway: US 61/Scott NB, MP 125, sta 525

Mix details: C-3WR

Coarse Aggregate: McCausland
 Fine Aggregate : McCausland Pit
 Cement : Lehigh
 Fly Ash : None

Observations: Visual inspection and light microscopy

Core Location & Details	Aggregates	Voids	Cracks	Comments
Trans. Joint Section A	Dolomite sound Sand sound	Some distorted entrapped voids	None evident	No surface cracks
Trans. Joint Section C	Dolomite not sound Sand sound	Many voids filled	Many cracked dolomite particles	Little cracking except at base of core – most cracks pass through dolomite and paste
Midpanel Section A	Dolomite sound Sand sound		None evident	No surface cracks
Midpanel Section B	Dolomite sound Sand sound		None evident	
Horizontal slice at crack	Dolomite sound Sand sound	Many voids filled	None evident in section	This slice was taken just above a major crack in the core

Observations: scanning electron microscopy

Location & Details	Air Content, % (mortar basis)	Area Weighted Mean Diameter. (microns)	Comments
Trans. Joint Section A	6.0	249	No fly ash
Trans. Joint Section C	5.4	373	Many filled voids
Midpanel Section A	8.7	249	No fly ash
Midpanel Section B	8.3	327	
Horizontal slice at crack	6.8	298	

APPENDIX E: RESULTS OF SHRINKAGE TESTING

Average Restrained Shrinkage Test Results					
sorted for plots					
Cement	fly ash%	WR*	cracktime (hrs)	treatment	plot values
Dix. Marq.	0	0	4.7	control	
Dix. Marq.	20	0	3.5	fly ash	
Dix. Marq.	0	5	4.5	water reducer	
Dix. Marq.	20	5	3.5	ash+water reducer	
Holnam	0	0	5.5	control	5.5
Holnam	20	0	10+ (but<23)	fly ash	10
Holnam	0	5	8+(but<23)	water reducer	8
Holnam	20	5	26.0	ash+water reducer	26
Kaiser	0	0	25.0	0	25
Kaiser	20	0	43.0	1	43
Kaiser	0	5	31+(but<46)	2	31
Kaiser	20	5	not performed	3	
LaFarge	0	0	3.0	control	
LaFarge	20	0	4.0	fly ash	
LaFarge	0	5	3.5	water reducer	
LaFarge	20	5	7.0	ash+water reducer	
Lehigh	0	0	2.7	control	
Lehigh	20	0	4.5	fly ash	
Lehigh	0	5	2.0	water reducer	
Lehigh	20	5	2.0	ash+water reducer	
Lehigh	20	10	7.5	4	
				*WR=water reducer	

Results of the Unrestrained shrinkage/expansion Tests												
Unrestrained Shrinkage												
Control Cements - all mixes at normal consistency												
% expansion time (days)	Lafarge			Kaiser			Dixon Marquette			Lehigh		
	0	0.167	1	0	0.167	1	0	0.167	1	0	0.167	1
Water Expansion												
% expansion time (days)	Lafarge			Kaiser			Dixon Marquette			Lehigh		
	0	0.167	1	0	0.167	1	0	0.167	1	0	0.167	1
Control Cements plus 20% Fly Ash - all mixes at normal consistency												
Unrestrained Shrinkage												
% expansion time (days)	Lafarge			Kaiser			Dixon Marquette			Lehigh		
	0	0.167	1	0	0.167	1	0	0.167	1	0	0.167	1
Water Expansion												
% expansion time (days)	Lafarge			Kaiser			Dixon Marquette			Lehigh		
	0	0.167	1	0	0.167	1	0	0.167	1	0	0.167	1
Lehigh Cement plus Fly Ash and Water Reducer- all mixes at normal consistency												
Unrestrained Shrinkage												
% expansion time (days)	3.3WR			6.7WR			0 WR			3.3WR		
	0	0.167	1	0	0.167	1	0	0.167	1	0	0.167	1
Water Expansion												
% expansion time (days)	3.3WR			6.7WR			0 WR			3.3WR		
	0	0.167	1	0	0.167	1	0	0.167	1	0	0.167	1
0	0	0	0	0	0	0	0	0	0	0	0	0
0.167	-0.027	-0.019	-0.031	-0.023	-0.028	-0.028	-0.023	-0.028	-0.028	0	0	0
1	-0.075	-0.052	-0.091	-0.071	-0.071	-0.071	-0.071	-0.071	-0.071	0	0	0
3	-0.125	-0.089	-0.160	-0.145	-0.110	-0.110	-0.145	-0.110	-0.110	0	0	0
7	-0.165	-0.128	-0.223	-0.202	-0.142	-0.142	-0.202	-0.142	-0.142	0	0	0
14	-0.198	-0.161	-0.268	-0.241	-0.171	-0.171	-0.241	-0.171	-0.171	0	0	0
31	-0.229	-0.188	-0.303	-0.272	-0.201	-0.201	-0.272	-0.201	-0.201	0	0	0
39	-0.231	-0.187	-0.311	-0.277	-0.207	-0.207	-0.277	-0.207	-0.207	0	0	0
73	-0.287	-0.238	-0.379	-0.338	-0.269	-0.269	-0.338	-0.269	-0.269	0	0	0
94	-0.327	-0.279	-0.428	-0.377	-0.315	-0.315	-0.377	-0.315	-0.315	0	0	0
Control Cements plus 20% Fly Ash - all mixes at normal consistency												
Unrestrained Shrinkage												
% expansion time (days)	Lafarge			Kaiser			Dixon Marquette			Lehigh		
	0	0.167	1	0	0.167	1	0	0.167	1	0	0.167	1
Water Expansion												
% expansion time (days)	Lafarge			Kaiser			Dixon Marquette			Lehigh		
	0	0.167	1	0	0.167	1	0	0.167	1	0	0.167	1
0	0	0	0	0	0	0	0	0	0	0	0	0
0.167	-0.02	-0.014	-0.027	-0.014	-0.019	-0.019	-0.014	-0.019	-0.019	0	0	0
1	-0.068	-0.043	-0.093	-0.062	-0.059	-0.059	-0.062	-0.059	-0.059	0	0	0
5	-0.132	-0.094	-0.183	-0.147	-0.115	-0.115	-0.147	-0.115	-0.115	0	0	0
12	-0.172	-0.124	-0.231	-0.186	-0.152	-0.152	-0.186	-0.152	-0.152	0	0	0
26	-0.202	-0.142	-0.265	-0.211	-0.182	-0.182	-0.211	-0.182	-0.182	0	0	0
34	-0.209	-0.146	-0.274	-0.215	-0.189	-0.189	-0.215	-0.189	-0.189	0	0	0
68	-0.262	-0.183	-0.337	-0.261	-0.248	-0.248	-0.261	-0.248	-0.248	0	0	0
89	-0.301	-0.214	-0.394	-0.293	-0.295	-0.295	-0.293	-0.295	-0.295	0	0	0
Lehigh Cement plus Fly Ash and Water Reducer- all mixes at normal consistency												
Unrestrained Shrinkage												
% expansion time (days)	3.3WR			6.7WR			0 WR			3.3WR		
	0	0.167	1	0	0.167	1	0	0.167	1	0	0.167	1
Water Expansion												
% expansion time (days)	3.3WR			6.7WR			0 WR			3.3WR		
	0	0.167	1	0	0.167	1	0	0.167	1	0	0.167	1
0	0	0	0	0	0	0	0	0	0	0	0	0
0.167	-0.029	-0.030	-0.018	-0.026	-0.025	-0.025	-0.026	-0.025	-0.025	0	0	0
1	-0.085	-0.086	-0.061	-0.068	-0.072	-0.072	-0.068	-0.072	-0.072	0	0	0
5	-0.161	-0.170	-0.116	-0.133	-0.136	-0.136	-0.133	-0.136	-0.136	0	0	0
7	-0.178	-0.190	-0.130	-0.150	-0.153	-0.153	-0.150	-0.153	-0.153	0	0	0
14	-0.201	-0.219	-0.148	-0.169	-0.176	-0.176	-0.169	-0.176	-0.176	0	0	0
28	-0.215	-0.254	-0.168	-0.191	-0.201	-0.201	-0.191	-0.201	-0.201	0	0	0
62	-0.215	-0.321	-0.218	-0.249	-0.263	-0.263	-0.249	-0.263	-0.263	0	0	0
83	-0.215	-0.378	-0.259	-0.293	-0.312	-0.312	-0.293	-0.312	-0.312	0	0	0

ASTM C 827 Tests									
	Lehigh	LaFarge	Lehigh	LaFarge	Holnam	Kaiser	Dix-Mar		
ceMENT	CBF	CBF	no	no	no	no	no	no	
fly ash	yes	yes	no	no	no	no	no	no	
WR	224	224	242.5	242.5	242.5	242.5	242.5	242.5	
Water	108	132	100	122	118	101	121	121	
flow	8+	6+	3	5	5.5	7+	6	6	
set time (hr)	75.00	73.55	76.00	74.84	73.23	72.10	72.42	72.42	
Mag factor	Raw data plus interpolation between points								
time (min)	Dist. (mm)	Dist. (mm)	Dist. (mm)	Dist. (mm)	Dist. (mm)	Dist. (mm)	Dist. (mm)	Dist. (mm)	time hours
10	6.5	13	10	12	6.5	2	10	10	0.17
20	10.5	20	24	22.5	18.5	15.5	16	16	0.33
30	14.5	23.5	36	29	30.5	24.5	21.5	21.5	0.50
40	17.5	27.5	46	31.5	38.5	27.5	26.5	26.5	0.67
50	22	31	53	34.5	44	28.5	30	30	0.83
60	25.5	33.5	60	36	48	30	32	32	1.00
75	28.5	36.5	65	36.5	57	30	35	35	1.25
90	32	39	67	37.5	66.5	30	37.5	37.5	1.50
105	34	40.5	69	37.5	73	30	39	39	1.75
120	36	42	66	37.5	79	34	41.5	41.5	2.00
135	37.5	43	66	38	82.5	37.5	44	44	2.25
150	39	44	66	38.5	86	41	45	45	2.50
165	40	45	66	38.5	88	43.5	45	45	2.75
180	40.5	45	64	39	89.5	45.5	46	46	3.00
210	42.5	47	64	38.5	91	46.5	46	46	3.50
240	43	48	64	38.5	91	46.5	46	46	4.00
270	44.5	48	64	38.5	92	46.5	46	46	4.50
300	44.5	49.5	64	38.5	92	46.5	46	46	5.00
330	44.5	49.5	64	38.5	92	46.5	46	46	5.50
360	44.5	51	64	38.5	92	46.5	46	46	6.00
390	44.5	51	64	38.5	92	46.5	46	46	6.50
420	44.5	51	64	38.5	93	46.5	46	46	7.00

Data adjusted for magnification and cylinder size									
ASTM C 827 Tests									
	Lehigh	LaFarge	Lehigh	LaFarge	Holnam	Kaiser	Dix-Mar		
cement	CBF	CBF	no	no	no	no	no		
fly ash	yes	yes	no	no	no	no	no		
WR	224	224	242.5	242.5	242.5	242.5	242.5		
Water									
time (min)	shrinkage,%	time hours							
10	0.085	0.174	0.130	0.158	0.087	0.027	0.136	0.17	0.17
20	0.138	0.268	0.311	0.296	0.249	0.212	0.217	0.33	0.33
30	0.190	0.314	0.466	0.381	0.410	0.334	0.292	0.50	0.50
40	0.230	0.368	0.596	0.414	0.517	0.375	0.360	0.67	0.67
50	0.289	0.415	0.686	0.454	0.591	0.389	0.408	0.83	0.83
60	0.335	0.448	0.777	0.473	0.645	0.410	0.435	1.00	1.00
75	0.374	0.488	0.842	0.480	0.766	0.410	0.476	1.25	1.25
90	0.420	0.522	0.868	0.493	0.894	0.410	0.510	1.50	1.50
105	0.446	0.542	0.894	0.493	0.981	0.410	0.530	1.75	1.75
120	0.472	0.562	0.855	0.493	1.062	0.464	0.564	2.00	2.00
135	0.492	0.575	0.855	0.500	1.109	0.512	0.598	2.25	2.25
150	0.512	0.589	0.855	0.506	1.156	0.560	0.612	2.50	2.50
165	0.525	0.602	0.855	0.506	1.183	0.594	0.612	2.75	2.75
180	0.531	0.602	0.829	0.513	1.203	0.621	0.625	3.00	3.00
210	0.558	0.629	0.829	0.506	1.223	0.635	0.625	3.50	3.50
240	0.564	0.642	0.829	0.506	1.223	0.635	0.625	4.00	4.00
270	0.584	0.642	0.829	0.506	1.237	0.635	0.625	4.50	4.50
300	0.584	0.662	0.829	0.506	1.237	0.635	0.625	5.00	5.00
330	0.584	0.662	0.829	0.506	1.237	0.635	0.625	5.50	5.50
360	0.584	0.683	0.829	0.506	1.237	0.635	0.625	6.00	6.00
390	0.584	0.683	0.829	0.506	1.237	0.635	0.625	6.50	6.50
420	0.584	0.683	0.829	0.506	1.250	0.635	0.625	7.00	7.00

APPENDIX F: HYPOTHESIS FOR PREMATURE CONCRETE DETERIORATION

A Hypothesis to Explain the Premature Concrete Deterioration in the Midwest (Pavement and Barrier Rails) by Vernon J. Marks, Scott Schiorholtz and David L. Gress

- I. Matrix Microcracking
 - a. Many current admixtures are exacerbating the drying shrinkage in the surface of the concrete.
- II. Over Vibration of the Concrete
 - a. Very low air content in the surface of the concrete.
 - b. Differential drying shrinkage crack in the vibrator trail (There is also significant drying shrinkage cracking between the vibrator trails).
 - c. Increased vibration due to early setting problem (due to combinations of admixtures, fly ash, cement, ambient temperature, wind and placement delays).
- III. Excessive Production of Calcium Sulfoaluminate
 - a. Higher sulfur content in the portland cement.
 - b. Class C fly ash contributes substantial aluminum and alkalis.
 - c. Substantial production of calcium sulfoaluminate that plugs or partially plugs the entrained air system.
- IV. Substantial Use of Deicing Salts
 - a. Makes the concrete near the surface hydrophilic so it retains a higher moisture content.
 - b. The sodium chloride causes the calcium sulfoaluminate near the surface of the concrete to swell and results in more volume and plugging of the entrained air system.
- V. The Low Air Content Renders the Concrete Susceptible to Freeze/Thaw Cracking
 - a. The microcracking and freeze/thaw cycles allow sodium chloride deicing salt and water to enter the concrete.
 - b. The freeze/thaw cracking allows more sodium chloride and water to enter the concrete.
 - c. The process repeats itself and the deterioration moves deeper into the concrete.
 - d. Joints and other areas with greater water availability deteriorate more rapidly because these areas become more saturated (sag vertical curves relatively impermeable bases).

Suggested Solution

1. Specify workability (?) (maximum and minimum slump) at the time of placement.
2. Restrict vibrator frequency and require them to be operated three inches below the surface of the finished pavement.
3. Batter the forms on the slipform paver.
4. Specify a minimum air content by image analysis of the hardened concrete 1/2" below the surface of the pavement.
5. The drying shrinkage problem and excessive production of calcium sulfoaluminate should be addressed.

VJM:kmd
12-01-97